Charles University

Faculty of Science

Study programme: Animal Physiology

Sorbonne Université

École Doctorale n°158

Cerveau, Cognition, Comportement

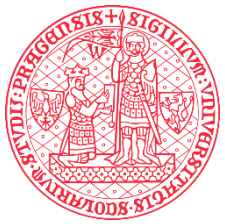

MSc. Alice ABBONDANZA

THE ROLE OF STRIATAL CHOLINERGIC SIGNALLING IN THE CONTROL OF BEHAVIOUR

Úloha cholinergní signalizace ve striatu v řízení chování

Le rôle de la signalisation cholinergique striatale dans le contrôle du comportement

DOCTORAL THESIS

Cotutelle de thèse

Supervisors:

Dr Jan JAKUBIK

Dr Véronique BERNARD

Examination Board:

Dr Camilla BELLONE - Reviewer

Dr Jan SVOBODA - Reviewer

Dr Jiri NOVOTNY - President (CU)

Dr Zdenka BENDOVA - Examinator (CU)

Dr Peter VANHOUTTE - Examinator (SU)

Dr Véronique BERNARD - Co-supervisor (SU)

Dr Jan JAKUBIK - Co-supervisor

Prague, 2023

γνῶθι σεαυτόν

Come in ogni viaggio, ciò che ci guida e indica la strada è la consapevolezza di noi stessi e dei nostri bisogni.

Prevedere ciò che ci sarà utile, formulare chiaramente gli obiettivi, imparare a conoscere i propri limiti e i propri punti di forza, è l'insegnamento maggiore che mi accompagnerà d'ora in poi sempre nel mio percorso.

Declaration:

I hereby declare that this doctoral thesis was elaborated independently and no other sources than quoted were used. Nor the thesis or any substantial part of it has been used to get any other academic title.

Prohlášení:

Prohlašuji, že tato disertační práce byla zpracována samostatně a nebyly použity žádné jiné než citované zdroje. Práce ani její podstatná část nebyla využita k získání jiného akademického titulu.

Déclaration:

Je déclare par la présente que cette thèse de doctorat a été élaborée de manière indépendante et qu'aucune autre source que celle citée n'a été utilisée. Ni la thèse ou une partie substantielle de celle-ci n'a été utilisée pour obtenir un autre titre académique.

Prague, 10th March 2023

Alice Abbondanza

Acknowledgements

At the end of this long path, I want to take some time and space to thank all the people I met, that helped me and taught me something in their own way. I have physically travelled quite a lot, and all this moving, besides making me meet many amazing people, also gifted me with some reference people.

First of all, I want to thank Helena, who shared with me her scientific passion and let me contribute to her ambitious project. Thank you for being always present for me, listening to my doubts, to my criticisms and transforming my eventually-too-realistic considerations in proactive new starting points. We formed a good team, I really enjoyed working at your side and I loved sharing many diverse considerations about life philosophies, cooking styles and tastes and cultures. For sure, we did our best. Thank to Veronique, for welcoming me in Paris, for patiently listening to my overwhelming considerations and ideas, for always trying hard with me before giving up. Thank you for all your support and being comprehensive in your way of understanding me. We gave a new meaning to the Paris-Prague, Prague-Paris connections. Thank to Sylvie, for teaching me so much about *in situ* hybridization and sharing her knowledge about science and life at any occasion, with always new inspiring examples and stories. Thank you for all your help and for your passion. Thank to Jan for welcoming me, trusting me and helping me understanding Czech rules and sorting out some of my never-ending problems. Thank you for teaching me that it does not matter how much we can complain about things, because if at the end we still find the strength and the toughness of keep pursuing them it really means we care about, and it is worthy.

I would like to thank all the members of the examination board, Dr Camilla Bellone, Dr Jan Svoboda, Dr Novotny, Dr Bendova, Dr Vanhoutte, Dr Bernard and Dr Jakubik for the time you dedicated in reading my manuscript and for the discussion about my research work. Thank to Dr Jan Svoboda and Dr Camilla Bellone for agreeing to be the reviewers of my thesis and for the interesting and useful feedbacks and comments.

Thank to Dana, for always trying to help me, beyond any language barrier and for taking care of me with her attentions. Thank you for making me feel supported and for helping so much. Thank to Alena, for your kindness and for really working on making the lab more cohesive, organizing lab meetings and proposing stimulating activities. Thank to my full Czech lab, to Dr Donezal, Eva, Ewa,

Nikolai, Dominik, Martina for becoming my ''Czech home'' and to all the students I shared some knowledge, time and space with, Anicka, Matias, Noemi, Shaed, Saeed, Jana, Jane, Irina, Trisha, Jakub, Zaki, Alex. Thank to Milan, for being always such a good guide and sharing with me many stories and habits about Czech culture and helping me with the car in different occasions.

Thank to Milica and Misa for being a team in sharing expertise, doubts, ideas and enjoying new experiences together. Thank to Dr Sumova and Dr Balastik for the fruitful discussions and suggestions and finding the time for our meetings. Thank to Pavel, for his skilful help and availability. Thank to the people at my favourite microscopy facilities, to David and Dr Hadraba for my first official trainings at confocal microscopes; to Martin, Ivan, Helena, Jirka, Jan and Ondrej for being there helping me solving always new challenges, helping a lot and making me experiment with different microscopes; to Ales and Maruska for showing me the beauty. Thank to our neighbour lab, to Jakub, Monica, Anirban, Mario, Katka, Pavel for being always nice and helpful. Thank to Daniel for being so supportive and cheering me up with your jokes and coffees and for sharing your experienced and wise philosophy of life with me. Thank to Natasha, for ''watching on me'', taking care and having funny adventures together. Thank to Simona, for sharing with me many moments and laughs, and showing me how to always find a bright side in approaching things and problems and the value of being original. Thank you for trying to teach me some Czech and for organizing the beer sessions. Thank to Nela, for all the suggestions and warnings about the cotutelle and for having such a good time together. Thank to Sofita, for being family, sharing so many moments and sustaining me, encouraging to ''hold-on'' no-matter what, for being authentic and enjoying dancing and having fun together. Thanks for being, together with Sonja and Carlos the best ''coronamigos'' I could ever wish to have as support. Thank to all the PhD students I met in these years and with whom I shared considerations and parts of the ''PhD-life'': Davide, Anna, Sofia, Sonja, Bohdan, Klevinda, Guillermo, Ivan, Rita, Milorad, Gabriella, Eduardo, Noelia. Thank to Daniel and Victor for bringing some of Brazilian calm ''love for life'' and perspective in a moment I really needed it. Thank to Mrs. Soukupova, Mrs. Havrdova, Mrs. Pouskova, Prof. Novotny and Mrs. Tomaskova for all the help in dealing with administration issues.

Thank to Mazarine, for being the best ''little-sister'' I wish I could have. Thank you for welcoming me and believing in me, being such a faithful reliable friend in any occasion, pulling always out the best part of me, sustaining me with your joy, kindness and affection. Thank to Augusto, for sharing so much and making the best out of our French experience, for your bright and honest scientific

integrity, for our discussions and life considerations. Thank to Marine, for the hugs and laughs, for being always ready after a first ''no'' to say ''yes'', for making everything possible beyond any problem because there are no things that cannot be fixed with the right will. Thank to Victor, for the experienced considerations about scientific career, for being always ready to fix a bad day or a black mood with a beer and some good chat. Thank to Kerleys, Csilla and Paola for sustaining each other through the misadventures with the ''French system'' and for having good time together. Thank to Adele, Justine, Naomi, Camille, Flavio, Laura, Maria and Margherita for sharing doubts and experiences through the process, celebrating our victories together and sharing happy moments. Thank to Johnny for being always such an optimistic, cheering me up with a contagious smile and making me realize everything will pass. Thank also to Ludovica, for waiting for me coming back every time and for enjoying Paris together. Thank to Stephanie and Nicolas for welcoming me in the lab and for patiently sustain me through my ''never-ending'' PhD. Thank to Salah, Odile, Carole, Vincent, Catalina, Sofie, Frank for the help and the interesting inputs. Thank to Marc and Danilo, for all the suggestions about next steps and for being such amazing examples of good life-work balanced lives while you keep ''climbing up'' your passions. Thank to Alina, for being such a passionate lover of life and for remembering me how valuable little things can be if you give them enough care.

Thank to Wenny, for being such an inspiring example of strong, self-confident woman, careful and funny. Thank you for making every single one of our meeting around the World a special lesson. Thank to Ursula and Roland, Lina, Mattes, Lasse for making me feel loved and ''home'' every time I am in Germany. Thank you for being such a good listeners, caring and supporting me. Thank to Emma, Camila and Sofia, for sharing special time together and for showing me how to be such inspired, determined and passionate researchers.

Thank to Shona and Susan for welcoming me and helping arranging everything to experiment and implement together new ideas. Thank to Eileen for making every visit to Coleraine comfortable and memorable.

Un grazie speciale va sicuramente a mamma e papa', che mi sostengono sempre, mi stimano e fanno il tifo per me. Grazie perche' anche se non sempre capite a fondo cosa faccio o non approvate certe mie scelte, siete sempre presenti per me, pronti a consigliarmi e a darmi forza. Grazie per avermi insegnato che vale la pena inseguire le mie passioni e che impegno, rispetto e consapevolezza ripagano sempre. Grazie per esser stati modello per me, di integrita' e tenacia. Grazie a Carla, Andrea

e Alessandro perche' non importa quanto distanti siamo, l'affetto, la stima e la comprensione reciproca fanno si' che vi senta sempre al mio fianco, ad incoraggiarmi, sostenermi e a gioire con me.

Grazie a Gianluigi, per esserci per me, per l'aiuto e per le distrazioni. Grazie per spronarmi ad apprezzare cio' che ho, dove ho la fortuna di vivere e a riconoscere le possibilita' e i traguardi raggiunti. Grazie a Ludovica, che mi aiuta a ''centrarmi'' e a ridefinire le cose in una prospetiva piu' oggettiva e bilanciata. Grazie per ricordarmi che e' importante cio' che penso, e che mi devo ascoltare perche' i miei bisogni e desideri hanno una loro dimensione che va rispettata. Grazie a Stefania, per essere un modello e una guida ispiratrice verso una carriera da ricercatrice e mamma. Grazie per tutti preziosi momenti passati insieme e le chiacchierate illuminanti. Grazie a Cecilia Gotti, per essere un modello di passione ed integrita' scientifica, per essere disponibile e pronta a consigliarmi e guidarmi. Grazie a Michela e Claudia, per avermi accolta quando avevo bisogno e per lasciare ''la porta sempre aperta'', essendoci per me che si tratti di un'emergenza manicure o di offrirmi una spalla su cui piangere. Grazie ad Enrico, per le pause caffe', i costruttivi confronti sulla carriera scientifica, per la condivisione e l'aiuto nel fronteggiare le difficolta' legate a nuove metodiche e non solo. Grazie a Federico, per i suoi criticismi e la sua scettica disillusione nel fare il ricercatore. Grazie per l'immancabile supporto a 360 gradi e i produttivi commenti e consigli. Grazie a Vincenzo per l'aiuto e le consultazioni IT al volo. Grazie a tutte le persone, piu' o meno di passaggio a Praga, con cui ho condiviso momenti, piu' o meno seri, in questi anni: Ilaria, Marco, Sarka, Feliciana, Irene, Vincenzo, Luca e Kasha, Cristina, Erika, Laura, Daniela. Grazie agli amici di sempre, che anche se lontani, riescono a sostenermi, capirmi e offrirmi un'alternativa o una via di fuga: Raffa, Marta, Biagio, Lara, Francesca e Gianni, Giulia e Ferdi, Nena, Jacopo, Stefano, Boffi e ai colleghi di sempre Matteo, ADB, Laura, GiuliaFerro, Laura, Marco, Anna, Jessica, Davide, Lapo, Stefano, Andrea, Silvia.

List of publications related to this dissertation

Alice Abbondanza, Irina Ribeiro Bas, Martin Modrak, Martin Capek, Jessica Minich, Alexandra Tyshkevich, Shahed Naser, Revan Rangotis, Pavel Houdek, Alena Sumova, Sylvie Dumas, Veronique Bernard and Helena Janickova

Nicotinic Acetylcholine Receptors Expressed by Striatal Interneurons Inhibit Striatal Activity and Control Striatal-Dependent Behaviors,

JNeurosci 2022, 42 (13) 2786-2803; DOI: https://doi.org/10.1523/JNEUROSCI.1627-21.2022

Statement about the extent of participation

I undersigned Alice Abbondanza declare that I performed all the stereotaxic surgeries for the preparation of the four cohorts of animals used in the study, the RNA scope experiment, the qPCR on striatal punches, brains' sectioning and all the related immunofluorescence staining and analysis, I contributed to the behavioural testing and analysis of all the tasks presented in this thesis dissertation (cued Morris water maze, elevated plus maze, forced swimming test, grooming test, hole-board test, light/dark preference task, marble burying test, nest building, novel object recognition, open field test (including amphetamine administration), social preference task, tail suspension test, Y maze and T-maze) performing the experiments myself or by supervising students helping me with the testing. In addition, I contributed to the writing, revision and figures' preparation of the scientific paper related to the above stated publication.

Prague, 10th March 2023

Alice Abbondanza

We undersigned Dr Helena Janíčková and Dr Véronique Bernard certify on behalf of all co-authors that the above stated information about contribution of Alice Abbondanza to the above stated publication is correct.

Prague, 10th March 2023

Helena Janíčková, PhD

Véronique Bernard, PhD

Abstract

Cholinergic transmission regulates many behavioural domains, ranging from motor activity to cognition. Acetylcholine signalling is mediated by muscarinic and nicotinic acetylcholine receptors (mAChRs and nAChRs, respectively). While mAChRs are slow responding metabotropic receptors, nAChRs are ion channels, mediating fast neurotransmission. There is a growing body of evidence suggesting a role of nAChRs as important modulators of behavioural functions. However, as nAChRs consist of many subtypes, depending on their composition in subunits, and as they are expressed by various neuronal populations in different brain regions, their contribution to behavioural control is very complex. To decipher their contribution, it is necessary to selectively target nAChRs expressed not only in particular regions but also by particular neurons with a defined effect on local microcircuits. The goal of the present thesis was to use different genetic strategies to induce regional- and cell-specific deletion of β2-containing nAChRs in the mouse brain, in order to characterize the functional role of these receptors.

We focused our work in two brain areas, the striatum and the prefrontal cortex (PFC). In the striatum, we identified the striatal neurons that express one of the most common nicotinic subunits, the β2 subunit, using double-fluorescent *in situ* hybridization. Surprisingly, striatal cholinergic interneurons were identified as the neuronal population with the highest expression of β2 nicotinic subunits. To investigate the functional significance of β2-containing nAChRs in striatal neurons, we induced as a first approach, a local deletion of β2 by injection of an AAV vector expressing Cre recombinase in the dorsal striatum of Beta2-flox/flox mice. Then, we tested mice with the deletion in several behavioural tasks. We found that the absence of β2 in the striatum, led to alterations in several behavioural domains, including an increase in anxiety-like behaviour, a decrease in sociability, a deficit in discrimination learning and increased sensitivity to amphetamine. The behavioural changes were also associated with increased c-Fos expression in both saline- and amphetamine-treated animals. In addition to the Cre/loxP approach, we used CRISPR/Cas9-mediated gene editing to selectively delete β2 subunits in neuropeptide Y (NPY)-expressing interneurons in the PFC. This deletion resulted in increased sociability in the mutated mice that had been previously described for β2-global knock out mice and associated with the PFC. We conclude that even selective deletion of nAChRs expressed by specific and rare population of neurons leads to behavioural alterations. In addition, the behavioural

effect of nAChRs' deletion is not only dependent on the receptor subtype but also on the brain region and the type of neurons that were affected by the deletion.

Abstrakt

Cholinergní přenos reguluje celou řadu behaviorálních domén, od motorické aktivity po kognici. Cholinergní signalizace je zprostředkována muskarinovými a nikotinovými acetylcholinovými receptory (mAChR a nAChR). Zatímco mAChR jsou pomalu reagující metabotropní receptory, nAChR jsou iontové kanály zprostředkovávající rychlou neurotransmisi. Existuje rostoucí množství důkazů potvrzujících roli nAChR jako důležitých modulátorů behaviorálních funkcí. Protože se však nAChR skládají z mnoha podtypů, v závislosti na jejich podjednotkovém složení, a protože jsou exprimovány různými populacemi neuronů v různých oblastech mozku, jejich příspěvek ke kontrole chování je velmi komplexní. K jeho dešifrování je nutné selektivně cílit na nAChR exprimované nejen v konkrétních oblastech, ale i konkrétními neurony s definovaným účinkem na lokální nervové okruhy. Cílem této práce bylo použít různé genetické strategie k vytvoření delece β2-obsahujících nAChR v konkrétních oblastech myšího mozku a typech neuronů , aby bylo možné charakterizovat funkční význam těchto receptorů.

Naši práci jsme zaměřili na dvě oblasti mozku, striatum a prefrontální kůru (PFC). Ve striatu jsme identifikovali neurony exprimující jednu z nejběžnějších nikotinových podjednotek, β2 podjednotku, pomocí dvojitě fluorescenční hybridizace in situ. Překvapivě byly striatální cholinergní interneurony identifikovány jako neuronální populace s nejvyšší expresí β2 nikotinové podjednotky. Abychom prozkoumali funkční význam β2 nAChR v neuronech striata, použili jsme jako první přístup lokální deleci injekcí AAV vektoru exprimujícího Cre rekombinázu. AAV vektor jsme injikovali do dorzálního striata myší Beta2-flox/flox a pomocí Cre/loxP rekombinace jsme indukovali deleci 5. exonu genu pro β2 podjednotku. Poté jsme testovali myši s touto delecí v několika behaviorálních úlohách. Zjistili jsme, že nepřítomnost β2 podjednotky ve striatu vedla ke změnám v několika behaviorálních doménách, včetně zvýšení úzkostného chování, snížení sociálního chování, deficitu v diskriminačním učení a zvýšené citlivosti na amfetamin. Změny chování byly také spojeny se zvýšenou expresí transkripčního faktoru c-Fos u zvířat, která obdržela injekci jak fyziologického roztoku, tak i amfetaminu. Kromě přístupu Cre/loxP jsme použili také techniku CRISPR/Cas9 k selektivnímu

odstranění podjednotky β2 v interneuronech exprimujících neuropeptid Y (NPY) v PFC. Tato specifická delece vedla ke zvýšení sociálního chování u mutovaných myší, která byla dříve popsána pro β2-globální knock-out myši a spojena s nikotinovou signalizací v PFC. Došli jsme k závěru, že i selektivní delece nAChR exprimovaných specifickou a vzácnou populací neuronů vede ke změnám chování. Navíc behaviorální účinek delece nAChR není závislý pouze na podtypu receptoru, ale také na oblasti mozku a typu neuronů, které byly delecí ovlivněny.

Résumé

La transmission cholinergique régule de nombreux domaines comportementaux, allant de l'activité motrice à la cognition. La signalisation de l'acétylcholine est médiée par les récepteurs muscariniques et nicotiniques de l'acétylcholine (mAChR et nAChR, respectivement). Alors que les mAChR sont des récepteurs métabotropiques à réponse lente, les nAChR sont des canaux ioniques, assurant une neurotransmission rapide. Il existe un nombre croissant de preuves suggérant un rôle important des nAChR en tant que modulateurs des fonctions comportementales. Cependant, étant donné la diversité des sous-types de nAChR (dépendant de leur composition en sous-unités) et leur expression par diverses populations neuronales au sein de différentes régions cérébrales, leur contribution au contrôle comportemental s'avère être très complexe. Afin de mieux comprendre cette contribution, il est nécessaire de cibler les nAChR exprimés au sein de régions particulières mais aussi par des populations neuronales précises avec un effet défini sur les microcircuits locaux. L'objectif de la présente thèse était d'utiliser différentes stratégies génétiques pour induire une délétion régionale et spécifique des cellules des nAChR contenant β2 dans le cerveau de souris, afin de caractériser le rôle fonctionnel de ces récepteurs.

Nous avons concentré nos travaux sur deux zones du cerveau, le striatum et le cortex préfrontal (PFC). Dans le striatum, nous avons identifié des neurones striataux exprimant l'une des sous-unités nicotiniques les plus courantes, la sous-unité β2, en utilisant une hybridation in situ à double fluorescence. De manière surprenante, les interneurones cholinergiques striataux ont été identifiés comme la population neuronale avec la plus forte expression de la sous-unité nicotinique β2. Pour étudier la signification fonctionnelle des nAChR contenant β2 dans les neurones striataux, nous avons induit en première approche une délétion locale de β2 par injection d'un vecteur AAV exprimant la

recombinase Cre dans le striatum dorsal de souris Beta2-flox/flox. Ensuite, nous avons testé des souris avec la délétion dans plusieurs tâches comportementales. Nous avons constaté que l'absence de β2 dans le striatum entraînait des altérations dans plusieurs domaines comportementaux, notamment une augmentation du comportement anxieux, une diminution de la sociabilité, un déficit de l'apprentissage de la discrimination et une sensibilité accrue à l'amphétamine. Les changements de comportement étaient également associés à une expression accrue de c-Fos chez les animaux traités à la solution saline et aux amphétamines. En plus de l'approche Cre/loxP, nous avons utilisé l'édition de gènes médiée par CRISPR/Cas9 pour supprimer sélectivement la sous-unité β2 dans les interneurones exprimant le neuropeptide Y (NPY) dans le PFC. Cette suppression a entraîné une sociabilité accrue chez les souris mutées qui avait été précédemment décrite pour les souris knock-out β2-globales et associées au PFC. Nous concluons que même la suppression sélective des nAChR exprimés par une population spécifique et rare de neurones entraîne des altérations comportementales. De plus, l'effet comportemental de la suppression des nAChR ne dépend pas seulement du sous-type de récepteur, mais également de la région du cerveau et du type de neurones qui ont été affectés par la suppression.

Table of contents

Abbreviations and Acronyms

Acb	nucleus accumbens
ACC	anterior cingulate cortex
ACh	acetylcholine
AChE	acetylcholine esterase
ADHD	attention deficit hyperactivity disorder
AP	anteroposterior
AAV	adeno-associated virus
bas	basal nucleus of Meynert;
Beta2-del	mice with deletion of β2 subunits of nAChRs
Beta2KO or β2-/-	global knock out for beta2 subunit of nAChRs
BLA	basolateral amygdala;
Cas9	CRISPR-associated protein 9
ChAT	choline acetyl transferase
Chrnb2	gene coding for the beta2 subunit of nicotinic acetylcholine receptors
CINs	cholinergic interneurons
CNS	central nervous system
cp	cerebral peduncle;
CPu	caudate-putamen
CRISPR	clustered regularly interspaced short palindromic repeats
Ctrl	control
DA	dopamine

DIG	digoxigenin
DR	dorsal raphe
Drd1	dopamine receptor D1
Drd2	dopamine receptor D2
DS	dorsal striatum
DV	dorsoventral
EC	entorhinal cortex
EPM	elevated plus maze
Ex5	exon 5
FBS	foetal bovine serum
FISH	fluorescent in situ hybridization
FS	fast-spiking
FST	forced swimming test
GABA	γ-aminobutyric acid
GABAINs	GABAergic interneurons
GP	globus pallidus
GPCRs	G-protein coupled receptors
Gpe	globus pallidus pars externa
GPi	globus pallidus pars interna
hdb	diagonal band;
ICj	Islands of Calleja
IF	immunofluorescence
IHC	immunohistochemistry
IL	infralimbic part of the mPFC

INs	interneurons
ip	intraperitoneal injection
IPN	interpeduncular nucleus
ko	knock out
LC	locus coeruleus
ldt	lateral dorsal tegmental nucleus;
LH	lateral hypothalamus
mAChRs	muscarinic acetylcholine receptors
ML	mediolateral
mPFC	medial PFC
ms	medial septal nucleus;
ms	mouse
MSNs	medium-sized spiny neurons
MT	medial terminal nucleus;
MWM	Morris water maze task
nAChRs	nicotinic acetylcholine receptors
NFS	non fast-spiking
NGS	normal goat serum
NOR	novel object recognition task
NPY	neuropeptide Y
NPY/scr	NPY-Cre-Cas9-GFP mice inject with AAV containing sg13 targeting chrnb2
NPY/sg13	NPY-Cre-Cas9-GFP mice inject with AAV containing scr
obj	object
OFC	orbitofrontal PFC

OT	olfactory tubercle
PBS	saline phosphate buffer
PFA	paraformaldehyde
PFC	prefrontal cortex
Pn	pontine nuclei
PPN	peduncolopontine nucleus
ppt	pedunculopontine nucleus;
PrL	prelimbic area of the PFC
Pvalb	parvalbumin
RT	room Temperature
S	nucleus accumbens shell
scr	scramble RNA
sg13	single guide RNA 13
si	substantia innominate;
SN	substantia nigra
SNc	substantia nigra pars compacta;
SNr	substantia nigra pars reticulata;
SSC	saline-sodium citrate buffer
SST	somatostatin
STN	subthalamic nucleus
TBS	PBS with 0.25% of Triton 100x
TST	tail suspension test
VAChT	vesicular acetylcholine transporter
vdb	vertical diagonal band;

VIP	vasoactive intestinal peptide
VTA	ventral tegmental area
wt	wild-type

I. Introduction

A. Acetylcholine

a) Definition and function

Acetylcholine (ACh) was the first neurotransmitter discovered, discovery for which Sir Henry Dale and Otto Loewi were awarded with the Nobel Prize in Physiology in 1936. Many efforts were spent in exploring the role of ACh as neurotransmitter of the postganglionic parasympathetic system, of the preganglionic neurons of the sympathetic system and in redefining its involvement in the regulation of many peripherical organs, such as the skin, the musculoskeletal, respiratory, cardiac, urinary, digestive, reproductive and immune systems (Beckmann & Lips, 2014). In the brain, ACh is a neurotransmitter involved in the regulation of a wide variety of higher-order cognitive processes including attention, motivation, memory, emotional processing and reward (Changeux et al., 2015; Joshua et al., 2017; Nees, 2015). All those mechanisms in the body that use ACh as principal molecule, thus expressing cholinergic receptors, and that can synthetize and release ACh are considered part of the cholinergic system (Beckmann & Lips, 2014).

b) Acetylcholine metabolism

ACh is formed by an acetylic group and choline. The acetylic group is synthesized in the mitochondria as Acetyl-Coenzyme A. The choline is synthesized in the liver by using the Serine backbone. At nerve terminals, the cytoplasmic choline is acetylated by the choline acetyl transferase (ChAT) and transformed in ACh (Figure I-2). ACh is stored and concentrated into synaptic vesicles, by the vesicular acetylcholine transporter (VAChT), ready to be released at the synaptic terminal upon functional stimulation. ACh can act through two different classes of receptors: muscarinic (mAChRs) and nicotinic (nAChRs) acetylcholine receptors, and these can be located pre- or post-synaptically. Finally, ACh is efficiently inactivated by cleavage into non-efficacious substrates, acetate and choline by the enzyme acetylcholinesterase (AChE).

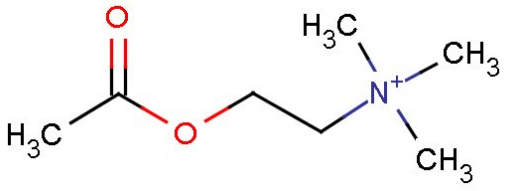

Figure I-1 Chemical structure of ACh – in red the carboxylic group is highlighted, while in blue is the quaternary ammonium cation.

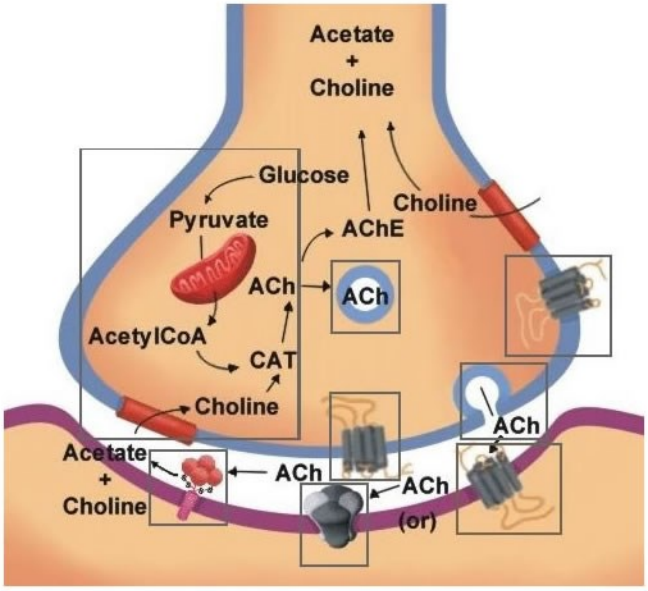

Figure I-2 Schematic representation of acetylcholine synthesis, storage and secretion, receptor interaction and termination. Contents © 1997-Present - McGovern Medical School at UTHealth

c) Acetylcholine as a neuromodulator

In the central nervous system (CNS), ACh acts on neural networks dynamics modifying and readapting neuronal excitability and presynaptic release of neurotransmitters in response to both internal and external inputs (Mineur & Picciotto, 2021; Picciotto et al., 2012). The diverse effects of ACh depend on site of release, types of receptor mediating the response, and the targeted neuronal population; however, in a simplistic view, it has been proposed that ACh potentiates adaptive behaviours and decreases responses to ongoing stimuli that do not require immediate action (Picciotto et al., 2012). For example, reward prediction results from the association of salient rewarding events with cues in the environment and it is mediated by an exactly precise firing regulation of the cholinergic interneurons in the striatum. Similarly, attention results from a finely regulated coordination of the excitation/inhibition tone promoted by cholinergic signalling acting on different adjacent neuronal types (activation of principal cortical neurons and contemporary decreased of the inhibitory tone exerted by interneurons) (Mineur & Picciotto, 2021; Bloem et al., 2014; Picciotto et al., 1995, 2012; Picciotto & Corrigall, 2002).

d) Acetylcholine receptors

ACh can act by stimulating two different kinds of receptors': muscarinic and nicotinic. mAChRs are metabotropic, G-protein coupled receptors (GPCRs), while nAChRs are ionotropic, fast-acting channels. There are five subtypes of mAChRs: M1 to M5. M1, M3 and M5 are excitatory because they are coupled to Gq proteins, activating phospholipase C and increasing intracellular Ca^{2+} levels, whereas the M2 and M4 subtypes signal through Gi/o, inhibiting adenylate cyclase and thus decreasing levels of cAMP. mAChRs play an important role in animal physiology, regulating heart rate, smooth muscle contraction, glandular secretion and many functions of the CNS (Groleau et al., 2015; Kruse et al., 2014). mAChRs are located both pre- and post-synaptically in the brain. Presynaptic M2/M4 mAChRs can act as inhibitory auto-receptors on cholinergic terminals reducing glutamate release from corticocortical and corticostriatal synapses, whereas M1/M5 receptors can stimulate, for example, dopamine (DA) release from striatal terminals and postsynaptic M1/M5 receptors can increase the excitability of cortical pyramidal neurons (Thiele, 2013).

e) Nicotinic acetylcholine receptors

The nAChRs are excitatory ligand-gated cation channels, formed by five transmembrane subunits, assembled around a central hydrophilic pore, selective for cations K^+, Na^+ and, mainly, Ca^{++}. nAChRs are highly conserved across species and represent the typical receptors of the skeletal neuromuscular junction. Given their abundant expression in Torpedo californica and Torpedo marmorata, many electrophysiology studies have been conducted on them, leading to the isolation of the receptor in its pentameric structure as early as 1970 (Changeux et al., 1970).

Nine α subunits (α2-α10) and three β subunits (β2-β4) are expressed in the mammalian brain, where they can assemble with different stoichiometry to form homomeric or heteromeric receptors (Dani & Bertrand, 2007; Hogg et al., 2003). The variety of possible combinations of the different subunits leads to the assembly of distinct types of nAChRs. The different subtypes of nAChRs vary in several structural properties, such as their permeability, affinity for substrates, kinetics, desensitization onset and, importantly, depending on their neuroanatomical localization (Gotti et al., 2006; Gotti & Clementi, 2004; Zoli et al., 2015). nAChRs exists in three conformational states: active-open, resting-closed and desensitized-closed. Upon binding of an agonist, the active conformation stabilizes, causing the pore to open and allow the subsequent influx of ions. Upon sustained binding of an antagonist, within an interval that may range from seconds to min, the receptor undergoes a

conformational change, stopping the influx of ions. Nicotine and ACh are nAChR agonists with a higher affinity for the receptor in its open state, whereas antagonists stabilize the desensitized or resting state. The X-ray crystallographic structure of the human α4β2 is presented. The receptor was resolved, at 3.9 Å resolution, by co-crystallization with nicotine (Morales-Perez et al., 2016). α4β2 are the most common heteromeric nAChRs in the brain and the main target of the present research. The homo-pentameric α7 receptors have five identical ACh-binding sites, one on each subunit, while hetero-pentameric receptors, like e.g. α4β2, has only two binding sites, located at the interface between α-β subunits by the location of the red spheres (Figure I-3 b).

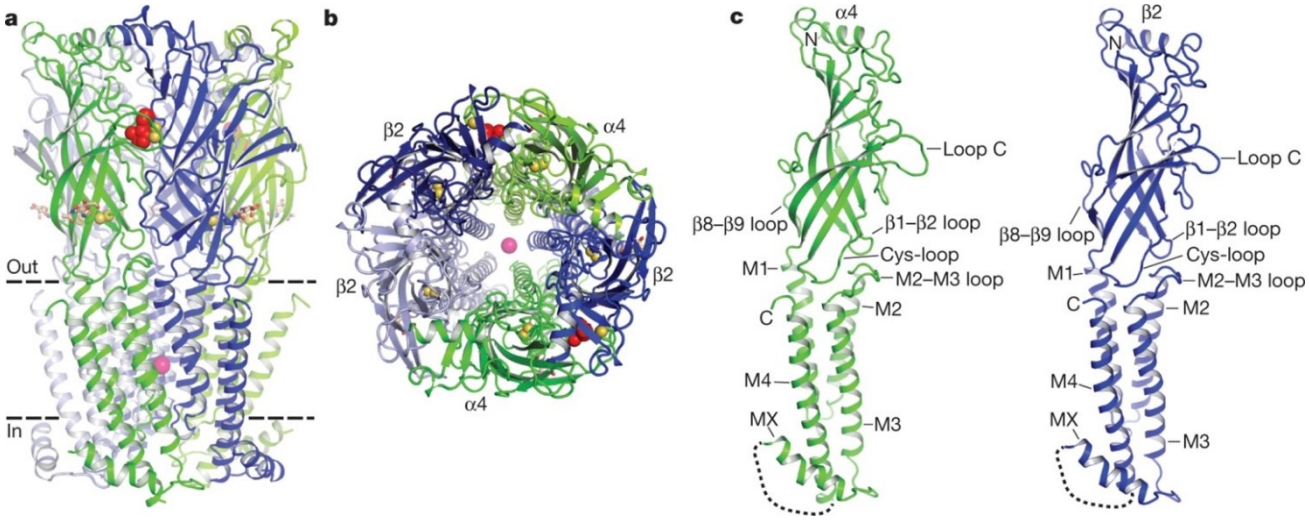

Figure I-3 X-ray crystallographic structure of the human α4β2 at 3.9 Å resolution, taken from (Morales-Perez et al., 2016). a) side view of the α4β2 receptor inserted in the plasma membrane (dashed lines). α4 subunits are in green and β2 in blue. Nicotine molecules are represented as red spheres at the binding sites at α-β junctions, while the pink sphere in the centre of the channel represents a sodium (Na^+) ion. b) perpendicular view from the extracellular side. c) single subunit unmerged from the full receptor structure shown in a).

Functional hetero-pentameric receptors usually comprise two α subunits carrying the principal component of the ACh-binding site (α2, α3, α4 or α6), two β subunits carrying the complementary component of the binding site (β2 or β4), and a fifth accessory subunit that does not participate in ACh binding (α5, β3, but also β2 or β4) (Dani & Bertrand, 2007; Levin, 2002; Sine, 2002; Soga et al., 2003; Wonnacott & Barik, 2007).

f) nAChRs distribution in the CNS

The most commonly represented nAChRs in the mammalian brain, are the homomeric α7 and the heteromeric α4β2* (the asterisk indicates that the accessory subunit can vary). α7 homo-pentameric receptors (red circles in Figure I-4) are widely expressed across the brain and particularly abundant

in the hippocampus, hypothalamus and cortex (Griguoli & Cherubini, 2012; Pohanka, 2012), where they can be pre-synaptic, facilitating the release of other neurotransmitters, like glutamate or GABA, or post-synaptic, mediating a fast synaptic transmission (Alkondon et al., 1999; Griguoli & Cherubini, 2012; Sinkus et al., 2015). Various combinations of α and β subunits can assembly to form hetero-pentameric nAChRs with distinct functions across the brain. α4β2 (green circles in Figure I-4) is the principal nAChR subtype in the cortex, striatum, superior colliculus, lateral geniculate nucleus and cerebellum (Gotti et al., 2006). β2 subunit, beside forming α4β2 receptors, is widely expressed across the brain, contributing to the formation of different types of nAChRs (Figure I-4, green lines).

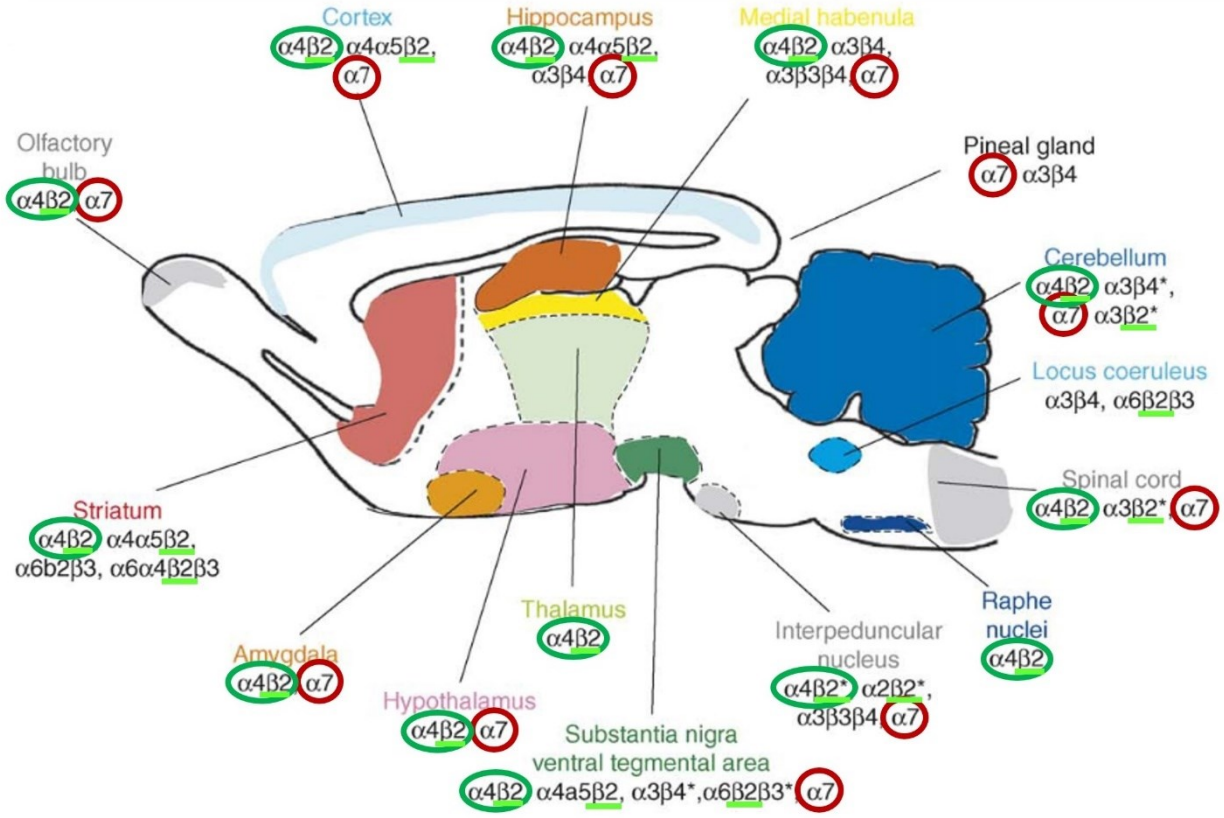

Figure I-4 Schematic representation of nAChRs expression across a sagittal section of a mouse brain, adapted from (Gotti et al., 2006). The red circles highlight α7 homomeric receptors expression in the different brain region represented, while the green circles remark α4β2 heteromeric receptors. In addition, the light green lines show the overall general expression of β2 subunits.

g) Animal model used to study nACHRs' functions

β2 global knock out

A combination of complementary technical approaches and the generation of knock out and knock in mice for specific nicotinic subunits allowed researchers to identify the subunit composition of the different subtypes of nAChRs (Picciotto et al., 1995, 1998, 2000; Picciotto & Corrigall, 2002; Zoli et

al., 2015). Of particular interest for the current thesis work is the β2 global knock out mouse model developed to investigate the functional role of the high-affinity, α-Bungarotoxin insensitive nAChRs (Gotti et al., 2006). In all the experimental mice utilised in the present work, we induced conditional knock outs of β2 nicotinic subunit to study its functional significance in individual regions and neuronal populations. Therefore, the previous findings related to the global knock out mice ($\beta2^{-/-}$) are highly pertinent to this work and the overview of these findings is presented below. The generation of the $\beta2^{-/-}$ line is described by Picciotto et al. (1995).

At first, various measurements in $\beta2^{-/-}$ mice, reported no differences in weight, mating and brain size. $\beta2^{-/-}$ mice exhibited normal motor functions and anxiety responses. No differences in goal-directed navigation and spatial orientation learning were detected by the cued and the classical version of the Morris water maze, respectively. Surprisingly though, $\beta2^{-/-}$ mice showed better performances in associative memory and a modified spatio-temporal organization of displacements, with increased navigation and decreased exploratory behaviour compared to wild-type mice (Maskos et al., 2005; Picciotto et al., 1995, 1998). These mice were characterised by a particular kind of hyperactive locomotion and an altered exploratory behaviour, with reported deficits in cognitive and social interaction tasks, only when they had to show flexible choices. Otherwise, their performances were normal, excluding any sort of anxiety-related behaviour (Avale et al., 2008; Besson et al., 2006, 2008; Bourgeois et al., 2012; Maskos et al., 2005; Picciotto et al., 2000; Serreau et al., 2011). This also applies to their performances in the light/dark task and in the elevated plus maze.

h) β2 global knock out and social behaviour

$\beta2^{-/-}$ mice exhibited impaired behaviour when offered a choice between conflicting motivations. They show an increased interest for social contact, especially when presented with the possibility of interaction with novel conspecific mouse. In particular, in $\beta2^{-/-}$ mice, Avale and colleagues (2011) showed increased c-Fos expression in neurons located in the prelimbic (PrL) area of the PFC when mice had an opportunity to interact with an unfamiliar mouse (Avale et al., 2011). Moreover, the authors GAdemonstrated that lesions of the PrL area in wild-type (wt) mice was sufficient to produce the same hyper-social phenotype observed in $\beta2^{-/-}$ mutants. The selective re-expression of β2-nAChRs in the PrL area of $\beta2^{-/-}$ mice restored the social interaction to normal levels. These findings

proved that the presence of nAChRs, formed by functional β2 subunits in PrL, is necessary for social interactions. Similarly, impairment of attentional performance has been related to the lack of β2-nAChRs in PrL, a deficit restored by the targeted re-expression of β2-receptors (Guillem et al., 2011).

B. The cholinergic pathways

In the peripherical nervous system, ACh is the main neurotransmitter at the neuromuscular junction, as well as a major effector of the autonomic system. In the central nervous system, there are four main cholinergic pathways, that differentiate by the localization of the nuclei containing the cell bodies of cholinergic neurons: 1. the **brainstem** pedunculopontine (ppt) and lateral dorsal tegmental (ldt) nuclei, innervating different cortical areas, hippocampus, basal amygdala, olfactory bulb (Figure I-5, green); 2. the **medial habenula** innervating the interpeduncular nuclei (Allaway & Machold, 2017; Mu et al., 2022); 3. the **striatum** (Figure I-5, blue) where cholinergic neurons serve as local interneurons (CINs); 4. the **basal forebrain** complex (Figure I-5, purple), including the nucleus basalis of Meynert (bas), the medial septal nucleus (ms), the nuclei of the vertical and horizontal limbs of the Diagonal Band of Broca (vdb and hdb), the substantia innominata (si), which collectively serve as the major sources of cholinergic projection neurons to neocortex, hippocampus, and amygdala (Ahmed et al., 2019; Li et al., 2017; Prado et al., 2017).

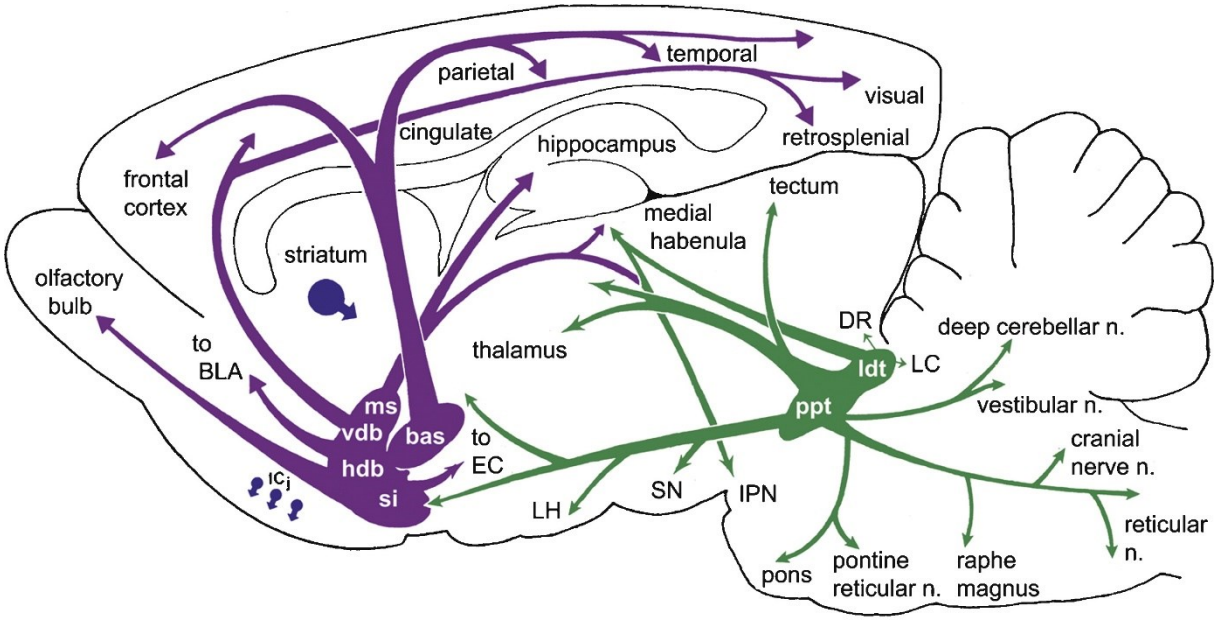

Figure I-5 Schematic representation of cholinergic pathways in the brain, taken from (Woolf & Butcher, 2011) BLA: baso-lateral amygdala; ICj: Islands of Calleja ms: medial septal nucleus; vdb: vertical limb of the Diagonal Band of Broca; hdb: horizontal limb of the Diagonal Band of Broca; si: substantia innominate; bas: basal nucleus of Meynert; EC: entorhinal

cortex; LH: lateral hypothalamus; SN: substantia nigra; IPN: interpeduncular nucleus; ppt: pedunculopontine nucleus; ldt: lateral dorsal tegmental nucleus; LC: locus coeruleus; DR: dorsal raphe.

C. Importance of nAChRs in brain functions

Because of their strategic location, ACh and cholinergic pathways have a prominent role in brain transmission and are essential for normal CNS functions, modulating cognitive, emotional, reward-related processes, attention and memory (King et al., 2003; Mineur et al., 2016a; Mineur & Picciotto, 2021; Picciotto et al., 2012b; Poorthuis & Mansvelder, 2013; Proulx et al., 2014; Rapanelli et al., 2017, 2018, 2023). The diversity of nAChR subtypes, with multiple possible combinations of subunits, together with the extent and the location of their expression at cellular and subcellular levels, plays a major role in the physiology and pathology of the nicotinic cholinergic system in the brain (Caton et al., 2020). For example, appropriate levels of ACh in the PFC are required to process relevant sensory information, for encoding environmental cues that drive goal-directed behaviour and for modulating functions related to conscious processing (Obermayer et al., 2019; Bloem et al., 2014; Luchicchi et al., 2014; Tian et al., 2011; Parikh et al., 2010; Ragozzino, 2000). Alterations in the expression of nAChRs formed by α7 subunits have been associated with the pathogenesis of dementia and psychosis through multiple mechanisms, while α5-containing nAChRs play an important role in schizophrenia (Caton et al., 2020; Benes & Berretta, 2003; Koukouli et al., 2017; Smucny & Tregellas, 2013). Abnormal expression of α4β2 nAChRs alters cholinergic neurotransmission, contributing to some aspects of the signalling failures reported in neuropsychiatric disorders, including autism spectrum disorders, nicotine addiction, and Parkinson disease (Lozovaya et al., 2018; Quik & Wonnacott, 2011; Vallés & Barrantes, 2021). Particularly studied is the role of α4β2* nAChRs in nicotine addiction due to their high affinity for both ACh and nicotine. Their systematic up-regulation found in smokers' brains has been related to the reinforcement properties of nicotine (Dajas-Bailador & Wonnacott, 2004; Maskos et al., 2005; Picciotto & Corrigall, 2002; Wonnacott, 1990, 1991; Wonnacott & Barik, 2007). Nevertheless, it is quite difficult to establish the specific contribution of nAChRs in these multifactorial disorders, where comorbidities, environmental and developmental factors, age-related brain-reshaping and genetics, result in a complex and overall unclear picture. A more causal example of the importance of β2 subunits of nAChRs, is represented by some gain-of-function mutations of its gene, CHRNB2, that result in a form of autosomal dominant nocturnal frontal lobe epilepsy (Schaaf, 2014). Since the mutations affect the transmembrane domains of β2-containing nAChRs, the kinetics of the ion pore

is altered resulting in an increased sensitivity to ACh or in a retardation in the desensitization of the receptor after its stimulation, causing partial epilepsies. These partial epilepsies are characterized by clustered attacks of brief motor seizures, mostly occurring during non–rapid eye movement sleep (Schaaf, 2014).

Nicotinic agonist drugs are currently approved and marketed for smoking cessation and in advanced clinical trials for depression, attention deficit hyperactivity disorder, schizophrenia, Alzheimer disease, and Parkinson disease (Schaaf, 2014). Despite the fundamental role of cholinergic signalling in the CNS, remarkably little is known about how ACh precisely modulates neural activity in different brain regions and the behaviours these circuits subserve (Luchicchi et al., 2014). Thus, there is a growing necessity for further and more integrative investigations to link receptor dynamics with circuit regulation.

D. The striatum

The striatum is the largest nucleus of the basal ganglia, controlling motor, procedural and reinforcement-based behaviours (Valjent & Gangarossa, 2021). Basal ganglia, is a group of subcortical nuclei responsible for the cognitive integration required for the regulation of motor control and learning, executive functions, emotions and behaviour (Lanciego et al., 2012). Basal ganglia refers in its strict sense to that structures that are sitting deep on the bottom of the telencephalon, the caudate-putamen nuclei of the striatum and the globus pallidus (GP). Then, basal ganglia related nuclei are the subthalamic nucleus (STN) in the diencephalon, the substantia nigra (SN) in the mesencephalon and the pedunculopontine nucleus (PPN) in the pons (Lanciego et al., 2012).

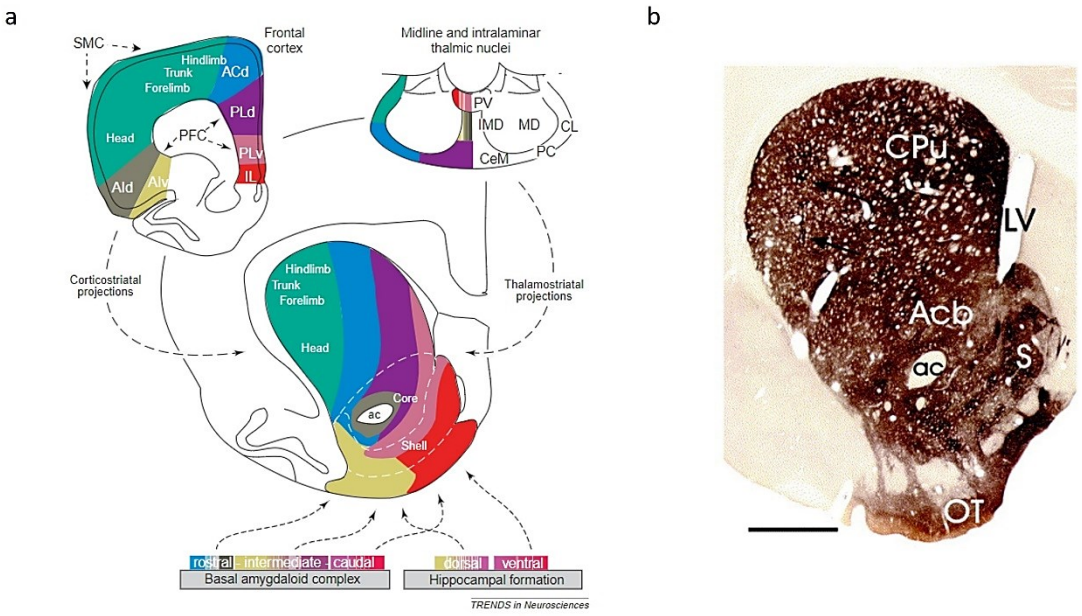

Figure I-6 Striatal anatomy and dorso-lateral-to-ventromedial functional striatal organization, adapted from Voorn et al., 2004. a, Scheme representing the topographically dorso-lateral-to-ventromedial striatal division, color-coded, on coronal sections cartoons. In the centre stands the striatum divided in colourful longitudinal oblique zones, while, on the sides, there are the striatal main afferents: the frontal cortex (upper left), midline and intralaminar thalamic nuclei (upper right), basal amygdaloid complex (lower left) and hippocampal formation (lower right). b, Coronal section of a rat striatum immunostained for dopamine. Arrows point at 'striosomes' structures. CPu: caudate–putamen complex; Acb: nucleus accumbens; S: nucleus accumbens shell; ac: anterior commissure; LV: lateral ventricle; OT: olfactory tubercle. Scale bar: 1 mm.

Neuroanatomical classification of the striatum distinguishes between the caudate nucleus and putamen (also indicated as caudate-putamen complex in mice, CPu, in Figure I-6 b) forming the dorsal striatum and nucleus accumbens (Acb) with the olfactory tubercle (OT), composing the ventral striatum. More recent classifications promote a dorso-lateral-to-ventromedial functional division, taking into account the specific connectivity with different striatal input regions. For example, with regard to cognitive functions, a distinction between dorsolateral, dorsomedial and ventral striatum is highly relevant (Voorn et al., 2004). The dorsolateral striatum mediates procedural or stimulus–response learning, whereas the dorsomedial striatum is involved in goal-directed and spatial learning (Barbera et al., 2016; Voorn et al., 2004). The main excitatory striatal afferent projections coming from the PFC and thalamus (Figure I-6 a, upper left and right, respectively), but also amygdala and hippocampus (Figure I-6 a, lower left and right, respectively), are strictly topographically organised. The dorsolateral striatum receives sensorimotor information (Figure I-6 b, green), the ventromedial striatum receives visceral afferents (Figure I-6 b, red and pink), and striatal areas lying between these extremes receive higher order 'associational' information (Figure I-6 b, blue and purple) (Voorn et al., 2004).

About 95% of the striatal neural population are GABAergic projection neurons, medium-sized spiny neurons (MSNs), while the remaining 5% consists of several classes of interneurons (Calabresi et al., 2014; Gerfen & Bolam, 2010). The striatal GABAergic MSNs can be divided into two types, based on their axonal projections, on their co-transmitter and on the type of dopaminergic receptors they express. Specifically, MSNs signalling with substance P and dynorphin and expressing D1 dopamine receptors (Drd1) form a direct striato-nigral pathway, while those signalling with enkephalin and expressing D2 dopamine receptors (Drd2) contribute to an indirect striato-pallidal pathway. Integration of the two pathways is needed for control of movement and actions (Economo et al., 2018; Calabresi et al., 2014; Macpherson et al., 2014; Morita, 2014; Gerfen & Surmeier, 2011). The striatum receives cortical and thalamic inputs that processes via the direct (Figure C 2, red) or indirect (Figure C 2, blue) pathway. While the former projects directly to the globus pallidus pars interna (GPi) and substantia nigra pars reticulata (SNr), the latter reaches the globus pallidus pars externa (GPe) first, and then signals to the STN which indirectly connects with GPi and SNr. GPi and SNr are the two main basal ganglia output centres. In the striatum, local circuits are modulated by several neurotransmitters including DA, ACh and GABA (Abudukeyoumu et al., 2018). DA is released in the dorsal striatum by neurons from the substantia nigra pars compacta (SNc), and in the Acb by neurons from ventral tegmental area (VTA). ACh and GABA are predominantly released by local striatal interneurons. However, a minor portion of striatal ACh derives from projections of the pedunculopontine and laterodorsal tegmental nuclei of the brainstem (Dautan et al., 2014). Striatal interneurons represent a minority (less than 5 % in rodents) (Muñoz-Manchado et al., 2016), but they seem to play a key role in controlling striatal microcircuits and striatal-dependent behaviours (Goral et al., 2022; Kaminer et al., 2019; Laforet et al., 2001; Martiros et al., 2018; Martos et al., 2017; Rapanelli et al., 2017).

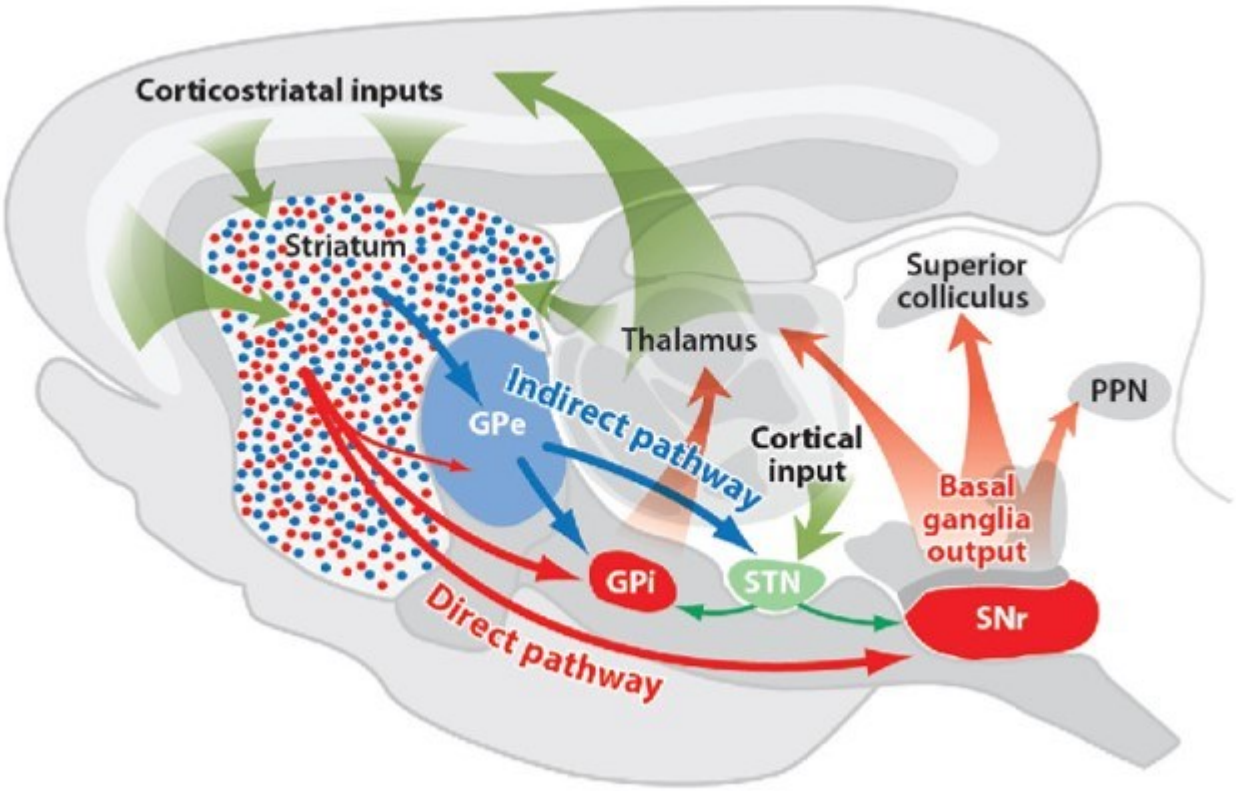

Figure I-7 Schematic representation of basal ganglia circuits on rat sagittal section, adapted from Gerfen & Surmeier (2011). The direct pathway (red), the indirect pathway (blue). GPi: globus pallidus pars interna; SNr: substantia nigra pars reticulata; GPe: globus pallidus pars externa; STN: subthalamic nucleus; PPN: pedunculopontine nucleus.

a) Striatal interneurons

Striatal cholinergic interneurons (CINs) possess rich axonal branching and tonic activity which enables them to extensively control striatal microcircuits despite their small number (Howe et al., 2019; Mallet et al., 2019; Mao et al., 2019). Cholinergic signalling in the striatum is possible through a variety of ACh receptors, expressed both by striatal neurons and striatal nerve terminals originating in other brain regions. Striatal MSNs express M1 and M4 mAChRs, while M2/M4 mAChRs are expressed both by projection terminals and different types of striatal interneurons including CINs (Bernard et al., 1992, 1998, 1999; Smiley et al., 1999). In addition, nAChRs with various subunit compositions are commonly expressed by striatal nerve terminals (see Figure I-4), while striatal neurons primarily express β2-containing nAChRs (Tanimura et al., 2019). Several types of GABAergic interneurons (GABAINs), have been identified in the striatum. Generally, they can be distinguished by their immunohistochemical and electrophysiological properties (Assous et al., 2018a; Muñoz-Manchado et al., 2016, 2018). Besides the more classical groups of parvalbumin-, somatostatin- and calretinin-expressing neurons, striatal GABAINs account for at least six distinct neuronal populations,

with some of them responsive to nicotinic stimulation, possibly via nAChRs (English et al. 2011). For instance, somatostatin-expressing (SST^+), 5HT3A-expressing and neuropeptide Y-expressing (NPY^+) GABAINs are activated by nicotine and this activation leads to an inhibition of MSNs activity (Assous et al., 2018a; English et al., 2012; Faust et al., 2016). While MSNs are considered not to express nAChRs (Luo et al. 2013; Maryka Quik et al. 2007), it seems that distinct GABAIN populations in the striatum can express different types of nAChRs. For example, it has been reported in tyrosine hydroxylase-expressing GABAINs, a distinctive expression of α3 nicotinic subunit. Unfortunately β2 subunit expression was not specifically described in the same study by (Muñoz-Manchado et al., 2018). Even though nAChRs are expressed by a relatively small number of striatal neurons, these receptors seem to have the ability to modulate striatal signalling and activity. Nonetheless, it remains unknown if this physiological effect can be translated into behaviour, a question that we will explore in this thesis.

E. The prefrontal cortex

The PFC is the most elaborated neocortical region in primates, where it accounts for their behavioural flexibility and diversity. As previously discussed, the PFC is connected in a topographically specific manner to basal ganglia circuits, to coordinate a wide range of neural processes (Miller & Cohen, 2001). The PFC is a region of the cerebral cortex that covers the anterior part of the frontal lobe, formed by interconnected neocortical areas, and that sends and receives projections from virtually all cortical sensory and higher-order association areas, motor systems, and subcortical structures associated with cognition, memory, and emotions (Haber & Robbins, 2022; Yang et al., 2021; Bedwell et al., 2014; Riga et al., 2014). Multiple studies have shown that the PFC plays an important role in cognitive processes such as attention (Opris & Casanova, 2014; Miller & Cohen, 2001; Ragozzino, 2000), memory and decision-making (Shadlen & Shohamy, 2016; Laroche et al., 2000), working memory (Riaz et al., 2019; Funahashi, 2015), social behaviour (Avale et al., 2011), emotions (Miller & Cohen, 2001) and personality (Kennis et al., 2013; Montag & Reuter, 2014; Valk et al., 2020). Attention and PFC-related behaviours are affected in many neuropsychiatric disorders, including schizophrenia, attention deficit hyperactivity disorder (ADHD), addiction, depression and autism, all of which are characterized by reduced activity in the prefrontal areas (Poorthuis & Mansvelder, 2013). A univocal integrated definition of which cortical areas correspond to the primates' PFC in rodents is still missing (Laubach et al., 2018). Electrophysiological studies and investigations into

foraging behaviour recognised a functional and anatomical correlate of the rat medial PFC (mPFC) with elements of the primate anterior cingulate cortex (ACC), orbitofrontal (OFC) and dorsolateral PFC, at a rudimentary level, mostly because of the limited size of the rodent brain (Kolk & Rakic, 2022; Rudebeck& Izquierdo, 2022; Seamans et al., 2008). The rodent mPFC is an anatomically and functionally heterogeneous structure consisting of the PrL and infralimbic (IL) cortices, which have largely distinct projection patterns to the Acb, thalamus, amygdala and hippocampus in order to monitor changing environmental contexts and respond with the most contextually appropriate behaviour by tuning cortical efferent projections (Riaz et al., 2019) in a top-down fashion. The rat PrL cortex is crucially involved in executive functions, making this region functionally homologous to the dorsolateral PFC in humans and other primates (Uylings et al., 2003). Like other cortical areas, the PFC is organized into layers and columns characterized by distinct connectivity but the rodent PFC lacks layer IV (Guillem et al., 2011; Poorthuis, Bloem, Schak, et al., 2013). Besides the classical concept of cortical lamination as an anatomical descriptor of the distribution of excitatory neurons and the definition of layer and cell type specificity are important characteristics to consider for neuronal excitability and synaptic activity mediated by neuromodulatory transmitters (Radnikow & Feldmeyer, 2018). Between these neuromodulators, cholinergic afferents are distributed at very high density throughout all layers of the neocortex, with particularly high axonal bouton densities in layers VI, V and I, mediating both tonic and phasic cholinergic signalling in the mPFC (Parikh et al., 2010; Poorthuis, Bloem, Verhoog, et al., 2013; Radnikow & Feldmeyer, 2018). It is unclear whether ACh functions through volume or synaptic transmission (Bloem et al., 2014; Parikh et al., 2010; Poorthuis, Bloem, Schak, et al., 2013; Poorthuis, Bloem, Verhoog, et al., 2013).

a) β2 in the PFC

nAChRs distribution in rodents and primate brains is quite similar (Gotti et al., 2006b; Zoli et al., 2015b). The PFC receives significant cholinergic innervation, and ACh signalling through nAChRs is crucial for the regulation of cognitive processes (Bloem et al., 2014). In parallel with receiving basal forebrain cholinergic projections, the mPFC itself projects to the basal forebrain, in a loop essential for attention performance and strictly dependent on functional nAChRs (Guillem et al., 2011). Nicotinic receptors in the PFC are expressed in a layer-specific manner (Poorthuis, Bloem, Verhoog, et al., 2013).

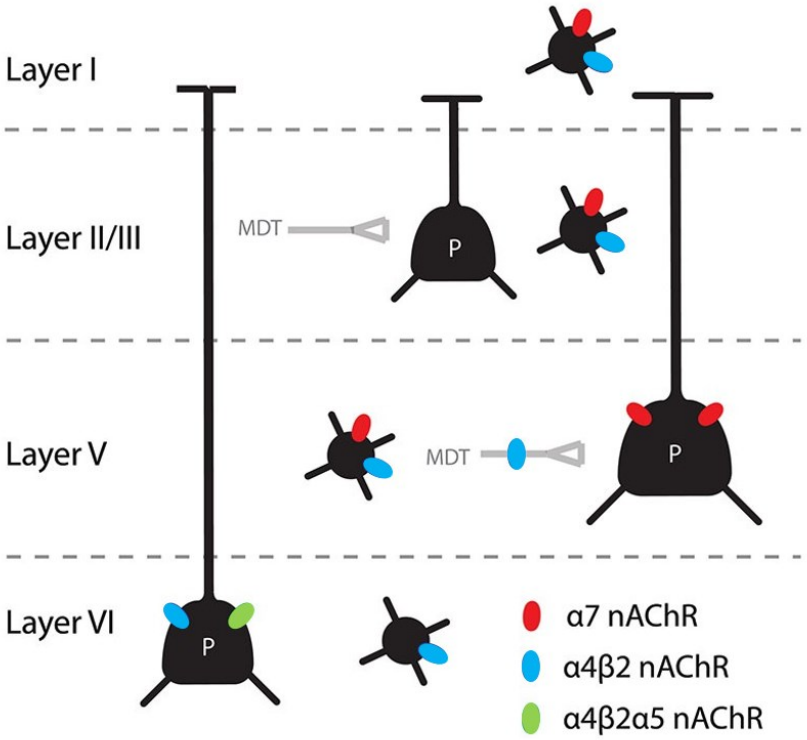

Figure I-8 Layer-specific modulation of the mouse PFC by nAChRs. While pyramidal cells (P) in layer V and VI are directly modulated through α7 and β2* nAChRs, respectively, interneurons of all layers (I, II/III, V) express β2-nAChRs. Adapted from (Bloem et al., 2014). MDT: thalamic input.

In the superficial layers I, II/III, only interneurons are activated by ACh via nAChRs, which can be α7 and α4β2 types (

Figure I-8). Glutamatergic inputs to layer V and local pyramidal neurons present α4β2 or α7, respectively, while pyramidal neurons in layer VI are modulated by α4β2 and α4β2α5 nAChRs. Interneurons across all layers contain mixed combinations of nAChRs although the distribution of homomeric and heteromeric receptors varies for different interneuron types and the different layers (Bloem et al., 2014; Poorthuis, Bloem, Schak, et al., 2013; Poorthuis, Bloem, Verhoog, et al., 2013).

It was shown that stimulation of basal forebrain fibres in layer I interneurons results in α7- mediated synaptic transmission, while activation of non-α7 receptors is triggered by volume transmission (Arroyo et al., 2012). Most likely both tonic and phasic release are possible, as well as both volume and synaptic transmission, making the precise release parameters crucial for determining the effects on the mPFC (Parikh et al., 2007). Furthermore, it has been shown that both point-to-point and tonic nicotinic transmission occur in the neocortex, depending on the regime of basal forebrain neurons. Low-frequency optogenetic stimulation results in point-to-point nicotinic transmission occurring synaptically via heteromeric receptors composed of α4, α5, and β2 subunits, whereas high-frequency

stimulation leads to a switch to tonic responses and the recruitment of extra synaptic receptors (Hay et al., 2016).

b) Interneurons in the PFC

INs are a subgroup of inhibitory neurons that keep neuronal timing, synchronicity and activity by generating inhibitory inputs over other neurons to modulate functions at the circuit and behaviour levels (Rapanelli et al., 2017). GABAergic interneurons in the mPFC play an important role in regulating working memory, decision-making and emotion associated with motivational and aversive behaviours (Poorthuis, Bloem, Schak, et al., 2013; Poorthuis & Mansvelder, 2013; Sun et al., 2017). There are different classifications of GABAergic interneurons in the mPFC. One can include parvalbumin-expressing ($Pvalb^+$), somatostatin-expressing (SST^+) and vasoactive intestinal peptide-expressing (VIP^+) interneurons (Krabbe et al., 2019; Obermayer et al., 2019), or another can distinguish between $Pvalb^+$, SST^+ and expressing the serotoninergic receptor 5HT3aR (Tremblay et al., 2016). Particularly interesting for us is the classification established by the Mansvelder's group, which distinguished between fast-spiking (FS) and non-fast-spiking (NFS) cells, including SST^+ cells, as a subgroup of NFS cells. They found that similarly to the FS neurons in layer V, half of the FS cells in layer II/III contain α7-nAChRs too. At the same time, all the NPS/SST^+ cells in layers II/III and V, expressed mainly β2-containing nAChRs. In particular, in layer II/III, β2*-nAChRs were exclusively expressed by interneurons. Altogether these findings show that nAChRs play an important role in modulating feedback inhibition among pyramidal neurons in cortical layers. They also confirmed that, in the PFC, distinct populations of neurons are activated by nAChR stimulation in a layer-specific manner (Poorthuis, Bloem, Verhoog, et al., 2013).

F. Genetic approaches for studying β2-mediated control of behaviour

Brain shape and functions result from a perfectly orchestrated structural organization regulated at a molecular level by signals integration into local circuits. Different brain regions are responsible for the control of particular aspects of specific behaviours. To understand the role of the neural transmission exerted via β2-containing nAChRs in the control of behaviour, we need appropriate genetic tools to delete the receptors in a more or less specific manner. In the present work, we

induced deletion of β2-expressing nAChRs in adult mice to observe behavioural changes associated with the deletion. We utilized two distinct genetic approaches for inducing deletion of β2-nAChRs: Cre-Lox recombination and CRISPR-Cas9 system.

Cre-Lox recombination is a site-specific recombinase technology, that uses the Cre enzyme and LoxP sequences derived from bacteriophage P1 to allow targeted DNA modification to a specific cell type. The system consists of a single enzyme, the Cre recombinase, that recombines a pair of short target sequences called the Lox sequences, and in our case, deletes the genomic part included between the two Lox sites resulting in a defective product that cannot assembly and therefore is not functional (Kim et al., 2018; McLellan et al., 2017).

CRISPR-Cas9 technology is another method for gene editing derived from Streptococcus pyogenes, developed by Emmanuelle Charpentier and Jennifer Doudna who got awarded the Nobel Prize in Chemistry in 2020 (Ledford & Callaway, 2020). CRISPR is the acronym for clustered regularly interspaced short palindromic repeats and consists of DNA sequences found in the genomes of prokaryotes as mechanisms of acquired immunity. After a first infection by a bacteriophage, some DNA fragments of phage, the CRISPR, are stored within the prokaryote genome, to recognise, detect and destroy similar bacteriophages DNA in case of subsequent infections. Cas9 (or "CRISPR-associated protein 9") is an enzyme that uses CRISPR sequences as a guide to recognize and cleave specific strands of DNA that are complementary to the CRISPR sequence (Adli, 2018; Moon et al., 2019; Pickar-Oliver & Gersbach, 2019; Redman et al., 2016). Jennifer Doudna and Emmanuelle Charpentier re-engineered the CRISPR/Cas9 endonuclease system into a more manageable two-component tool. It uses a synthetic "single-guide RNA" that consists of specific targeting sequence and a scaffold sequence to combine with Cas9, to find and cut the DNA target. In the present work, we used a mouse line with conditional cre-dependent expression of Cas9 as well as previously validated sequences of guide RNA (Peng et al., 2019) to target and delete β2-nAChRs.

General aims

Cholinergic regulation is complex, and every region in the brain follows different rules, dynamics and hierarchy. In the recent years, many research have pointed out not only the involvement of cholinergic system in the insurgence of developmental, psychiatric and age-related diseases but also how the diversification of the nicotinic receptors expression by different cell populations has a specific functional and pathological relevance. It is, therefore, crucial to understand how local circuits are formed and how the interplay between principal neurons and interneurons can finely modulate behaviour, adaptation and cognition.

Hypothesis

We hypothesised that disruption of cholinergic signalling by the deletion of β2-containing nAChRs in specific neuronal types will lead to behavioural changes, even if the deletion is selective and affects only a relatively small neuronal population.

Objectives of the thesis

To address our hypothesis, we have set these objectives:

1. For the striatum

    a. Identification of striatal neurons expressing β2-containing nAChRs.
    b. Behavioural role of β2-containing nAChRs expressed by neurons in the dorsal striatum.
    c. Evaluation of changes in neuronal activity measured by c-Fos expression.

2. For the PFC

    a. Use of CRISPR/Cas9 technology for β2 knock down in specific cellular types.
    b. Behavioural role of β2-containing nAChRs expressed by NPY neurons in the PFC.

II. Materials and methods

A. Animal models

All experimental procedures were approved by the Czech Central Commission for Animal Welfare as compliant with the directive of the European Community Council on the use of laboratory animals (2010/63/EU). Mice housing conditions provided free access to standard rodent chow and water ad libitum, controlled temperature and humidity, with a 12 hour light/dark alternation cycle (lights on from 6 a.m. to 6 p.m., local time). Mice were housed in groups of a maximum of five mice per cage but after the stereotaxic surgery they were separated into individual cages if they started to attack each other. To diminish any cage/litter effect, mice from the same cage were always included in both control and mutant groups whenever possible.

From now on, for simplicity in reporting the data in graphs and legends, I will note the β2 subunit in full characters as Beta2, especially when denoting genetically modified mouse strains or RNA transcripts of *chrnb2* gene. It is kept as β2 when explicitly referring to β2-nAChRs.

The two main mouse lines used within the project are described below. Additional mice used as controls for some experiments (wild-type mice or $\beta2^{-/-}$) or as breeders (mice expressing Cas9-GFP in the Cre dependent manner) are also mentioned shortly.

a) Beta2-flox/flox mice

The generation of Beta2-flox/flox mice is described by Burbridge et al. (2014). The schematic for the flox/flox insertion flanking the exon 5 (Ex5) of *chrnb2* (Figure II-1 a), together with the suggested primers for genotyping (Figure II-1 b).

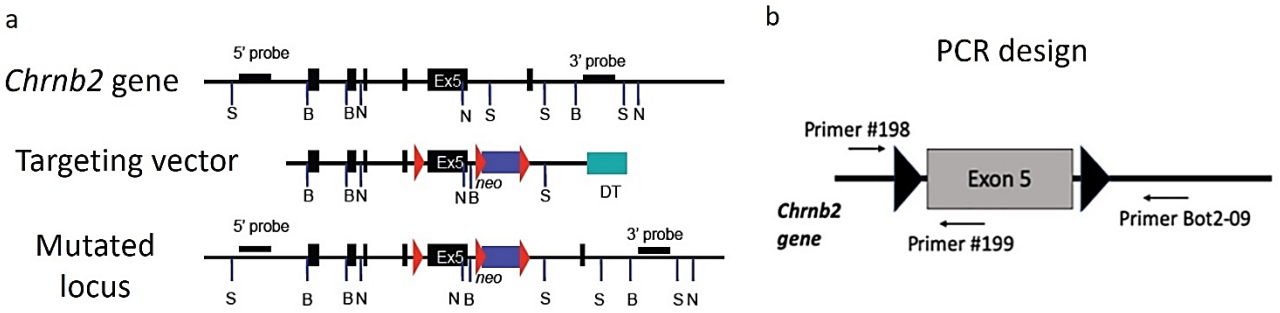

Figure II-1 Generation of Beta2-flox/flox mice - a, scheme for the flox/flox insertion flanking the exon 5 (Ex5) of Chrnb2 gene. Floxed sites are indicated by red arrowhead, adapted from Burbridge et al. (2014)s. b, scheme of the PCR design with the suggested primers for genotyping from Burbridge et al. (2014). Sequences: Primer #198 CAGGCGTTATCCACAAAGACAGA, Primer #199 TTGAGGGGAGCAGAACAGAATC, and Primer Bot2-09 ACTTGGGTTTGGGCGTGTTGAG.

The original Beta2-flox/flox breeding pairs were kindly provided by Prof. Michael Crair from Yale University (USA). Mice were maintained as homozygous on a mixed background for ten generations. The age range of mice used for behaviour was between 2 and 8 months, as indicated in details in Figure II-7.

Beta2-flox/flox male mice of 8 weeks underwent stereotaxic surgeries injecting the Cre-recombinase (packed in a AAV-viral vector) into the dorsal striatum . After 3 weeks, the maximal expression of the viral vector occurs and the local deletion of β2-nAChRs is in place, so the conditional-knock out model is ready to be tested (*Figure II-2*).

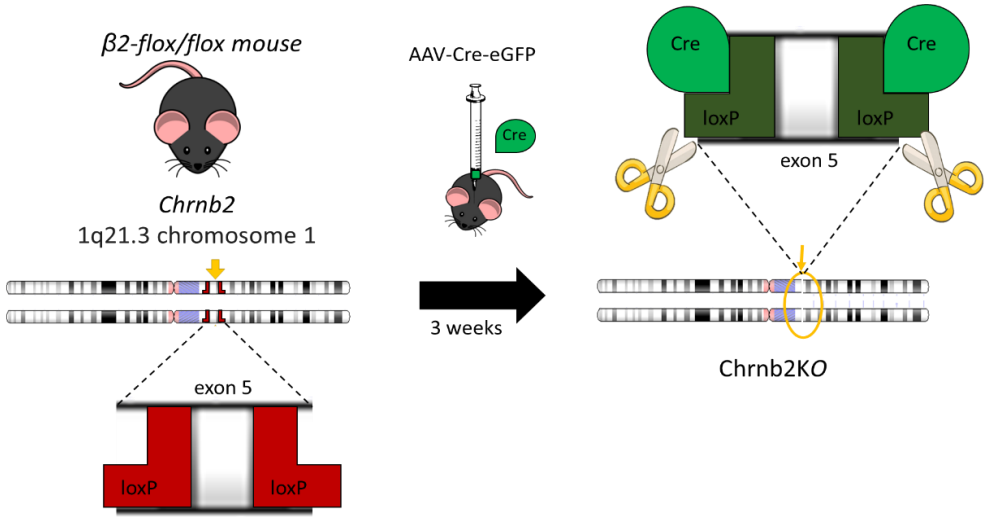

Figure II-2 Schematic illustration of the experimental approach used for the deletion of β2-nAChRs – When Beta2-flox/flox mice reached 2 months of age, they were injected in dorsal striatum with a virus with (Beta2-del, see the text) or without (ctrl) Cre recombinase (AAV-Cre-eGFP). After 3 weeks, the

maximal level of viral expression allows for the deletion of β2-nAChRs in all the transfected cells, resulting in Chrnb2KO.

For the fluorescence *in situ* hybridization (FISH) experiments characterizing β2-nAChRs expression in the striatum,C57BL/6J wild type male mice were used.

b) NPY/Cas9 mice

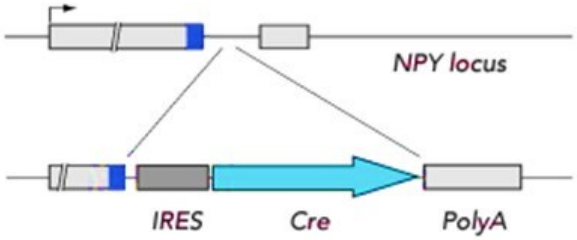

Figure II-3 Scheme of the generation of the NPY-IRES-Cre knock in mouse line by Zemelman's lab. The illustration by Milstein et al. (2015) shows the insertion of IRES (grey block) and Cre recombinase (turquoise arrow) within the NPY locus.

Mice with Cre recombinase inserted in the locus for NPY (Figure II-3) and therefore expressing Cre under the control of promoter for NPY (NPY-IRES-Cre mice) were purchased from The Jackson Laboratory (JAX#027851, B6.Cg-Npytm1(cre)Zman/J) and developed by Milstein et al. (2015). NPY-IRES-Cre mice were crossed with Rosa26-floxed STOP-Cas9 knock in (JAX#026175, B6J.129(B6N)-Gt(ROSA)26Sortm1(CAG-cas9*,-EGFP)Fezh/J, also purchased from Jackson Laboratory and developed by Platt et al. (2014). This mouse line is characterised by a Cre recombinase-dependent expression of CRISPR-associated protein 9 (Cas9) endonuclease and EGFP, directed by a CAG promoter (Figure II-4). Both strains were maintained on a C57BL/6 background.

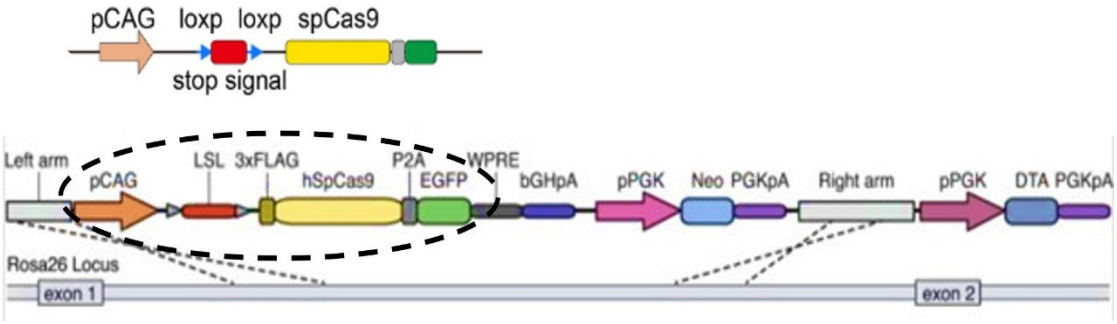

Figure II-4 Scheme illustrating the Rosa26-floxed STOP-Cas9 knock in, adapted from Platt et al., (2014). The black dashed line points out the sequence on the Rosa26 locus explicated above. After the CAG promoter sequence (orange arrow),

there are the 2 loxp sites (blue arrowheads) flanking the stop codon (red block) that precedes the Cas9 (yellow block) and EGFP (green) domains.

Crossing these two lines generated mice with Cas9-GFP expression limited to the cells that at some point during lifetime exhibited NPY expression. In order to achieve CRISPR-induced knock down of β2 nicotinic subunit in NPY-expressing cells, the mice had to be injected with a viral vector expressing sgRNA against *chrnb2* gene. Therefore, the NPY-Cre-Cas9-GFP mice were injected in the PFC with AAV vector expressing sgRNA targeting a sequence inside the *chrnb2* gene and a fluorescent marker, mCherry. The expression plasmid #87916 was prepared by Prof. Hewitt's lab and obtained from Addgene (Hung et al., 2016). From now on I will refer to NPY-Cre-Cas9-GFP line as NPY/Cas9 and to NPY/Cas9 injected with the virus containing the sg13, as NPY/sg13 (Figure II-5). For controls, we used NPY/Cas9 mice injected with AAV vector expressing scrambled sgRNA, to control for the impact of the stereotaxic surgery and the viral toxicity per se. I will refer to the control mice as NPY/scr. Thanks to the concomitant expression of a GFP tag with the Cas9, I could check for the fidelity of the Cas9 expression driven by NPY promoter in the NPY/Cas9 mice.

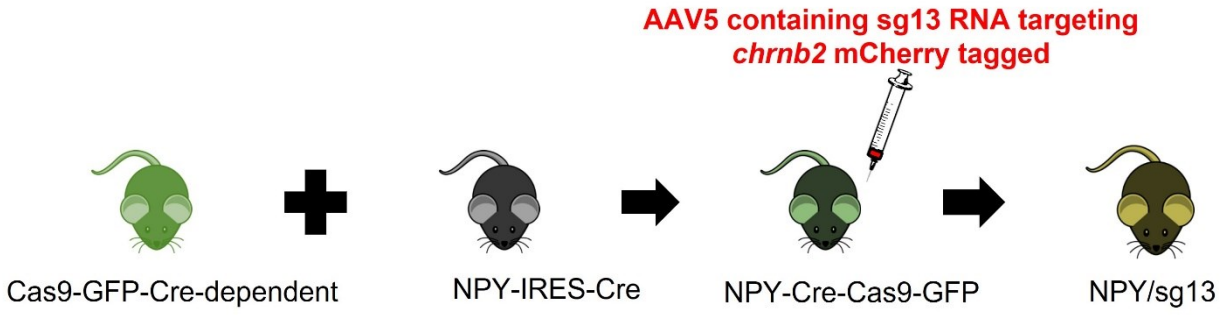

Figure II-5 Schematic representation of the mouse lines crossed to obtain the NPY-Cre-Cas9-GFP litters for viral injection with the virus containing the sg13 for the selective deletion of *chrnb2*.

c) Stereotaxic surgeries

Mice were injected when they reached 5 weeks of age. A deep level of anaesthesia was achieved, through the injection of a mixture of ketamine and xylazine (10 mg/kg and 1,3 mg/kg respectively; Vetoquinol). The head of the mouse was fixed in the stereotaxic frame (Stoelting Co.) and virus was injected bilaterally with 1000 nL of virus in total per hemisphere, administered in two different points per each hemisphere by MICRO2T-UMP3-NL2010 microinjections pump (WPI) with a infusion rate of 50 nL/min. To make sure each animal was injected in both hemispheres and to increase the striatal area expressing viral vector, mice were injected in two different point in each hemisphere. The

stereotaxic coordinates were determined according to *labs.gaidi.ca/mouse-brain-atlas*, an interactive mouse brain atlas available online that can simulate the position of selected coordinates.

d) Targeting the dorsal striatum

Beta2-flox/flox mice were injected in the dorsal striatum following the coordinates (in mm): anteroposterior (AP) 1.5; mediolateral (ML) 1.4; dorsoventral (DV) 3.0 and AP 1.3; ML 1.6; DV 3.3. AAV5-Cre-GFP (viral titre 4.5 x 10^12 vg/ml; UNC Vector Core) virus was injected to generate mutants, or AAV5-eGFP for control mice.

e) Targeting the PFC

NPY-Cre/Cas9-GFP were injected in the PFC, bilaterally, with 500nL of the virus per injection site, following the coordinates: AP 2.5; ML 0.4; DV 1.9 and AP 2.2; ML 0.3; DV 2.1. with AAV5-sg13RNA-mCherry (viral titre 4.5 x 10^12 vg/ml; UNC Vector Core) to generate mutants, or AAV5-scrRNA-mCherry for controls, at 50 nL/min.

f) Plasmid structure and cloning of the guide RNA mCherry

We referred to the work developed and published by Hung et al. (2016) and Swiech et al. (2015) for the production of the plasmid to pack in the viral vector to inject in NPY/Cas9 mice. We obtained the plasmid carrying an insertion cassette for the guide RNA (Figure II-6) and mCherry sequence and we cloned inside it the guide 13 sequence (g13 ATCAGCTTGTTATAGCGGG) taken from Peng et al. 2019), via SacI restriction site. After bacteria transformation and isolation of the successful clones, we sequenced the construct to verify the correct insertion of the sgRNA sequence and we shipped it to the UNC Vector Core to packaging into an AAV5 vector. The same procedure was used for creating the control vector expressing scramble sgRNA.

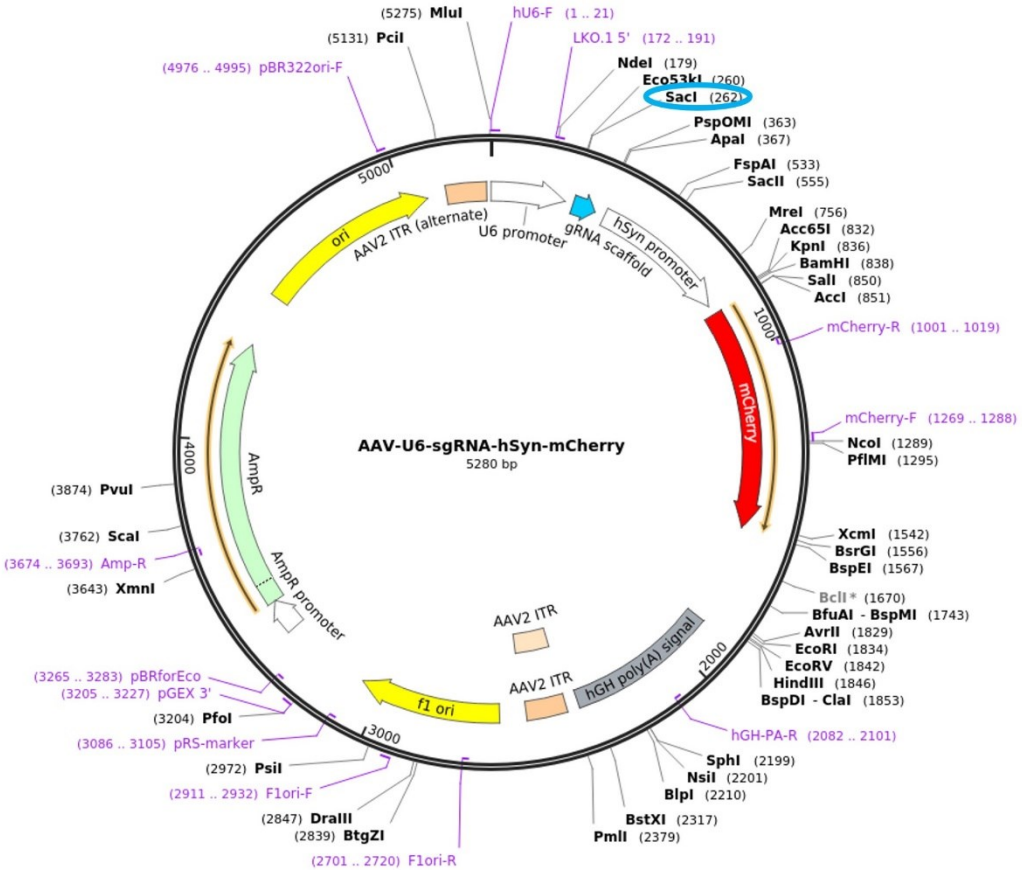

Figure II-6 Schematic structure of the plasmid used for virus preparation, from Addgene #87916, by Hung et al., (2016). In light blue the position of the gRNA scaffold cassette (arrow), and the SacI restriction site (circled) are indicated, followed by the promoter and the mCherry sequence in red.

B. Behavioural testing

a) Beta2-flox/flox mice cohort preparation

I have performed the stereotaxic surgeries to prepare all the cohorts, 1 to 4. I have run the presented behavioural tasks for cohorts 1 and 2, and when possible, for cohorts 3 and 4, otherwise tested by bachelor and master students in the lab, supervised by Dr Helena Janickova.

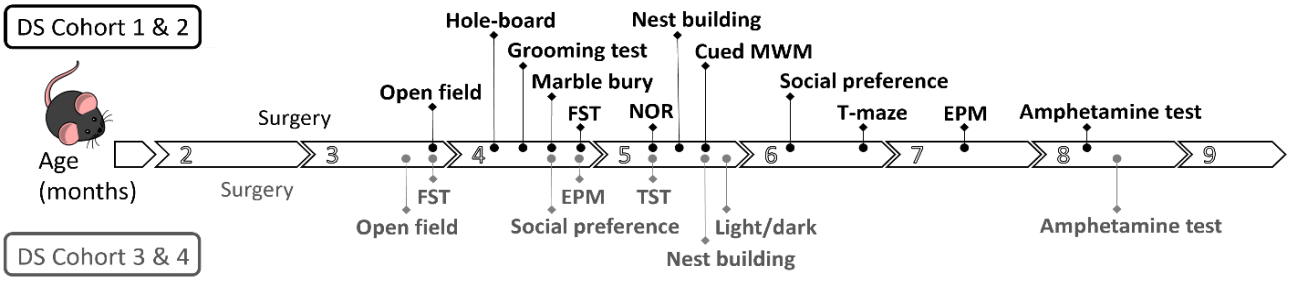

Figure II-7 *Timeline showing the order of the tasks followed in the different cohorts of animals – cohort 1 & 2 underwent Open Field, Hole-Board, Grooming test, Marble bury, Forced swimming test (FST), Novel object recognition (NOR), Nest building, Cued Morris Water Maze (MWM), Social preference, T-maze, Elevated plus maze (EPM), Amphetamine test; while cohort 3 & 4, Open Field, FST, Social preference, EPM, Tail suspension test (TST), Nest building, Light/dark, Amphetamine test. Cohort 1 & 2, 16 controls and 16 Beta2-mutants; cohort 3 & 4, 13 and 16 respectively.* DS indicates mice were injected with the virus into the dorsal striatum.

Mice were tested in 4 separate cohorts for the behavioural characterization and the data from the individual cohorts were merged. The cohorts that underwent exactly the same testing are grouped together in Figure II-7. Therefore, Cohorts 1 & 2 were used for an initial broader behavioural characterisation, while Cohorts 3 & 4 were added later on, focusing mainly on reproducing the most relevant tasks that emerged during the screening of the first two cohorts. In particular, we decided to add tasks such as the EPM, TST and light/dark alternation, to better investigate changes in the anxiety-like behaviour that emerged during the first battery of tasks. The main arrow in the middle of Figure II-7 represents the timeline followed for scheduling the behaviour and every block of the arrow stands for a month. The behavioural tasks are ordered on the timeline respecting the succession used, paired with the age of the animals.

In the tasks performed in all of four groups, 29 control animals were used and 32 mutants. When split, cohorts 1 & 2 had 16 controls and 16 mice carrying β2-nAChRs deletion and cohort 3 & 4 had 13 and 16, respectively. In all the behavioural graphs presented within the respective sections within the Results (β2-nAChRs in the striatum – behaviour), the following convention is used: white colour with black boarders is associated with control animals (injected with AAV5-GFP) while the green colour and 'Beta2-del' naming stands for mice injected with AAV5-Cre-GFP, thus carrying the deletion of β2-nAChRs in the dorsal striatum (DS).

C. Behavioural tasks

a) Open field test (including amphetamine administration)

A square Plexiglas arena (40 cm x 40 cm) was used as open field where mice were introduced and let free to explore for 30 min, being recorded. The task was repeated in two consecutive days. We used ToxTrac software by Rodriguez et al. (2018) to analyse the total distance travelled in both days, together with the time spent in centre and edges of the arena.

At the end of the study, both controls and mutants Beta2-fx/fx mice, before being sacrificed, were split into two groups. After 30 min of habituation, mice were alternatively injected intraperitoneally (ip) with saline or amphetamine (2mg/kg as described by (Yates et al., 2007)) and returned to the arena where their locomotion was recorded for another hour. Locomotor activity was scored both during the habituation (30 min), and after injection (90 min).

b) Nest building

Mice were moved into individual cages in the morning. After 5h of habituation in the home cage and at least 3h before the onset of the dark phase, 3g of cellulose nestlet material was distributed in each cage and the nest-building activity was evaluated using the scoring scale by Deacon (2006), that classifies as 0 the starting untouched material, up to 4 describing a complete, round, 3D nest. The cages were inspected at 10, 30, 60, 180 min and after 24h, when also we weighted the total amount of untorn material.

c) Grooming test

The grooming test was performed as described by Wang et al. (2017). Mice were habituated to a novel empty cage for 5 min and then recorded for other 5 min (pre-spray phase). Subsequently, mice were taken from the cage, sprayed with water and returned to the test cage. The recording continued for other 10 min (post-spray phase). Videos were scored off-line by two blinded experimenters and their scores were averaged. Number of events grooming events and their duration were considered.

d) Hole-board test

The testing was performed according to Martos et al. (2017) Wang et al. (2017). Mice were placed in the 40 cm x 40 cm Plexiglas arena containing Plexiglas insertion with 16 equidistant 2-cm-wide holes and recorded for 30 min. Numbers and positions of head-dippings were scored by two blinded experimenters whose scores were averaged.

e) Marble burying test

Twenty glass marbles were positioned as 5 rows of 4 marbles on the surface of a 5 cm high layer of clean bedding in a standard holding cage as described by Angoa-Pérez et al. (2013). Mice were placed in a corner of the cage with the marbles and then recorded for 15 min. The number of marbles buried was evaluated by a blinded experimenter. The marble was considered buried if at least two-thirds were covered with bedding.

f) Elevated plus maze

The method and the equipment were set as indicated by (Walf & Frye, 2007). Mice were placed in the middle of a cross-maze formed by two closed arms and two open arms, facing one of the open arms. The number of entries and time spent in the open or closed arms were recorded for 5 min and scored by a blinded experimenter.

g) Light/dark preference task

Half of a square Plexiglas arena (40 cm x 40 cm) was enclosed in a black cardboard envelope and divided with a black partition with a small opening in the front into two halves, creating one dark side of the maze and leaving the other half exposed to the light (Arrant et al., 2013; Takao & Miyakawa, 2006). The test was performed during the dark phase of the light cycle (active phase for mice) in a bright room. Mice were placed in the centre of the light side of the arena and allowed freely to explore both the light and the dark parts of the maze for 10 min. The session was recorded and the time spent in each part of the arena was manually scored.

h) Forced swimming test (FST)

The FST (Commons et al., 2017; Rada et al., 2006) was performed by using a 2 L beaker filled with 1.8 L of tap water. The temperature of the water was maintained at 25-27°C throughout the experiment, while the water was changed every 3 or 4 animals. Mice were gently placed into the beake and recorded for 6 min. Only 5 min of the test were scored as the first min was not evaluated. The time mice spent immobile was scored by two blinded experimenters and their scores were averaged.

i) Tail suspension test

Using laboratory tape, mice were attached upside down by their tail to a rectangular wooden bar placed across the top of an open field box, as described by Can et al. (2011). The tape was placed approximately 2 cm from the end of the tail, so the animal did not fall during testing while it was not able to turn around and climb onto the wooden bar. A camera was positioned on the box facing the animal from the front. A 6 min-session was recorded and time spent struggling for escape vs. time immobile was scored from min 2 to 6 of the test.

j) Social preference test and Social novelty

We addressed the sociability of the tested mice with a three-chamber apparatus setup inspired by the ones developed by Crawley's group (M. Yang et al., 2011; Moy et al., 2009; Nadler et al., 2004). A 90 cm long, 23 cm wide and deep Plexiglas box was divided into three chambers with the same dimensions by the insertion of two spacer with little doors that could be closed by a doorway. The mouse was placed in the middle of the central compartment to habituate for 5 min. After the habituation, doorways were open and the animal was free to explore for 10 min all the three chamber: one containing the inanimate novel object (non-social stimulus) consisting in a wired cup; the empty central one used for the habituation and one containing an unfamiliar mouse (social stimulus) placed inside a same kind of wired cup used as a non-social stimulus. The mouse used as a social stimulus was a young male of 5-7 weeks. The total time spent in each of the 3 chambers, the time spent exploring the empty wired cup and the time spent with the social stimulus were measured. For the social novelty task, after the first 10 min of social interaction, the non-social stimulus was replaced with a novel unfamiliar mouse, while in the opposite chamber the same mouse as before was presented. Again, the total time spent in each chamber and the fraction of time spent interacting with the novel or the familiar conspecific was scored over 10 min.

k) Novel object recognition

The procedure was adapted from (R. Zhang et al., 2012). On day 1, mice were habituated for 20 min to a clean empty home cage. On day 2, mice were placed in the same cage as day 1 and they underwent a training session during which they were presented with two identical objects (small plastic black and white striped cups) for 10 min. After the training, mice were placed back in their home cages and let undisturbed for 1 h. Then, during the test session, mice were placed back into the same cage as day 1 with two objects for 5 min. This time, one of the cups used during the training was replaced with a similar novel object (a small plastic toy with a black stripe). Both sessions on day 2 (training and test) were recorded and a blinded observer manually scored the time mice spent in the exploration of all the individual objects used during the task. We scored as exploration of the object when the mouse was pawing the object and/or directing its nose towards the object within a 2 cm distance. Climbing or sitting on the object was not scored as exploration. Based on the scores, the recognition index was calculated and expressed in percentage as Recognition index = time exploring novel object/(time exploring novel object + time exploring familiar object) x 100. The unbiased preference for the used objects was ensured in a previous pilot study.

l) Cued MWM

The cued version of the MWM was performed as described in (Rossato et al., 2006). Mice were tested over two days. The platform was visible, placed at water level with a black and white striped flag as cue. On day 1, the training consisted of 8 consecutive trials with a 60 s inter-trial interval. The platform position and starting point were changed each time. After 24 h, mice were probed for their retention in 2 trials of maximum 60 s, starting from positions never used during the training. Animals' performances were recorded with a Tracker software (Biosignal Group). Distances travelled, latencies to reach the platform and quadrant location were analysed by CM Manager version 0.4.0 (open source by Stepan Bahnik, available at: https://github.com/bahniks/CM_Manager_0_4_0).

m) T-maze task

Prior to the task, mice were mildly food-restricted at 85%-90% of their regular weight when offered food ad libitum. Sweetened condensed milk, diluted 1:2 in water, and offered as 40ul/portion, was used as reward to motivate mice for performing the task. Before the training, mice were first habituated to the reward and to the maze, a cross-maze apparatus where one of the arms was

systematically blocked, offering the animals just a T-shaped space where to move (Okada et al., 2018; Deacon and Rawlins, 2006). The position of the blocked arm and the starting point were always chosen as opposite but their position was alternated so the starting positions were pseudo-randomly changing for each animal. During habituation, mice were taught to move in the apparatus to reach and consume the rewards placed in both target arms within 90 s. During the acquisition phase a single reward was placed in the goal arm. When animals reached the goal by performing the correct body turn with an accuracy above the chance level (≥ 50% in Cohort 1, ≥ 70% in Cohort 2), they were moved to the reversal phase. In Cohort 2 the learning criterion was adjusted since mice learnt faster than Cohort 1. Data were anyway pooled together and expressed as percentage of performance of control animals. During the reversal phase of the task, mice had to learn that the correct body turn to reach the reward was switched. Mice that failed to reach the criterion during the acquisition were not moved to the reversal phase, but their acquisition data were included in the analysis.

D. Biochemical approaches

a) Immunofluorescence

After intracardiac perfusion with 4% paraformaldehyde (PFA) in saline phosphate buffer (PBS 1X), brains were extracted and post-fixed overnight (o/n) in 4% PFA at 4°C. Brains of Beta2-fx/fx mice were switched to PBS 1X and cut with vibratome (Leica VT1000S) in 40 µm slices for free-floating immunofluorescence (IF) or stored in cryoprotective solution at -20°C for later use. Brains of NPY/Cas9 mice, instead, underwent sequential incubations with sucrose 10% and 30% after post-fixation with PFA and were sliced with cryostat at 20 µm thickness and collected directly on coated slides to ensure proper sampling of the full PFC. The immunohistochemical (IHC) protocol performed afterwards, was the same for all the types of samples. All steps, except for the primary antibody incubation, were performed at room temperature (RT). Prior and after the permeabilization step (PBS 1X, Triton X100 1.2% at RT for 20 min), slices were washed three times in PBS 1X with Triton x100 0.25% (TBS1X) for 10 min each. For DARPP-32 and mAb 270 staining, the permeabilization step has been replaced by three consecutive washes of 5 min in ethanol 50%, 70%, 50%. For blocking non-specific binding, the sample was incubated with PBS 1X, Triton X100 0.2%, and normal goat serum (NGS) 5% for 1h at RT. Washes in TBS1X (10min) followed. Primary antibodies) were added at the

Abs solution (PBS 1X, Triton X100 0.2%, NGS 2%) and incubated o/n at 4°C. The next day, after 3 TBS 1X washes, after 1h of incubation with the secondary antibodies, diluted in the Abs solution, samples were mounted on a slide, covered with Fluoroshield (Sigma) and coverslipped. Images were acquired through Leica SP8 AOBS WLL MP confocal microscope at different magnifications, using HC PL FLUOTAR 5x and 10x, HC PL APO 40x and 63x objectives. Cell count and evaluation of areas of interest were performed using Fiji and CellProfiler. All the antibodies used with their working concentration are summarized in the table below.

Table II-1 List of the antibodies used for immunostaining

Antibody Type	Target	Manufacturer	Host species	Used concentration
1ry	Anti-GFP	Abcam - ab13970	chicken	1/1000
1ry	Anti-c-Fos	Abcam - ab190289	rabbit	1/500
1ry	Anti-RFP	Chromotek	rat	1/500
1ry	Anti-DARPP-32	R&D Systems - 10641854	goat	1/500
1ry	Anti-VAChT	Gras et al., 2008	guinea pig	1/5000
1ry	Anti-NPY	Abcam - ab112473	mouse	1/250
1ry	mAb270	Developmental Studies Hybridoma Bank	rat	1/100
2ndry	Alexa Fluor 488 anti-chicken	Jackson ImmunoResearch Laboratories	goat	1/500
2ndry	Alexa Fluor 594 anti-rabbit	Jackson ImmunoResearch Laboratories	goat	1/500
2ndry	Alexa Fluor 594 anti-guinea pig	Jackson ImmunoResearch Laboratories	goat	1/500

2ndry	Alexa Fluor 594 anti-goat	Jackson ImmunoResearch Laboratories	donkey	1/500
2ndry	Alexa Fluor 680 anti-rabbit	Jackson ImmunoResearch Laboratories	goat	1/500

Cultures of primary neurons were used to test the specify of mAb270 in vitro. Neurons were transfected with a plasmid carrying β2-nAChRs sequence with an m-Cherry tag (Addgene, #45097) to induce over-expression of the tagged receptor in the transfected cells (Srinivasan et al., 2010). We used Lipofectamine 3000 reagent (ThermoFisher, #L3000001) according to the manufacturer's instructions, we incubate for 48h and then we washed with PBS once, fixed the cells with PFA4% for 10 min and, after washing out the PFA, we proceeded with immunocytochemical staining following the same protocol reported above used for brain tissue.

b) In situ hybridization

Adult mice (12.5 weeks) were killed by cervical dislocation. Brains were extracted and frozen in cold isopentane (-30°/-35°C) and stored at -80°C. Then, they were serially sectioned on a cryostat at 16 µm thickness and stored at -80°C. Double-probe fluorescent *in situ* hybridization (FISH) was performed as described in (Dumas & Wallén-Mackenzie, 2019). Probes' preparation: antisense riboprobes for the detection of the following mRNAs were prepared: *Chrnb2*, NM_009602 sequence 597-1517; *Drd1*, NM_010076 sequence 1756-2707 and *Drd2* NM_010077 sequence 268-1187; *Chat*, NM_009891 sequence 526-1065; *Pvalb*: NM_013645 sequence 74-591; *Npy*, NM_023456 sequence 13- 453; *Sst*, NM_009215 sequence 143-401; *Htr3a*, NM_013561 sequence 641-1552. Digoxigenin (DIG) or fluorescein labelled nucleotides (Sigma-Aldrich, #11277073910 and #11685619910) were incorporated by a transcriptional reaction to synthetize the specific digoxigenin and fluorescein-labelled RNA probes specified above. The specificity of the probes for the targeted sequences was simulated and confirmed using NCBI blast.

FISH experiments: Cryosections were air-dried and fixed in 4% PFA for 10 min. It followed a 10 min acetylation step with 0.25% acetic anhydride in 100 mM triethanolamine (Sigma, #T58300) at pH 8.

After 3 washes in PBS 1X, sections were hybridized overnight for 18 h at 65°C in formamide-buffer containing different combinations of 1 µg/ml DIG-labelled riboprobe and 1 µg/ml fluorescein-labelled riboprobe in a final volume of 100 µl per slide. We mostly used *Chrnb2*-DIG probe because in this specific case, during the revelation, we could obtain a better signal/noise ratio for the DIG-labelled probe compared to the fluorescein-labelled one. On day 2, sections were washed at 65°C with saline-sodium citrate (SSC) buffers of decreasing strength (5X first and 0.2X after) and blocked for 1 h with 20% of foetal bovine serum FBS (Invitrogen, #10106-169) in 1% blocking solution (Roche, #11096176001). DIG epitopes were conjugated with HRP anti-DIG fab fragments at 1:2500 (Roche, #11207733910) and revealed using Cy3-tyramide (Sigma, #GEPA13104) at 1:100. Fluorescein epitopes were detected with HRP anti-fluorescein fab fragments at 1:5000 (Roche, #11426346910) and revealed using Cy2-tyramide (Thermo Fisher, #46410) at 1:250. Nuclear staining was performed with DAPI (Sigma, #D9542). Sections were mounted with Fluoromount (Southern Biotech, #0100-01) and cover-slipped.

Analysis: All slides were scanned at 20x resolution using the NanoZoomer 2.0-HT (Hamamatsu Photonics). Exposure and acquisition time were set separately for each riboprobe. Images were analysed using the NDP.view2 software (Hamamatsu Photonics) and manually counted. ROIs were identified according to the Paxinos mouse brain atlas (Franklin & Paxinos, 2007). We estimated the colocalization when the signals for both probes were co-expressed in the soma of the same cell. A mean of 700, 1200, 520, and 830 Chat, Npy, Pvalb, and Sst neurons, respectively, were analysed per brain, on adjacent sections at 6 levels of the rostro-caudal axis. For illustration purposes, the NanoZoomer images were exported in TIFF format using NDP viewer and were then corrected for contrast and cropped in Photoshop 2021 (Adobe Systems), and assembled with Illustrator 2021 (Adobe Systems).

c) qRT-PCR on striatal punches

To obtain samples for the PCR, mice were killed by decapitation, brains were quickly removed, and individual brain regions were dissected on ice, frozen on dry ice, and stored at -80°C until use. RNA for the qRT-PCR from the striatum-expressing AAV virus was prepared from punches taken specifically in the AAV-expressing area and isolated by RNeasy Micro Kit (QIAGEN). For the qRT-PCR, the reverse transcription of the RNA samples was performed with LunaScript RT SuperMix (New England Biolabs) and the qPCR with LCC 480 SYBR Green Master at LCC 480 instrument (Roche)

according to the manufacturers' instructions. Primers used in qRT-PCR were targeted against exon 5 of the Chrnb2 gene: forward 5'-TGGCCATCCTGGTCTTCTAC-3' and reverse 5'-CGCCAGCAGCACAGAAATAC-3'. For the normalization of the data we used the expression of β-actin gene as reference, using primers reported by Frahm et al. (2011). The relative quantification of gene expression was calculated using the $2^{-\Delta\Delta CT}$ method (Saito et al., 2005Livak & Schmittgen, 2001;).

d) RNA-scope

After decapitation, mouse brain was removed from the skull and immediately embedded in OCT medium (Thermo Fisher Scientific) and frozen in isopentane precooled at -35°C in dry ice. Brains were stored at -80°C for up to 3 months. Before being sectioned sagittally at 16 µm, the OCT block was placed in the cryostat (Leica CM 3000), precooled at -20°C, for 1 h. Sections corresponding to the intraneural lateral distance of 0.96 mm, according to the mouse brain atlas (Franklin & Paxinos, 2007) and containing both the DS and SNc, were selected for the *Chrnb2* visualization. RNAScope kit (ACDBio) with a custom-made probe for exon 5 of the Chrnb2 RNA was used following the manufacturer's instructions for fresh-frozen tissue. Brain sections were fixed in 4% PFA for 15 min and dehydrated in increasing concentrations of ethanol (50%, 70% and 2 times in 100%) for 5 min each. Following a 30 min incubation with Protease IV (ACDBio), the brain slices were hybridized with the target probes (*Chrnb2*, positive and negative controls) for 2 h in a humidified incubator at 40°C. Then, the washes described in the protocol and the incubations at 40°C with the supplied amplification reagents (Amp-1, Amp-2, Amp-3, and Amp-4) followed. Finally, the samples were stained with DAPI (ACDBio) for 30 s and mounted with Prolong Gold antifade reagent (Thermo Fisher Scientific). Puncta corresponding to *Chrnb2* RNA were detected with a Leica SP8 WLL MP confocal microscope with HC PL APO 63x/ 1.40NA objective. For each animal, three confocal images of the DS and three of the SNc were analysed by Fiji's manual multi-counting function throughout the z stacks (3 mm steps, 7 pictures). Five cells per picture were randomly selected, and the total number of puncta in 5 cells was counted.

E. Statistics

Data were analysed using GraphPad Prism (GraphPad Software, San Diego, CA) by two-tailed Student's t-test or (repeated measures) two-way ANOVA followed by post hoc test as appropriate. The Mann–Whitney U non-parametric test was used for the analysis the nest building and hole-board tests due to the non-normal distribution of the data collected. Statistical tests used are also reported in the figure's legends and summarized in the appendix. Significance was set at $p < 0.05$.

Results of individual statistical tests are presented and discussed throughout the main text when significant, while the other statistical descriptive data and the statistical methods employed are organised in the annex presented in at end of the Results section.

III. Results

The results section comprises three main parts. Each of them uses a specific mouse model and it focuses on a targeted brain region. The functional evaluation of β2-nAChRs starts with the analysis of β2-nAChRs expression, followed by the model characterization and the behavioural investigation. I conceive the research work as result of collaboration, so I will use the pronoun ''we'' to report the results obtained. I will clearly state when experiments were not performed directly by me or under my supervision.

A. β2-nAChRs in the striatum

a) β2 expression

i. The problem of visualizing β2-nAChRs

β2-nAChRs represent the central subject of my research project. It would be ideal if we could directly visualize them in the brain tissue through an immunohistochemical approach. The few published data about a working antibody targeting neuronal β2-nAChRs, correspond to the so-called mAb 270, prepared by Lindstrom's team (Govind et al., 2012; Whiting & Lindstrom, 1987) and available at Developmental Studies Hybridoma Bank (DSHB). At first, we tested mAb 270 antibody on fixed primary cultured neurons from mouse embryos transfected with a plasmid carrying *chrnb2*, the gene coding for β2-nAChR, tagged with mCherry. We co-detected mCherry and the mAb 270 labelling with a similar pattern of expression on the transfected neuron (*Figure III-1* a). Then, we tested mAb 270 on fixed brain tissue.

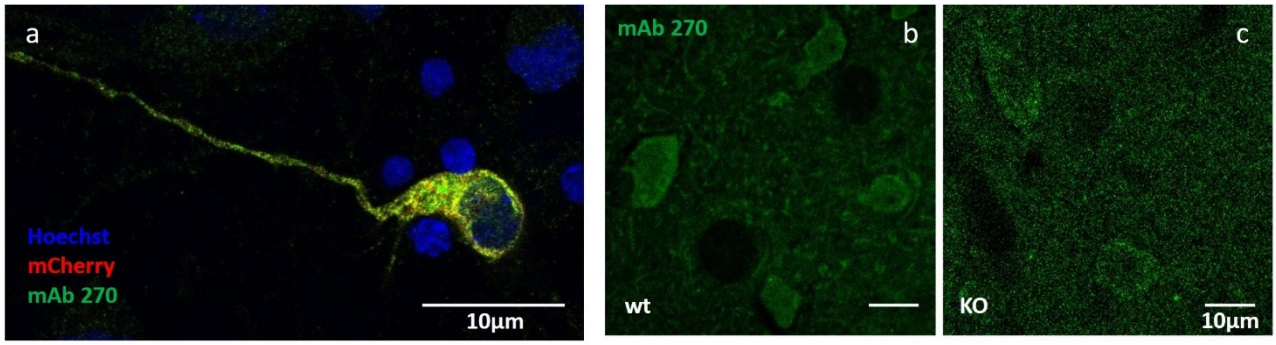

Figure III-1 mAb 270 testing – Confocal images of a neuron in primary culture (a) and mouse brain tissue sections of a wild-type (wt; b) and Beta2KO (c) stained for anti-mAb 270, antibody anti-β2-nAChRs. Nuclei are counterstained with Hoechst.

On the suggestion of Dr Morgane Besson (Institut Pasteur, Paris), who kindly provided me with wild-type (wt) and Beta2-global knock out (Beta2KO; mouse line generation originally described in Picciotto et al., (1995)) littermate brain samples, we tried different protocols for the immunolabelling of β2-nAChRs. None of them resulted in a specific signal clearly distinguishable from the background and totally absent in the Beta2KO (*Figure III-1* c vs b). Unfortunately, there is no evidence of working antibodies for selective and specific targeting of neuronal β2-nAChRs (Moser et al., 2007). As an alternative approach, thanks to a collaboration with Dr Sylvie Dumas (Oramacell, Paris), we used fluorescent *in situ* hybridization (FISH) to visualize the mRNA encoding for the β2 subunit of the nAChR gene (*Chrnb2*). In our FISH experiments, instead, the detection of Chrnb2 it is possible and it is specific when compared to the Beta2KO (*Figure III-2*).

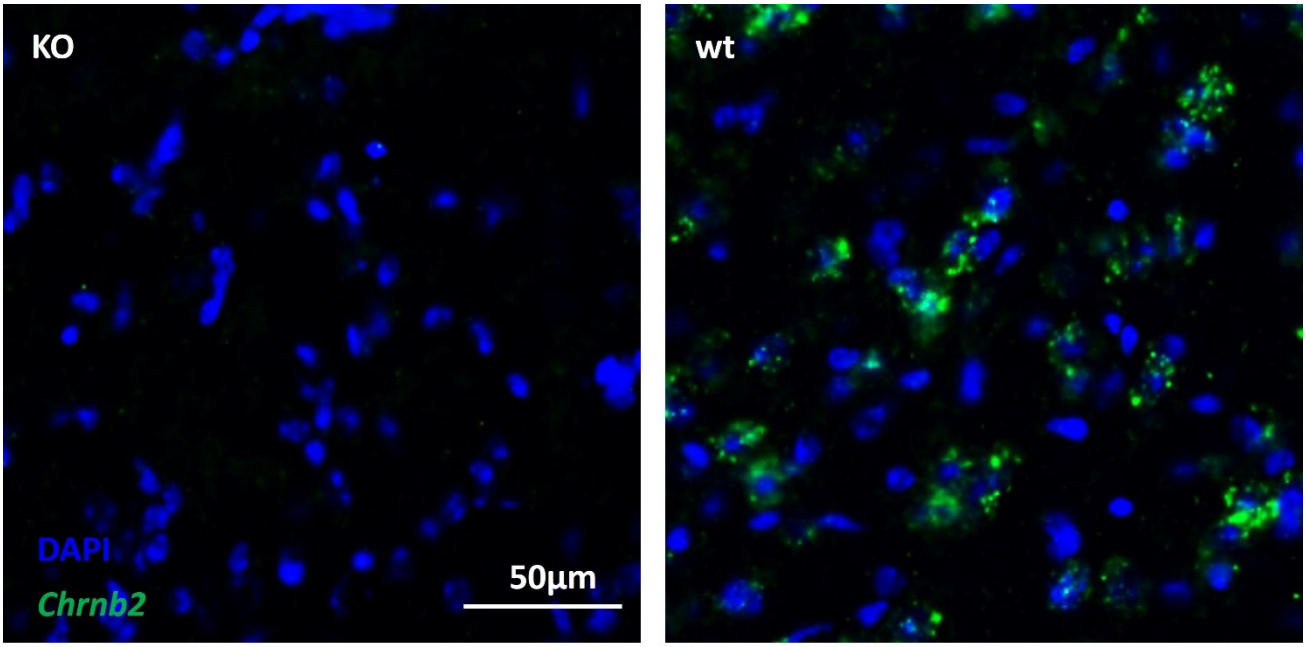

Figure III-2 Fluorescent in situ hybridization (FISH) for the detection of chrnb2 in the thalamus – Comparison of chrnb2 signal (green) between Beta2KO, on the left, and wt (right) adult male mouse in a brain section. DAPI in blue stains the nuclei.

ii. β2-nAChRs expression in the striatum

We decided that double FISH was the best approach to visualize the concomitant expression of β2-nAChRs together with other neuronal markers to identify specific populations expressing the receptor. We used different markers to identify the phenotype of the neurons expressing β2-nAChRs. First, we investigated the *in situ* cplocalisation of *Chrnb2* in combination with the choline acetyltransferase (Chat) mRNA (*Figure III-3* a, b). Besides Chat (*Figure III-3* b), parvalbumin (Pvalb, *Figure III-3* d), neuropeptide Y (Npy, *Figure III-3* e), somatostatin (Sst, *Figure III-3* f), D1 and D2 dopamine receptors (Drd1 and Drd2, *Figure III-3* g, h) were co-analysed with *Chrnb2*. In most cases, three different possibilities appeared: cells Chrnb2-positive (Chrnb2^{+}) only, cells positive for the other marker only, and cells double-positive, both for the marker and Chrnb2^{+}.

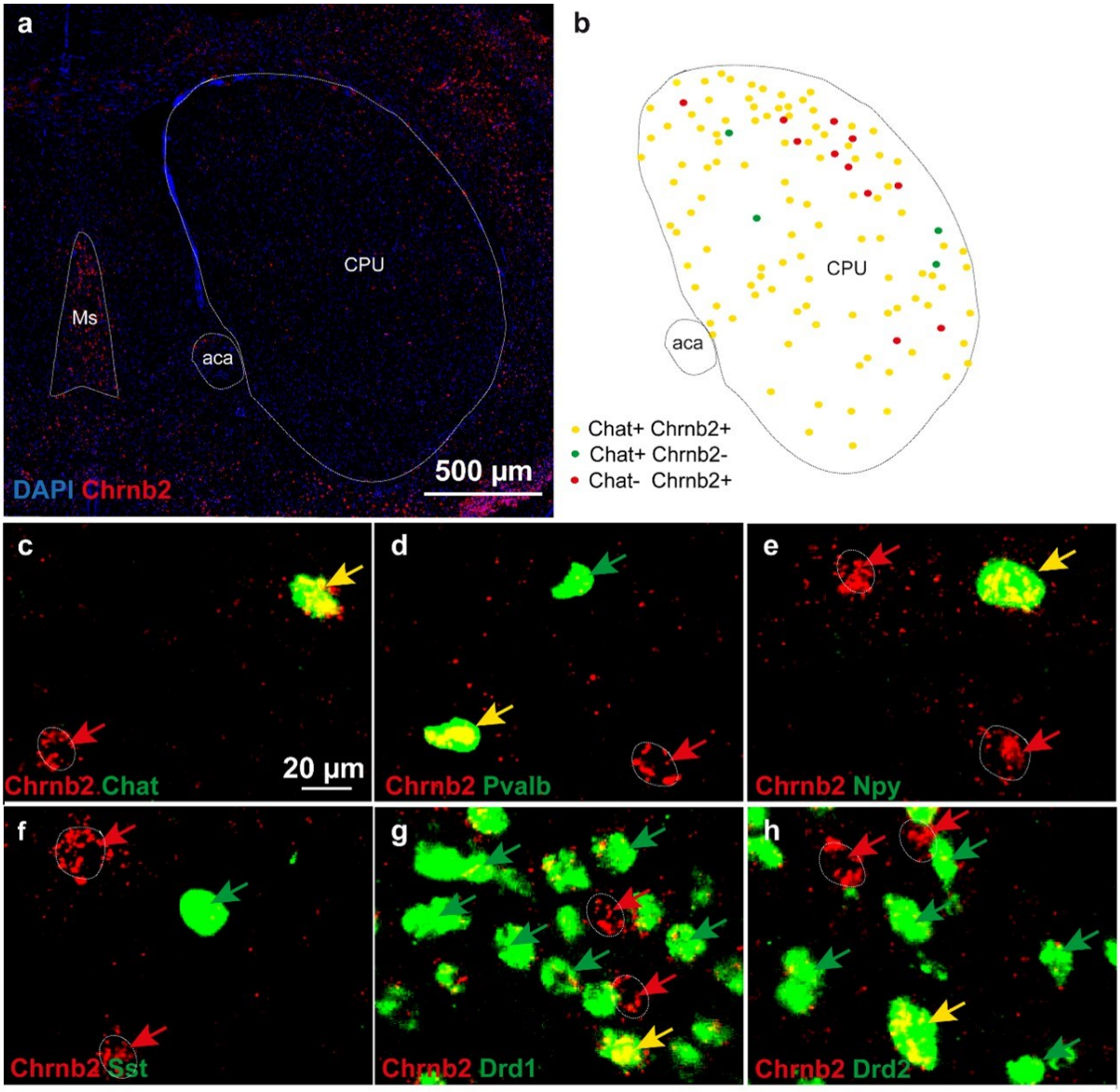

Figure III-3 Main neuronal types expressing Chrnb2 in the mouse striatum visualized by FISH – (a) Pattern of expression of Chrnb2 in the striatum, at bregma 0.5. (b) Scheme representing the cell distribution within the caudate-putamen [CPU]. Yellow dots represent Chat⁺ and Chrnb2⁺ neurons; green ones, Chat⁺ but Chrnb2⁻; red ones, Chrnb2⁺ but Chat⁻. (c – h) show close-ups for Chrnb2 co-expression with the main markers for interneurons (Chat for CINs; Pvalb, Npy, Sst, for different populations of GABAINs) and Drd1, Drd2 for MSNs. See the text for an explanation of abbreviations.

Therefore, we performed a systematic quantitative analysis of expression in the entire striatum by selecting 6 different bregma levels, from the rostral to the caudal part of the CPU (bregma 0.98; 0.74; 0.5; 0.26; 0.02 and -0.22). Most of the Chat⁺ neurons, 96%, express Chrnb2 (*Figure III-4* a), while just 24% and 5.5% of Pvalb⁺ (*Figure III-4* b) and Npy⁺ cells (*Figure III-4* c) are also Chrnb2⁺. In addition, the rostro-caudal distribution of Chat and Chrnb2 double-positive neurons differed from Pvalb⁺/Chrnb2⁺

and Npy$^+$/Chrnb2$^+$, the firsts being more homogeneously distributed across the CPU whereas the latter were found only in the dorsolateral part of the striatum.

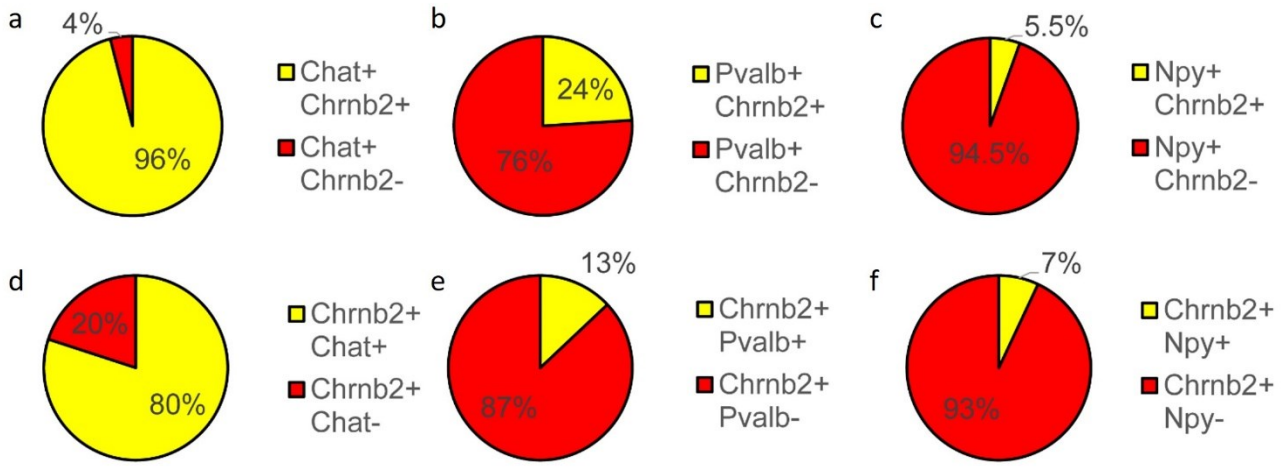

Figure III-4 Pie charts showing the quantification of the FISH data – (a-c) Percentage of Chat$^+$ (a), Pvalb$^+$ (b) and NPY$^+$ (c) striatal neurons, that also showed expression of Chrnb2. (d-f) Percentage of total Chrnb2$^+$ expressing neurons that are also Chat$^+$ (d), Pvalb$^+$ (e) and Npy$^+$ (f).

When Chrnb2-expressing cells were counted, we found that 80%, 13%, and 7% of Chrnb2$^+$ neurons were also Chat$^+$, Pvalb$^+$, and Npy$^+$, respectively, thus adding up to the full 100% (*Figure III-4* d-f). Interestingly, only 0.5% of Drd1$^+$, presumably neurons displayed Chrnb2 mRNA, while the 20% of Chrnb2$^+$ but Drd2$^-$ cells, corresponded to the sum of the Chrnb2$^+$ neurons that were Drd1$^+$ (Chrnb2$^+$/Pavalb$^+$ and Chrnb2$^+$/Npy$^+$). The Drd2$^+$/Chrnb2$^+$ neurons were mostly large-sized, putatively representing CINs (Le Moine, Normand, et al., 1990; Le Moine, Svenningsson, et al., 1990; Le Moine, Tison, et al., 1990). We could conclude that, in the striatum, Chrnb2 is selectively expressed by specific groups of striatal interneurons (INs), with the CINs, Chat$^+$, representing the vast majority.

b) Model characterization

i. Beta2-flox/flox mouse model

Given the rare presence of β2-nAChRs in the dorsal striatum and the selective expression on INs, the main aim of the present research project was to investigate the functional role of striatal β2-nAChRs. In the striatum, INs represents all together about 5% of the neuronal population and they have a modulatory function on striatal circuitry regulation. As a first approach, we used the Cre-loxP strategy

to delete β2-nAChRs. While the cell-specificity was dictated by the physiological expression of β2-nAChRs, we obtained a regiospecificity by injecting Cre-recombinase exclusively in the dorsal striatum of Beta2-flox/flox mice.

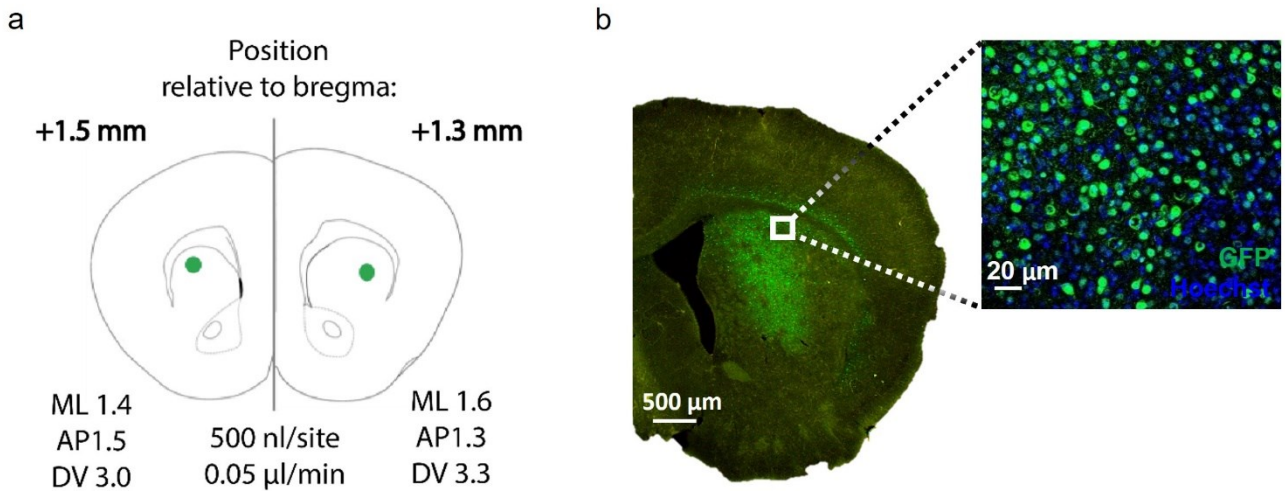

Figure III-5 Stereotaxic coordinates and viral transduction efficiency – a) a scheme adapted from Franklin & Paxinos (2007) Mouse Brain Atlas shows the 2 different bregma levels used for the stereotaxic injections and the full coordinates. In b), a representative image of a section of a mouse dorsal striatum after AAV-Cre-GFP injection. Spreading of the virus and the transduction efficiency in vivo (close up). ML: medio-lateral; AP: antero-posterior; DV: dorso-ventral.

Mice were injected contralaterally at 1.4 medio-lateral (ML), 1.5 antero-posterior (AP), 3.0 dorso-ventral (DV) from bregma, and 1.6 ML, 1.3 AP, 3.3 DV, with 500 nl of virus per injection site and 0.05 µl/min of delivery rate.

We evaluated post-mortem, for each mouse used for the behavioural testing, the spreading of the virus in the dorsal striatum and the transduction efficiency of the virus in targeting striatal cells (*Figure III-5* b).

ii. Deletion of β2-nAChRs in the mouse striatum

Besides the qualitative assessment following the viral expression patterns, we have isolated pools of the green cells by punching out parts of the striatal tissue in fresh frozen brains to perform quantitative RT-PCR (qRT-PCR). The prevalent nicotinic receptor in the mouse striatum is the heteromeric α4β2 subtype (Picciotto et al., 2000). The mRNAs expression of *Chrnb2* and *Chrna4* (gene coding for nAChRs expressing α4 subunit) was compared in mice injected with AAV-GFP or AAV-Cre-GFP (*Figure III-6* a, b, respectively). While Beta2 mRNA decreased in mice with deleted β2-nAChRs, there was no difference in Alfa4 expression ($t(11)= 16.95$, $p= 0.0001$, vs $t(11)= 0.5191$, $p= 0.6140$, respectively, two-tailed t-test). In parallel, we used another approach to visualise changes in Beta2 mRNA expression *in situ*, focusing on the striatum and also on striatal projection (in the midbrain), to

prove the regiospecificity of the genetic approach and to be sure that Beta2-deletion was not occurring unpredictably. We performed RNA-scope on brain slices of Beta2- flox/flox mice injected with control virus or AAV-Cre and we quantified the number of puncta per randomly selected cell in three animals for each condition. The *Chrnb2* mRNA puncta markedly decreased in AAV-Cre-injected mice comparing to controls (average in controls: 95 ± 7 SEM; in AAV-Cre-injected mice: 29 ± 45 %; p=0.0014, two-tailed t-test) in the striatum (*Figure III-6* c and d), while no change was detected in cells of the SNc (*Figure III-6* c and e), (average in controls: 115 ± 12 SEM; in AAV-Cre-injected mice: 130 ± 26 SEM; p=0.6228).

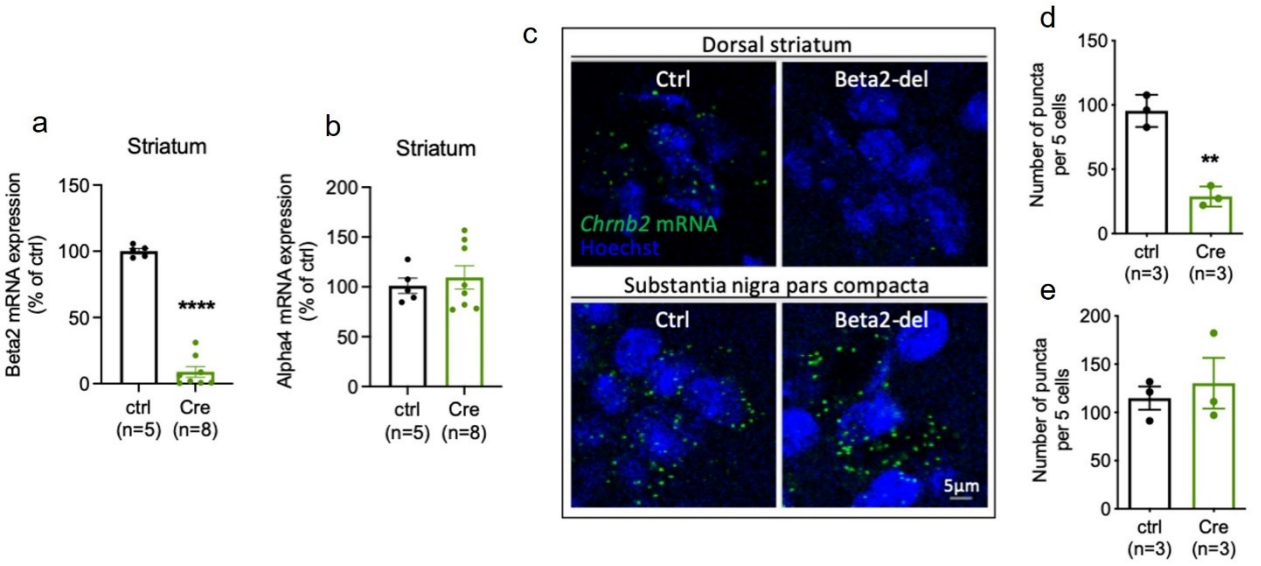

Figure III-6 Assessment of β2-nAChRs deletion in the mouse striatum – (a, b) qRT-PCR on brain punches for Chrnb2 and Chrna4, gene coding for nAChRs expressing Beta2 and Alfa4 subunit respectively. RNA-scope characterisation of Chrnb2 expression in striatal neurons and the substantia nigra pars compacta, both in control and Beta2-del mice. (d, e) quantification of the RNA-scope data expressed as the number of Chrnb2 puncta per 5 cells (Hoechest blue signal in the figures) in the field of view. Confocal images, 63x objective.

As a complementary approach, we controlled the specificity of the viral expression by following the pattern of the GFP signal in whole brain sagittal sections of mice injected with the AAV-GFP or AAV-Cre-GFP virus. In *Figure III-7* it is possible to appreciate how much the fluorescent signal given by the GFP expression is restricted to the dorsal striatum, CPu.

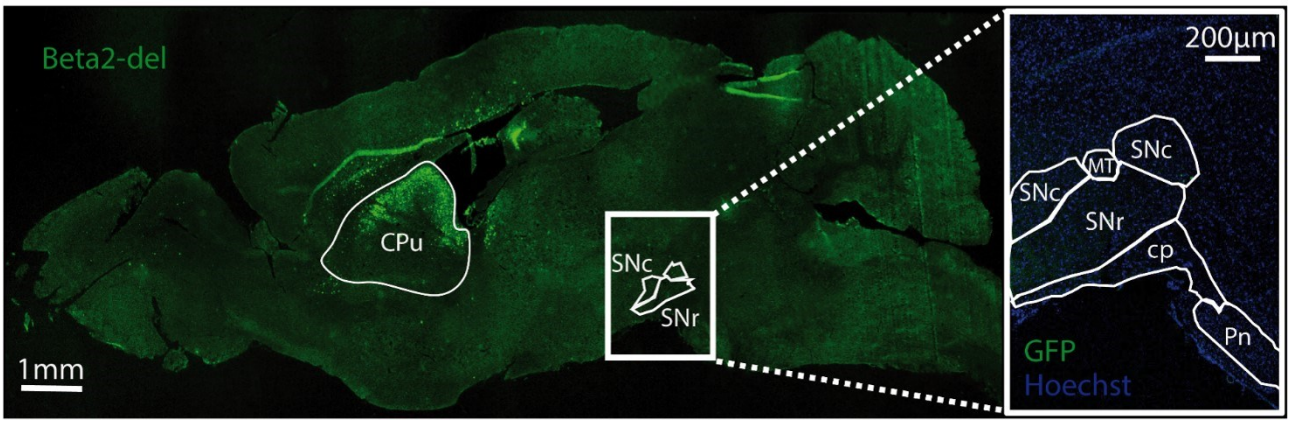

Figure III-7 Striatal restricted viral expression – Sagittal section of beta2-flox/flox adult mouse brain injected with AAV-Cre-GFP virus in the dorsal striatum representing the spreading of the virus. CPu: caude-putamen; SNc: substantia nigra pars compacta; SNr: substantia nigra pars reticulata; MT, medial terminal nucleus; cp, cerebral peduncle; Pn, pontine nuclei.

c) Behaviour

i. Rationale and general overview

Striatum is the main nucleus of the basal ganglia associated with the regulation of several aspects of behaviour, such as locomotion, reward-related processes, and motivation(Gonzales & Smith, 2015; Kaminer et al., 2019; Lovinger, 2010; Macpherson et al., 2014). Similarly, nAChRs have been identified as contributors in the regulation of a variety of comportments (Besson et al., 2006; King et al., 2003; Mineur et al., 2016a; Picciotto & Corrigall, 2002; Zoli et al., 2002). To answer the core question of my PhD project, can striatal β2-nAChRs, even if expressed in low levels and by rare interneurons, modulate behavioural outcomes, we tested different groups of animals.

ii. *Basal behaviour*

Due to the association between β2-nAChRs with the regulation of fundamental behaviours (Konsolaki et al., 2016; Léna et al., 2004; Léna & Changeux, 1999) we started with basal behaviour investigation of the mice after surgery. As the first task, we evaluated the spontaneous locomotor activity in an open field, in a novel (day 1) or familiar (day 2) environment, by repeating the task on 2 consecutive days.

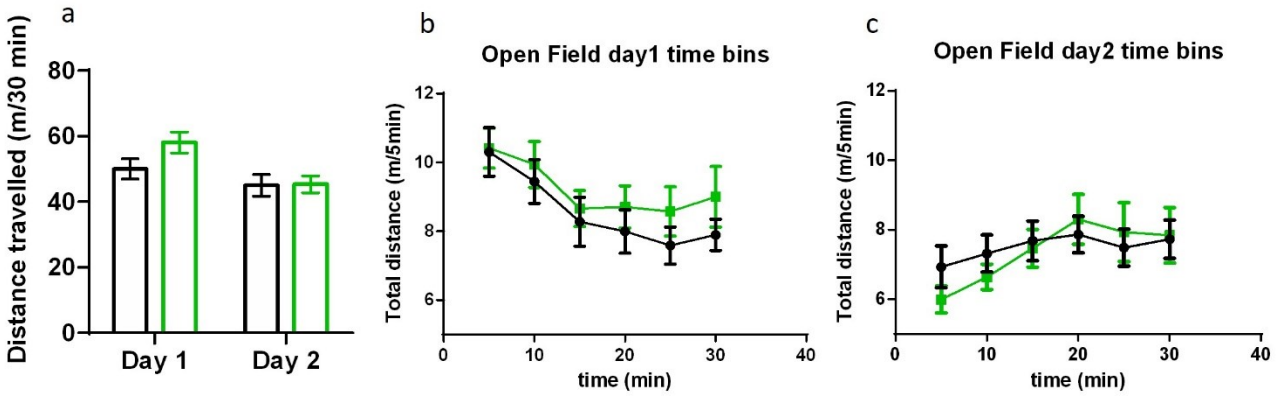

Figure III-8 Locomotor activity in the open field – (a) Total distance travelled by control and mutant mice, in the open field arena over 30 min, on two consecutive days. (b, c) Distance travelled by 5 min time bins steps, during day 1 and day 2 respectively. Ctrl=29, Beta2-del=32. Data are shown as mean ± SEM. In black: ctrl mice injected with AAV5-GFP, in green: Beta2-del mice injected with AAV5-Cre-GFP.

As expected, the overall locomotor activity on day 2 is decreased compared to day 1 (*Figure III-8* a; effect of the day: $F(1,59) = 17.81$, $p = 0.0001$; two-way ANOVA), but there is no difference between controls and mutants (effect of group: $F(1,59) = 1.255$, $p = 0.2672$). Beta2-del mice showed a slight, but not significant hyperactivity compared to controls when exposed to the open field as a novel environment (*Figure III-8* a; group x day interaction: $F(1,59) = 3.409$, $p = 0.0699$).

Interestingly, when we analysed the time spent in the centre rather than in the periphery of the open field (Figure III-9 a), besides a general decrease in the time spent in the centre of the arena during day 2 compared to day 1 (effect of the day: $F(1,59) = 38.56$, $p < 0.0001$; two-way ANOVA), there was a difference between control and mutant groups (main effect of group: $F(1,59) = 8.925$, $p = 0.0041$ and day x group interaction $F(1,59) = 6.494$, $p = 0.0134$). Animals carrying the deletion of β2-nAChRs, spent less time in the centre of the open field during day 1 (adjusted $p = 0.0004$ with the post hoc test, Sidak's multiple comparisons), as symbolised by the 3 asterisks. Generally, the central area of a novel environment is the place where it feels less comfortable and more dangerous since it is more openly accessible from all directions, therefore avoiding the centre of the open field arena denotates a more anxious-like kind of phenotype. A mutant mouse is clearly preferring corners of the arena rather than spending time exploring the central part (Figure III-9 b).

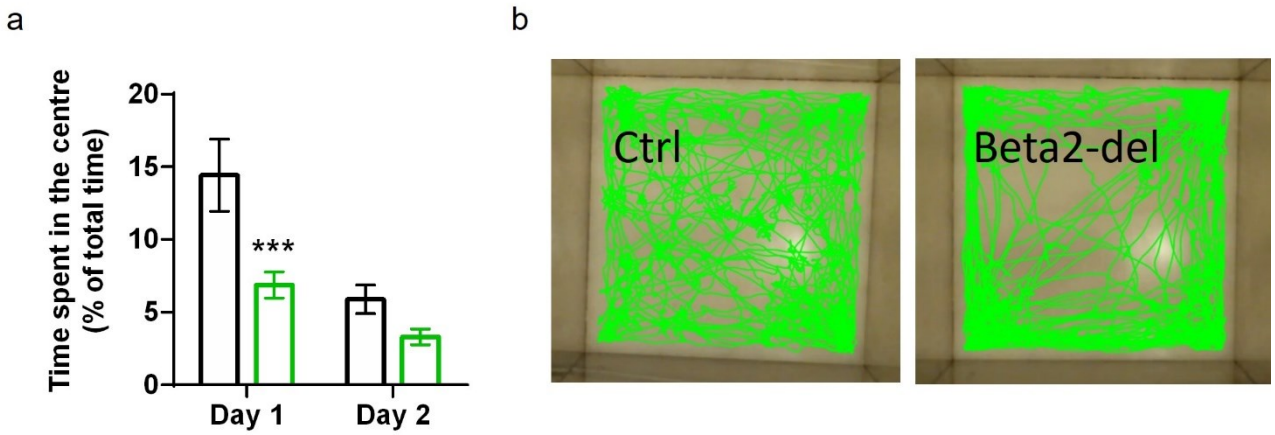

Figure III-9 *Time spent in the centre of the open field – a: time spent in the centre as % of total time spent exploring an open field arena in two consecutive days in control and Beta2-del mice. b: representative examples of the pattern travelled by animals of different genotypes. Ctrl=29, Beta2-del=32. Data are shown as mean ± SEM; *** = p < 0.0001. In black: ctrl mice injected with AAV5-GFP, in green: Beta2-del mice injected with AAV5-Cre-GFP.*

Between the tasks considered for the investigation of basal behaviours, the nest building test shows if mice can present any welfare impairment in the home cage. We reported here that deletion of β2-nAChRs does not cause any changes in animals' attitude towards nesting, with no difference in the amount of untorn nestlet material (*Figure III-10*; p = 0.3994, Mann–Whitney U test).

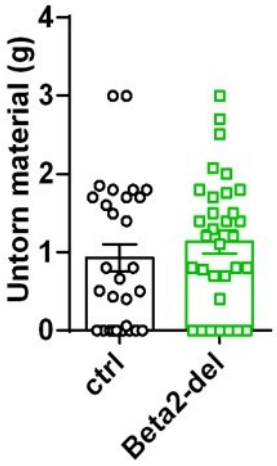

Figure III-10 Nest building task – Quantity of untorn nesting material. Ctrl=29, Beta2-del=32. Data are shown as mean ± SEM. In black: ctrl mice injected with AAV5-GFP, in green: Beta2-del mice injected with AAV5-Cre-GFP.

Another task that measures typical mouse behaviour, is the grooming test. The number of grooming events is scored before and after the splashing stressful event. Even if there was a difference between grooming pre- and post-splash (*Figure III-11*), there was no difference both in the total time spent grooming (*Figure III-11* a) and in the number of events (*Figure III-11* b) between Beta2-del and ctrl (effect of group F (1, 58) = 0.5290, p = 0.4699 and F (1, 58) = 0.0078, p = 0.9297, respectively, two-way ANOVA).

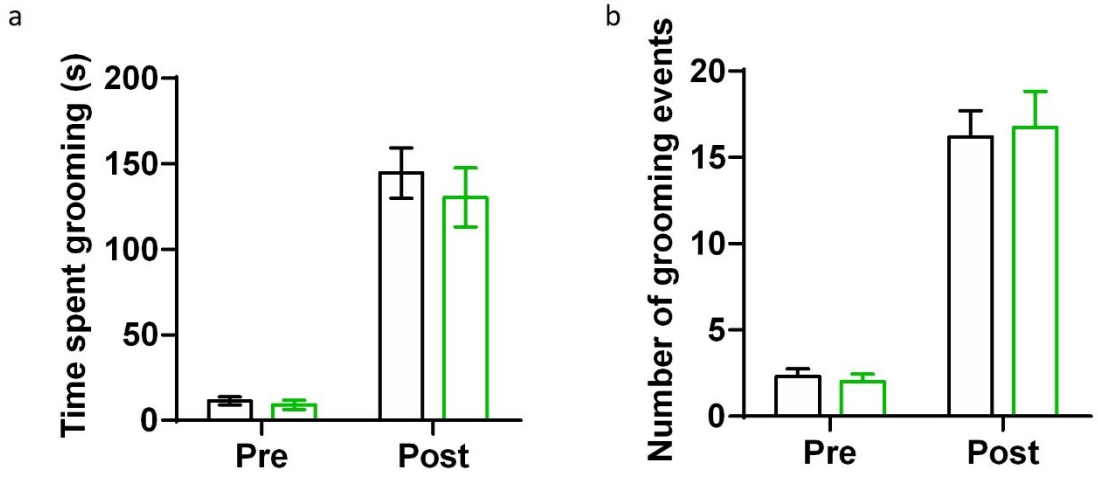

Figure III-11 Grooming test – (a) Time spent grooming pre- and post-splashing. (b) Total number of grooming events pre- and post-splashing. Ctrl=16, Beta2-del=15. Data are shown as mean ± SEM. In black: ctrl mice injected with AAV5-GFP, in green: Beta2-del mice injected with AAV5-Cre-GFP.

Grooming is a kind of repetitive behaviour that could be also an index of stereotypical behaviour. Even if anything significant emerged from the grooming task, we followed up with other two tests, the hole-board test and the marble bury task to check for basal behaviours that could potentially transform into stereotypies if triggered.

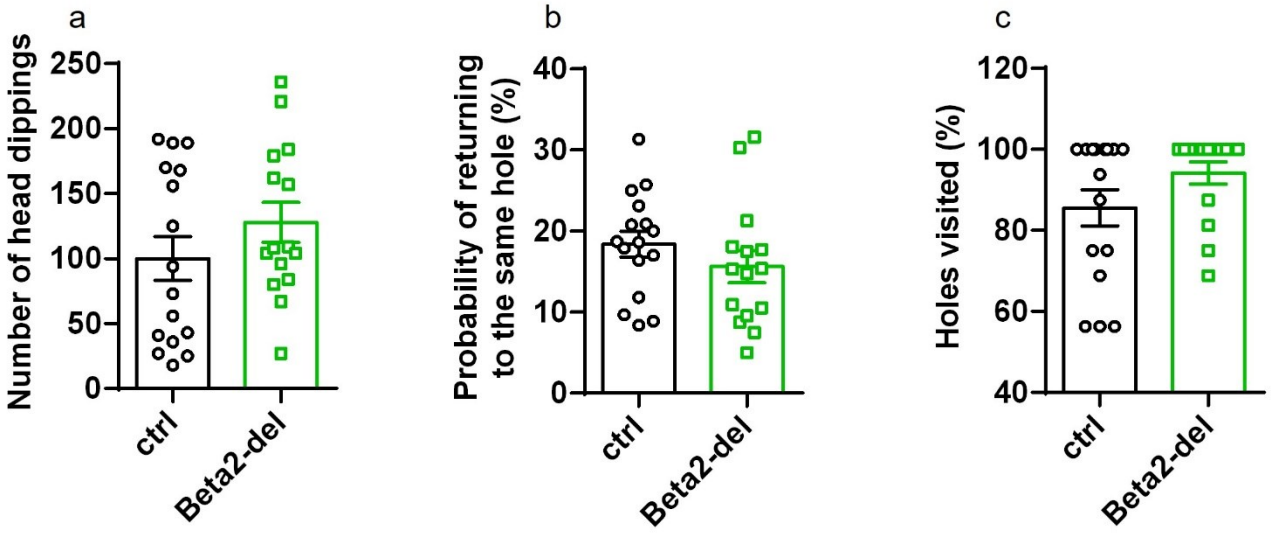

Figure III-12 Hole board test – (a) Number of head dipping; (b) probability of returning to the same hole and (c) % of hole visited are presented as indexes of repetitive behaviour evaluated with this task. Ctrl=16, Beta2-del=15. Data are shown as mean ± SEM. In black: ctrl mice injected with AAV5-GFP, in green: Beta2-del mice injected with AAV5-Cre-GFP.

The total number of head dipping, probability of returning to the same hole and the number of holes visited during the hole-board test were totally comparable between mutants and controls (*Figure III-12*, no differences in the groups p = 0.2354, Mann–Whitney U test; t = 1.096, p = 0.2823, unpaired t-test; p = 0.1427, Mann–Whitney U test). Similarly, no changes were detected in the marble bury task performances of Beta2-del mice compared to controls (*Figure III-13*, t = 0.2103, p = 0.8349, unpaired t-test).

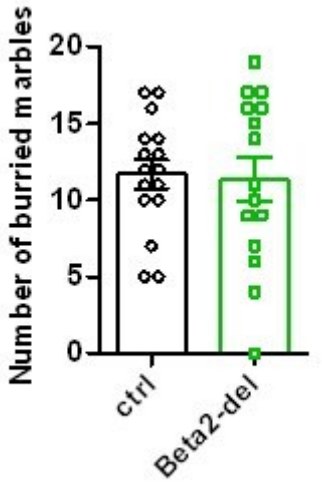

Figure III-13 Marbles bury test – The number of buried marbles was counted both in control and Beta2-del animals and no difference emerged. Ctrl=16, Beta2-del=15. Data are shown as mean ± SEM. *In black: ctrl mice injected with AAV5-GFP, in green: Beta2-del mice injected with AAV5-Cre-GFP.*

iii. *Anxiety-like behaviour*

To better investigate the anxiety-like behaviour of Beta2-del mice that emerged in the open field task (Figure III-9) with decreased time spent in the centre of the arena, we performed other complementary tasks, such as the elevated plus maze, the force swimming test, Light/Dark alternation task, and tail-suspension test.

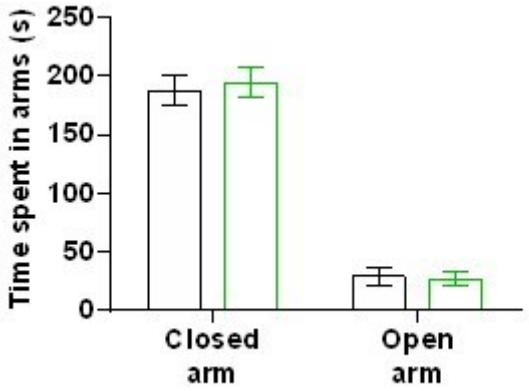

Figure III-14 Elevated plus maze – Time mice spent in the closed or open arms of the maze. Ctrl=29, Beta2-del=32. Data are shown as mean ± SEM. In black: ctrl mice injected with AAV5-GFP, in green: Beta2-del mice injected with AAV5-Cre-GFP.

As expected, mice preferred overall the closed arm to the open (effect of the arm: $F(1, 110) = 252.6$, $p < 0.0001$, two-way ANOVA) but both controls and mutants had the same kind of behaviour (effect of the group: $F(1, 110) = 0.0375$, $p = 0.8467$) (*Figure III-14*).

Conversely, when tested in the light/dark alternation paradigm, the two groups showed a different attitude towards the exploration of the environment exposed to the light (*Figure III-15*). Beta2-del mice spent less time, on average 223.8 s ± 15.86 vs 283.2 s ± 23, in the light compartment of the maze with respect to controls ($t (27) = 2.184$, $p = 0.0378$; unpaired two-tailed t-test).

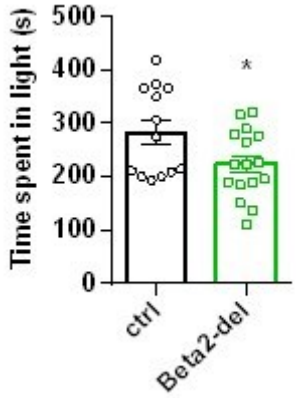

*Figure III-15 Light/dark alternation task – Time mice spent in the half part of the arena in the light. Data are shown as mean ± SEM; *= p < 0.05. Ctrl=13, Beta2-del=16. In black: ctrl mice injected with AAV5-GFP, in green: Beta2-del mice injected with AAV5-Cre-GFP.*

This finding is in line with the avoidant behaviour Beta2-del animals had in exploring the central part of a novel environment in the open field task. In the same way, they showed a sort of resilience towards a more stressful environment, like being exposed to the light when they could stay in a dark more favourable environment, resulting in an anxiety-like phenotype. To further evaluate behavioural despair, we used the forced swimming and the tail suspension tests (*Figure III-16*). The time mice were immobile was scored in the two tasks. No difference was detected in the behavioural response of the two groups in the two tasks: t (17) = 0.2401, p = 0.8131 in the TST; t (59) = 0.4466, p = 0.6568 in the FST.

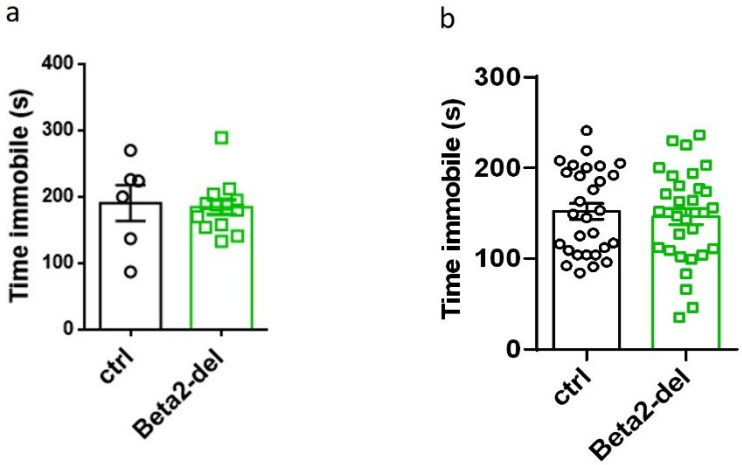

Figure III-16 TST and FST – Time that mice spent immobile when suspended by the tail (a) or immersed in water (b). Data are shown as mean ± SEM. TST: Ctrl=6, Beta2-del=11; FST: Ctrl=29, Beta2-del=32. *In black: ctrl mice injected with AAV5-GFP, in green: Beta2-del mice injected with AAV5-Cre-GFP.*

iv. *Social behaviour*

To investigate if social behaviour would be affected by the deletion of striatal β2-nAChRs, we performed the social preference task. At first, we considered the time mice spent in each chamber of the 3 chambers apparatus (*Figure III-17*).

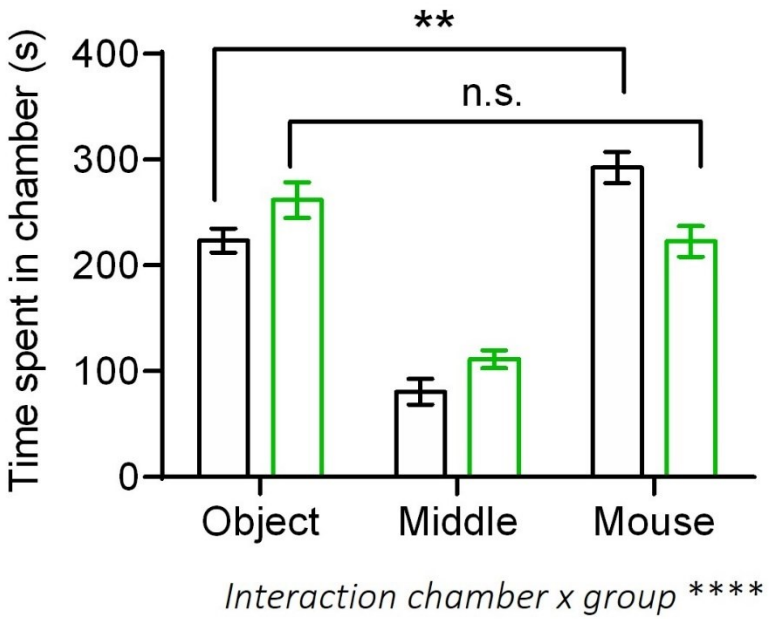

*Figure III-17 Social preference task – Time spent by mice in each chamber of a three-chamber apparatus. Data are shown as mean ± SEM; **: p < 0.001; ****: p < 0.0001. Ctrl=29, Beta2-del=32. In black: ctrl mice injected with AAV5-GFP, in green: Beta2-del mice injected with AAV5-Cre-GFP.*

Control mice clearly preferred spending more time in the chamber where the social stimulus was presented (indicated as 'mouse', along the x-axis on the right; adjusted p = 0.0016 for 'mouse' vs 'object' comparison with Sidak's post hoc test) rather than in the other two, 'object' and 'middle' ones; Beta2-del animals exhibited an opposite trend, favouring the 'object' chamber over the 'mouse' and 'middle' ones. Beta2-mutants did not show chamber preference between the 'object' and the 'mouse' ones (adjusted p = 0.1008, with Sidak's post hoc test), whereas there was a chambers x group

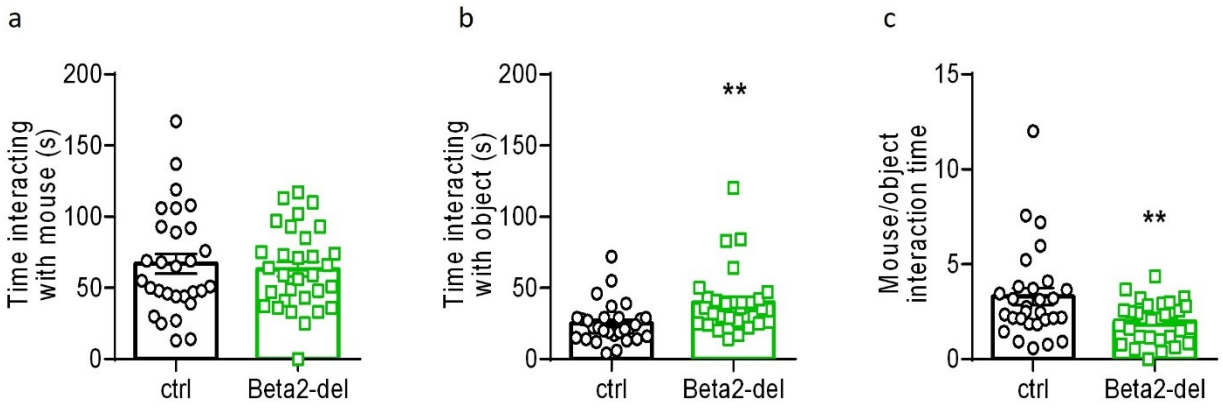

*Figure III-18 Social interaction task – (a) Direct interaction time with a social stimulus (mouse); (b) direct interaction time with a simple object; (c) interaction time with the social stimulus/ interaction time with the object. Ctrl=29, Beta2-del=32. Data are shown as mean ± SEM; **: p < 0.001. In black: ctrl mice injected with AAV5-GFP, in green: Beta2-del mice injected with AAV5-Cre-GFP.*

interaction (F (2, 174) = 10.13, p < 0,0001, 2-ways ANOVA) effect. Taking a closer look at the time spent interacting with both the empty object and the object populated with the social stimulus, revealed that surprisingly the mutants spent more time exploring the empty object (*Figure III-18* b, t = 3.064, p = 0.0035, Welch's correction of two-tailed t-test) rather than interacting with the other mouse (*Figure III-18* a; t (58) = 0.4590, p = 0.6480, unpaired two-tailed t-test). Since the average social interaction time is 67.07 ± 6.9 and 63.16 ± 5.10 SEM, for control and Beta2-del respectively, the difference in the mouse/object interaction time is driven by the longer interaction with the non-social stimulus of Beta2-mutants (*Figure III-18* c; t = 2.692, p = 0.0105, Welch's correction of two-tailed t-test).

v. *Learning and memory*

In the broad exploration of how the deletion of β2-nAChRs on striatal interneurons can affect different cognitive domains, learning and memory evaluation followed. We used the novel object recognition task to test the episodic-like type of memory. There was no difference in performance between Beta2-del and controls, as shown in *Figure III-19* by the recognition index (t = 1.708, p = 0.1021; unpaired t-test with Welsh's correction).

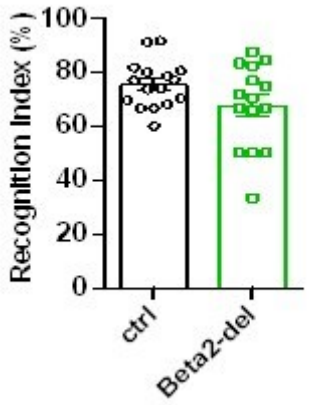

*Figure III-19 Novel object recognition task - The recognition index was calculated as Recognition index = time exploring novel object/(time exploring novel object + time exploring familiar object)*100. Ctrl=29, Beta2-del=32. Data are shown as mean ± SEM. In black: ctrl mice injected with AAV5-GFP, in green: Beta2-del mice injected with AAV5-Cre-GFP.*

We have also tested the two groups of animals in the cued version of the Morris water maze, to estimate their goal-directed behaviour. Two main parameters were considered: the time needed to reach the platform (latency) and the distance swam to get to the platform (*Figure III-20*).

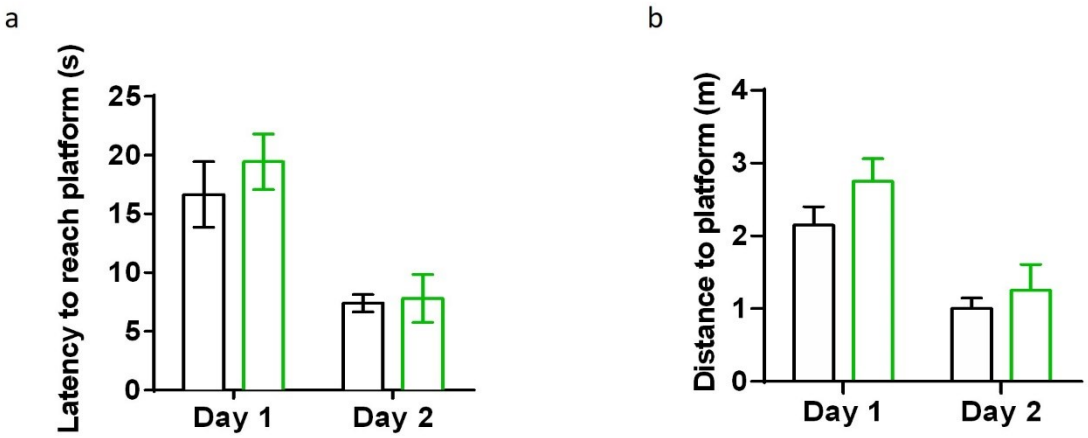

Figure III-20 Cued Morris water maze – latency to reach the platform (a) and distance travelled to reach the cued platform (b) are represented, during the training (day 1) and probe (day 2), with a 60 s intertrial interval. Ctrl=29, Beta2-del=32. *Data are shown as mean ± SEM. In black: ctrl mice injected with AAV5-GFP, in green: Beta2-del mice injected with AAV5-Cre-GFP.*

Day 1 represents the training, while day 2 is the probe day. The improvement in the latency time and the reduced distance travelled in day2, proved that the animals learnt the task. The performance of Beta2-del mice did not differ from controls' (effect of group: $F(1,29) = 0.3785$, $p = 0.5432$; effect of

the day: F(1,29) = 48.16, p < 0.0001; group versus day interaction: F(1,29) = 0.6274, p = 0.4347; two-way ANOVA).

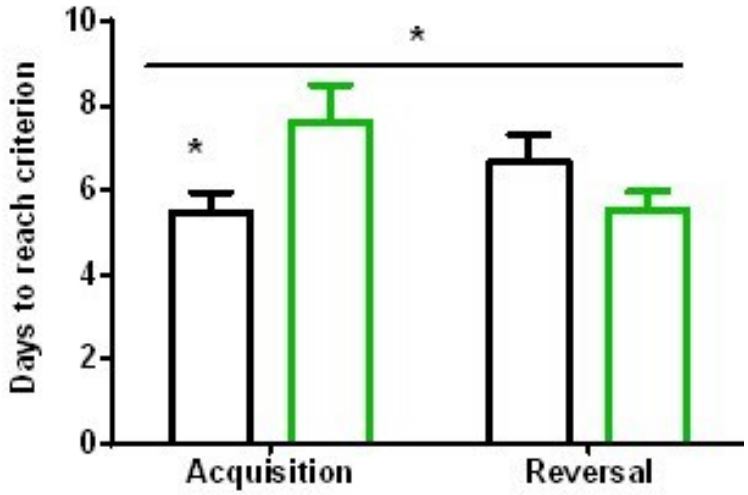

*Figure III-21 T-maze task – Time required by mice (days) to learn to reach the reward in the correct arm of the maze (Acquisition phase), based on an acquired egocentric navigation, and time required by mice (days) to learn to reach the reward placed in a new location (Reversal phase). The learning criterion in the acquisition phase was set as at least 50% of correct choices in Cohort 1 and 70% in Cohort 2. Data are shown as mean ± SEM.; *: p < 0.05. In black: ctrl mice injected with AAV5-GFP, in green: Beta2-del mice injected with AAV5-Cre-GFP. Acquisition:* Ctrl=15, Beta2-del=16; *Reversal:* Ctrl=12, Beta2-del=13.

Beta2-mutants did not show any impairment in procedural memory and consolidation, hence we trained the animals for the T-maze task, with the idea of exploring their egocentric navigation skills and their performance in reversal learning. During the acquisition phase, mice had to learn the correct body turn to execute in the T-maze to successfully reach the reward (*Figure III-21*). Different starting points (two alternative arms of the maze) were pseudo-randomly utilized alternatively. In the reversal phase, the body's turn to execute to reach the reward was the opposite as per the acquisition (*Figure III-21*). We show here, that Beta2-del mice needed more training, during acquisition, to satisfy the criterion (t(13.96) = 2.521, p = 0.0245; Welsh's t-test), while, on the contrary, they performed better than controls in the reversal phase (t(20) = 1.497, p = 0.1499, two-tailed t-test). Mutant mice showed difficulties in learning a new task based on egocentric navigation, but they did not have any problems, but actually, they were faster in reversing the learnt strategy once the change in conditions required that.

vi. *Pharmacological approach and neuronal activity*

Finally, before sacrificing the animals, we designed a last behavioural paradigm to have an insight in the neuronal adaptation occurring in the dorsal striatum when deletion of Beta2-nAChRs is in place.

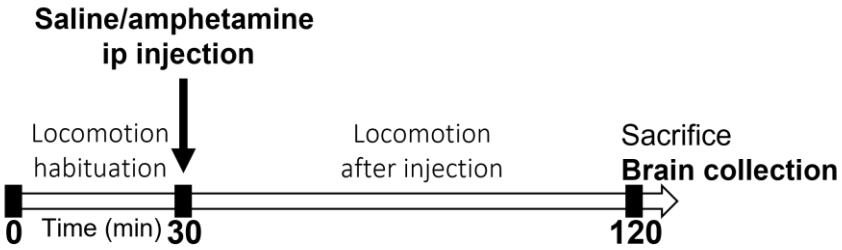

Figure III-22 Experimental design for amphetamine/saline administration and locomotor activity determination – Schematic protocol: mice were tested for 30 min in the open field (habituation), injected intraperitoneally (ip) with either saline or amphetamine and placed back in the arena where their locomotor activity was recorded for other 90 min before being sacrificed. Brains were collected for further immunohistochemical analysis.

Amphetamine is a stimulant drug that, by increasing the availability of monoamines at the synapses, favours excitatory neurotransmission. Striatal regulation of locomotor activity relies on the activation of medium spiny neurons (MSNs). The purpose of the described experiment, was to compare the neural activity in Beta2-del to control mice in the presence or absence of amphetamine. Through the use of c-Fos, an immediate early response gene used as marker for neural activity, we could evaluate the identity of the neurons activated during the task and identify the differential effect exerted by saline or amphetamine on MSNs or INs in the presence or absence of functional nAChRs.

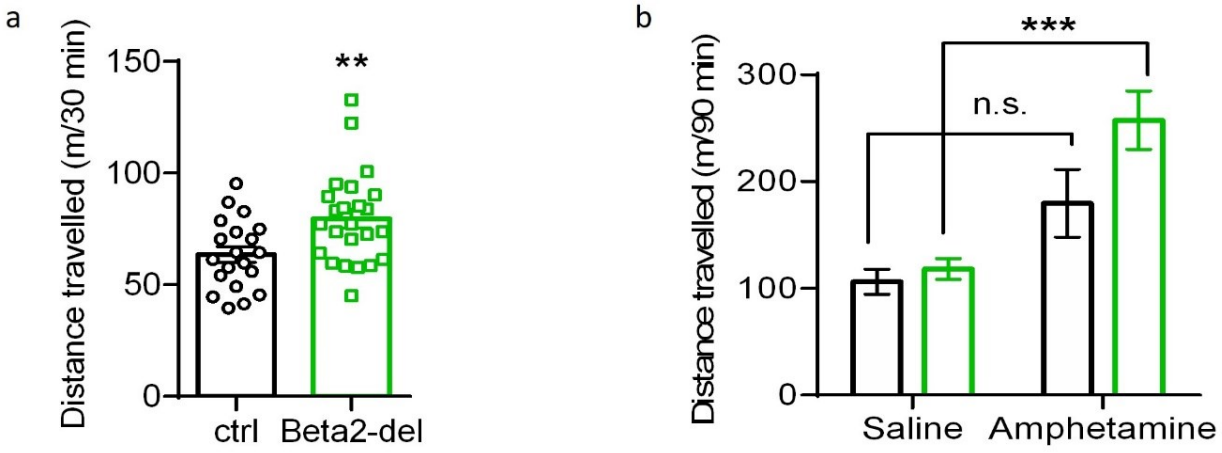

Figure III-23 Locomotor activity following saline or amphetamine administration – Distance travelled during the first 30 min of habituation (a), or during the 90 min following saline or amphetamine

*injection (b). Beta2-del: 11 got saline and 13 amphetamine; ctrl: 9 saline and 11 amphetamine. Data are shown as mean ± SEM. **: p <0.001; ***: p < 000.1. In black: ctrl mice injected with AAV5-GFP, in green: Beta2-del mice injected with AAV5-Cre-GFP.*

Interestingly, the locomotion measured in the first 30 min, showed a significant increase in Beta2-del mice (t(42) = 2.887, p = 0.006; t-test) that confirmed and strengthen the trend seen at first in the open field (*Figure III-8*) on day 1 (*Figure III-23*). After injection, amphetamine-induced hyperlocomotion was visible both in controls and mutants (effect of treatment: F(1,40) = 19.75, p < 0.0001; effect of group: F(1,40) = 3.519, p = 0.068; group x treatment interaction: F(1,40) = 1.886, p=0.1773; two-way ANOVA) but there was a remarkable increase in the locomotor activity of amphetamine-treated compared to saline-treated mice just in Beta2-del (ctrl, saline vs amphetamine: p = 0.1780; Beta2-del, saline vs amphetamine: p = 0.0006; Tukey's post-test).

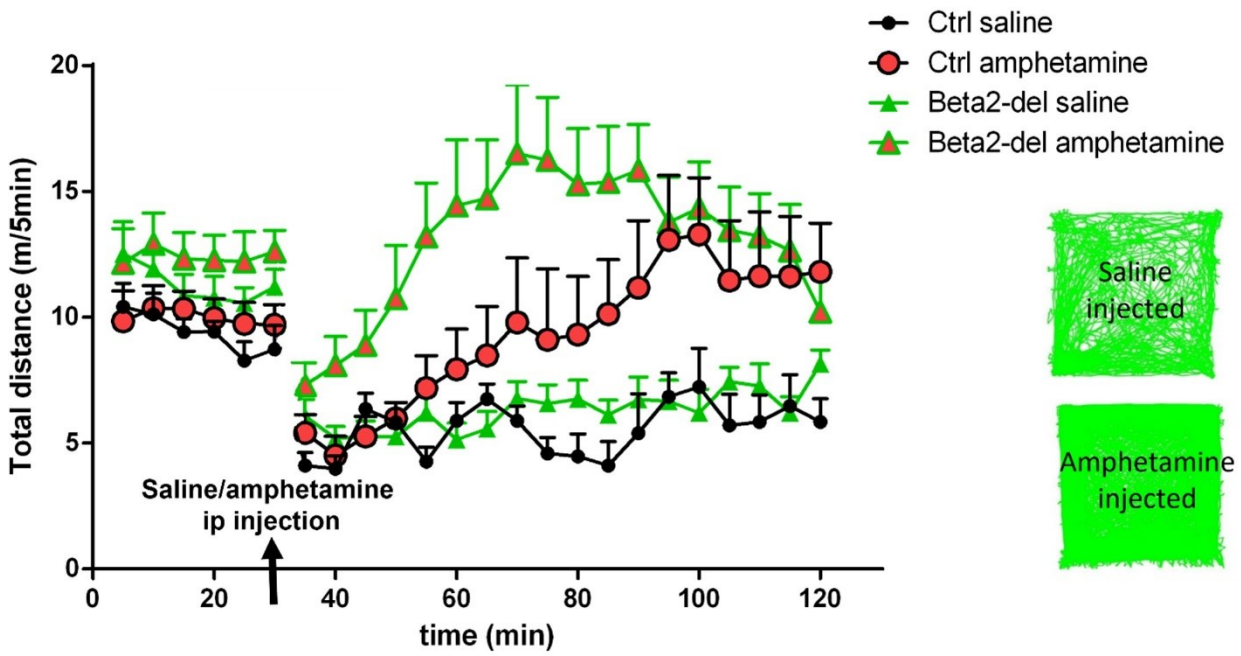

Figure III-24 Locomotor activity after pharmacological treatment – (main) The total distance, travelled by mice in the Open Field arena, split in 5 min time bins intervals. The black line shows ctrl mice injected with saline or amphetamine (black with orange dots), at min 30. The green lines, instead, stand for Beta2-mutants, administrated with saline (green triangles) or amphetamine (orange triangles). (right side) Tracking representations for Beta2-del mice after saline or amphetamine injection.

When the locomotor activity was analyzed as total distance travelled (m) in 5 min as a function of the total time considered (120 min), the effect of amphetamine administration on Beta2-del mice locomotion was clear (*Figure III-24*, main). The activity peaks between 30 and 70 min after the injection. The visualization of the locomotor patterns followed in the open field arena by two Beta2-

del animals injected with saline or with amphetamine shows the hyperlocomotion induced by amphetamine administration (*Figure III-24*, right side).

Besides the behavioural outcome, we analysed striatal activation by immunohistochemical evaluation of the c-Fos expression. In control mice, with or without amphetamine, only few c-Fos immunoreactive neurons were identified. In contrast, in Beta2-del mice, an higher density of c-Fos^{+} neurons was appreciated already in saline injected mice and it was maximal in amphetamine treated mutants (*Figure III-25*, left).

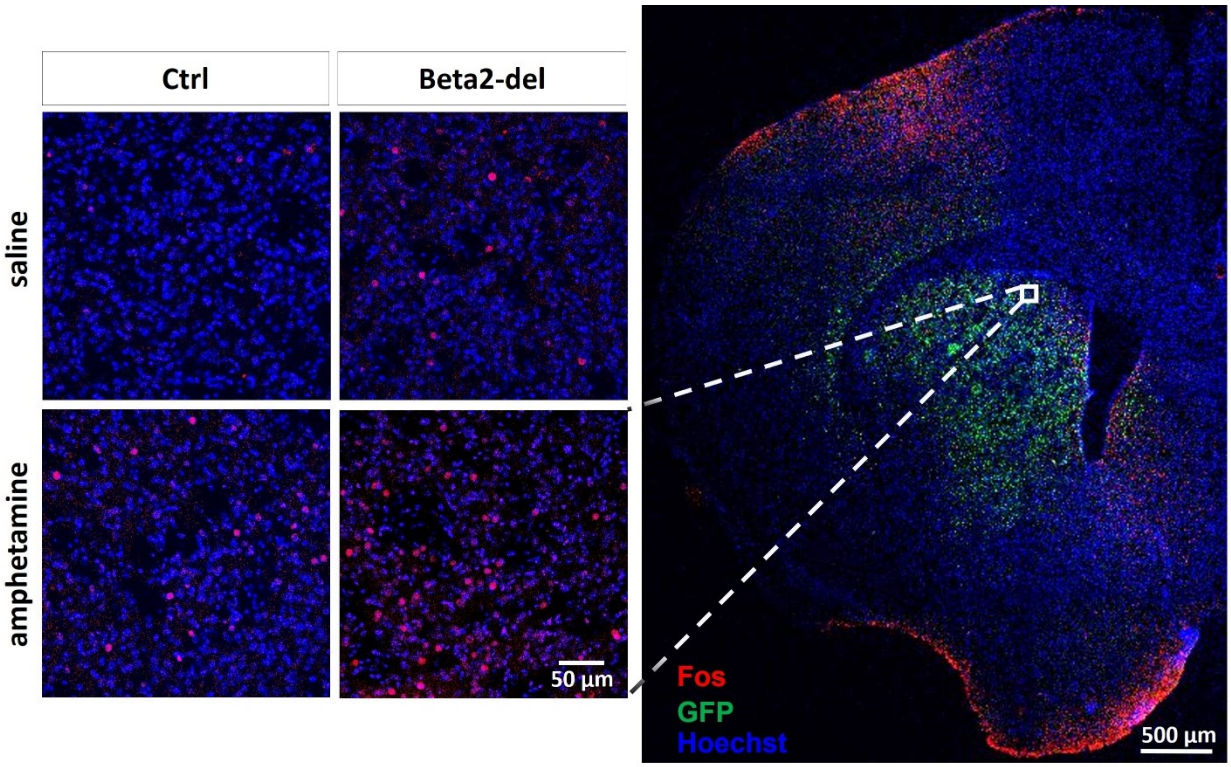

Figure III-25 c-Fos expression after saline or amphetamine administration – (right), a representative striatal section counterstained with Hoechst shows GFP and c-Fos expression. The white square identifies a typical area in the DS used for c-Fos analysis, that was acquired at the confocal with a higher magnification (40x). (left), representative close-ups, counterstained with Hoechst, showing baseline and amphetamine-induced c-Fos expression in Beta2-del and control animals.

This evidence made us question a possible correlation between the two findings and, indeed, the distance travelled in the 90 min after injection, positively correlated with the percentage of c-Fos-expressing cells in the dorsal striatum (*Figure III-26* b). The c-Fos expression data congruently reflected the locomotion observed, with the effect of group: $F(1,33) = 5.958$, $p = 0.0202$; effect of treatment: $F(1,33) = 10.15$, $p = 0.0031$; group x treatment interaction: $F(1,33) = 0.9106$, $p = 0.3469$;

in the two-way ANOVA (*Figure III-26* a). Post-tests pointed out only a difference between the saline- and amphetamine-injected Beta2-del mice (p = 0.0222, Tukey's multiple comparisons test).

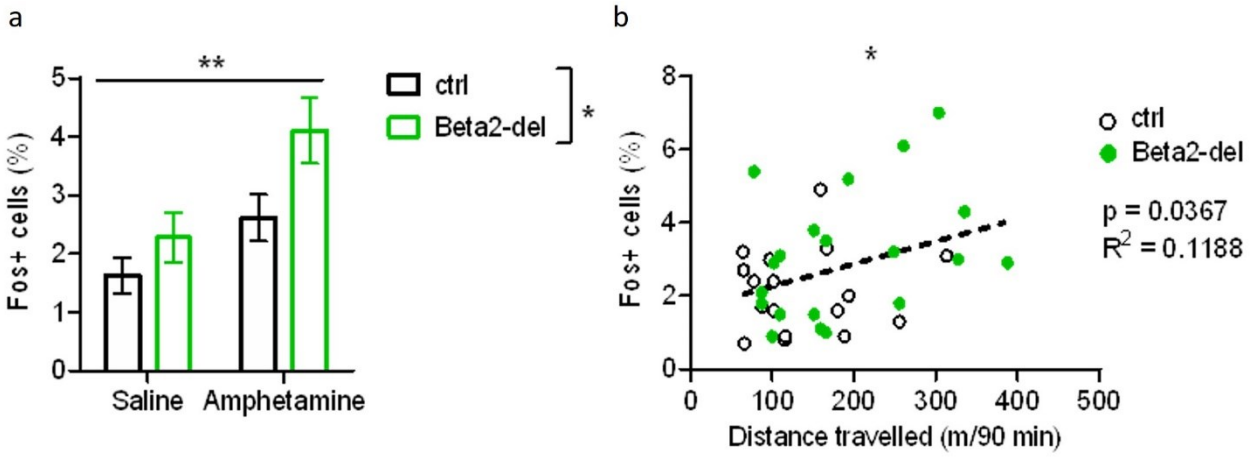

Figure III-26 c-Fos quantification and correlation with locomotion – (a) Quantification of cells expressing c-Fos (% of Fos⁺ cells/nuclei). (b), Fos quantification is plotted as a function of the distance travelled after injection. (Figure III-23). Fos increase correlated with locomotion (*) and reproduced the observed differences in locomotion between genotypes.
**: p <0.05; **: p < 00.1. Data obtained from 11 Beta2-del saline-injected and 9 amphetamine-treated; 8 and 9, respectively, for controls. Six brain sections per mouse were analyzed (1000 nuclei on average per picture). In black: ctrl mice injected with AAV5-GFP, in green: Beta2-del mice injected with AAV5-Cre-GFP.*

Next, we wanted to explore more to identify which kind of striatal neurons were the ones expressed c-Fos. We coupled GFP and c-Fos detection, dopamine- and cAMP-regulated neuronal phosphoprotein (DARPP-32) or vesicular acetylcholine transporter (VAChT) to distinguish MSNs or CINs, respectively. GFP helped us to localize cells transduced by the virus; c-Fos showed the cells activated by the pharmacological treatment; DARPP-32 in combination with c-Fos told us how many MSNs were activated (*Figure III-27*), while, similarly, VAChT in combination with c-Fos identified the CINs activated (Figure III-29).

As expected, since MSNs represent 95% of striatal neuronal populations, the cyan signal associated with the anti-DARPP-32 antibody is highly represented and, due to its cytoplasmatic expression, it looks like very diffuse staining (*Figure III-27*). We needed to use a multi-stacks acquisition approach with the confocal microscope to be sure we could visualize the entire cells for co-localization evaluation with c-Fos (magenta signal). Most of the cells (85-90%, *Figure III-28* a) as complementary data to reach the full 100% - meaning that what is not DARPP-32⁻/c-Fos⁺ is DARPP-32⁺/c-Fos⁺ out of

the entire pool of c-Fos$^+$ cells), in all four conditions, were double-positive for DARPP-32 and c-Fos, proving striatal involvement in the control of locomotor activity.

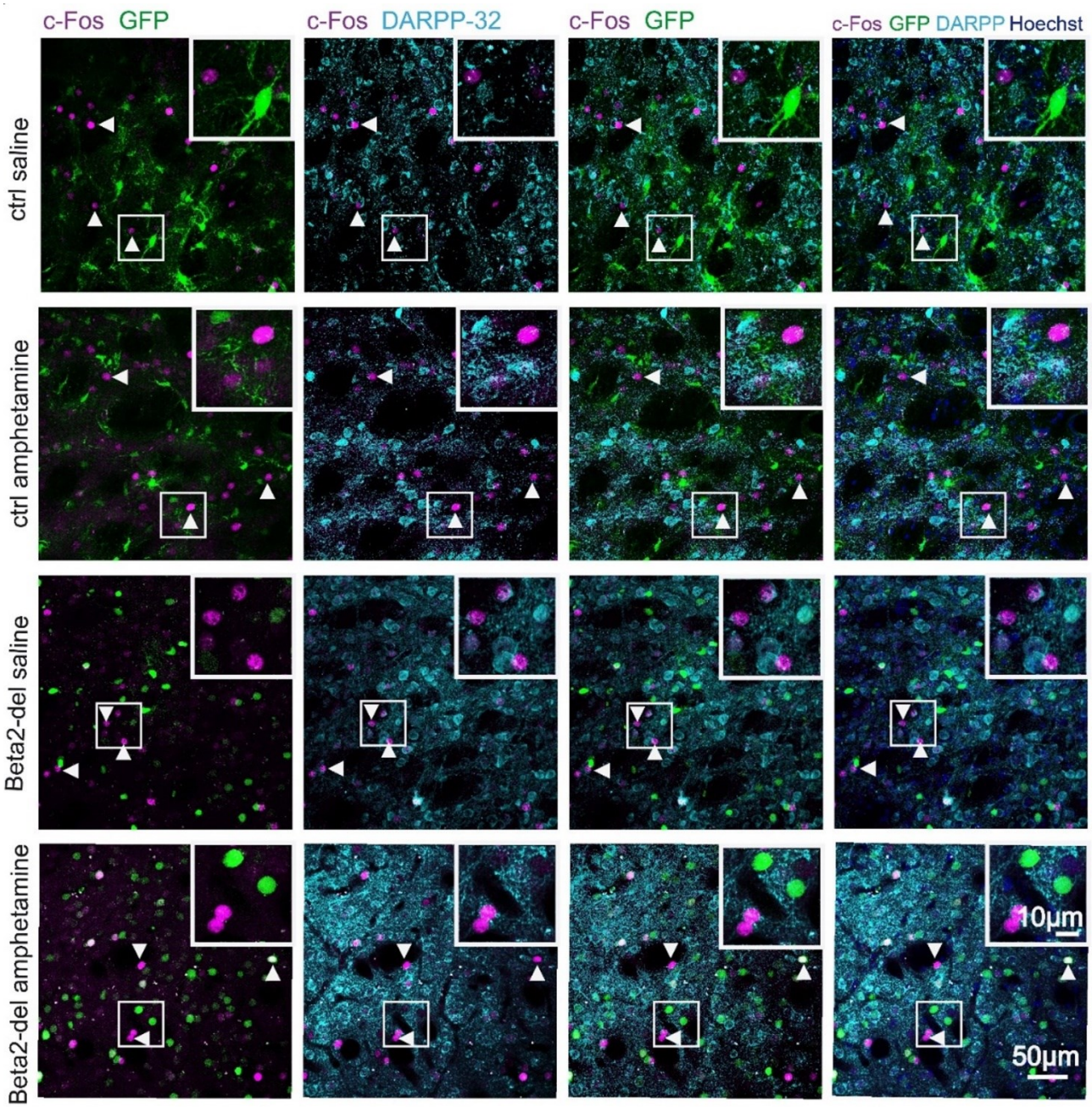

Figure III-27 c-Fos in MSNs – Representative panel of images showing baseline and amphetamine-induced c-Fos expression in Beta2-del and control animals in combination with DARPP-32 and GFP staining (indicating the AAV-expressing area with presumed Beta2-deletion). From the left, merged images represent the following: c-Fos double labelling with GFP; c-Fos double labelling with DARPP-32; c-Fos triple labelling with GFP and DARPP-32; the combination of the three markers over Hoechst counterstain for nuclei. White arrowheads highlight c-Fos-positive cells, not expressing DARPP-32. White squares represent close-ups of the c-Fos$^+$/DARPP-32$^-$ cells.

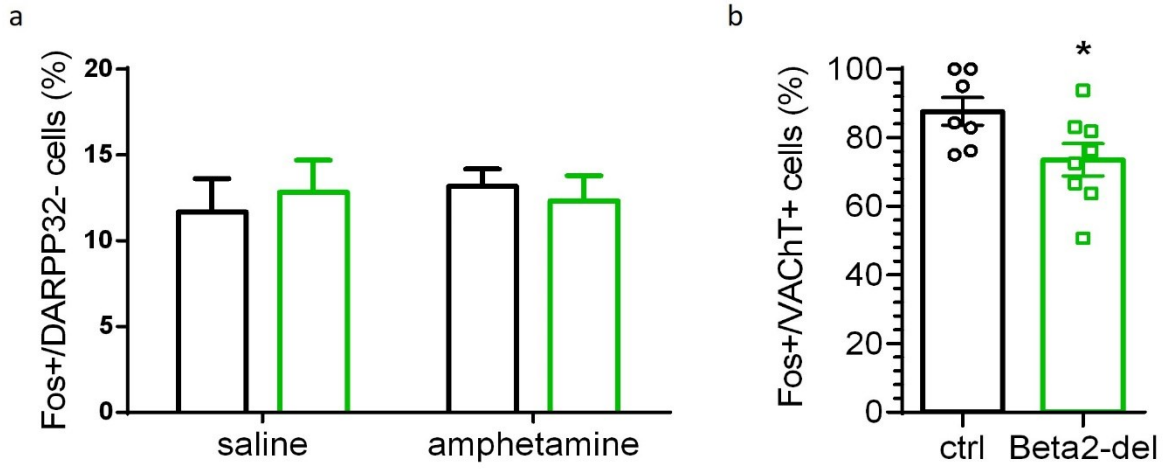

Figure III-28 Quantification and identification of Fos positive neurons as MSNs or CINs – a), the number of c-Fos⁺/DARPP-32⁻ cells is expressed as percentage of all c-Fos⁺ neurons in Beta2-del and control mice injected with either saline or amphetamine (3 mice used per each condition). Two striatal sections were analysed per mouse, with an average of 25 c-Fos⁺/DARPP-32⁻ neurons. b) shows the number of c-Fos⁺ neurons out of all VAChT⁺ neurons in control and Beta2-del mice. Saline (7 mice) and amphetamine-injected (8) mice were pooled together in each group. An average of 23 VAChT⁺ neurons were analysed in 4 brain sections per mouse. Ctrl=13, Beta2-del=13. *Data are shown as mean ± SEM. *: p <0.05. In black: ctrl mice injected with AAV5-GFP, in green: Beta2-del mice injected with AAV5-Cre-GFP.*

Then, we focused on the cells not expressing DARPP-32 (DARPP-32⁻) but expressing c-Fos (c-Fos⁺), presumably representing non-MSNs neurons, therefore, being INs. This time, we analyzed the c-Fos⁺ cells out of the VAChT⁺ expressing cells (*Figure III-28* b). Striatal Beta2 deletion decreases CINs activation (c-Fos⁺), t(13) = 2.231, p = 0.0440 in a two-tailed t-test and results in an increase in the locomotor activity.

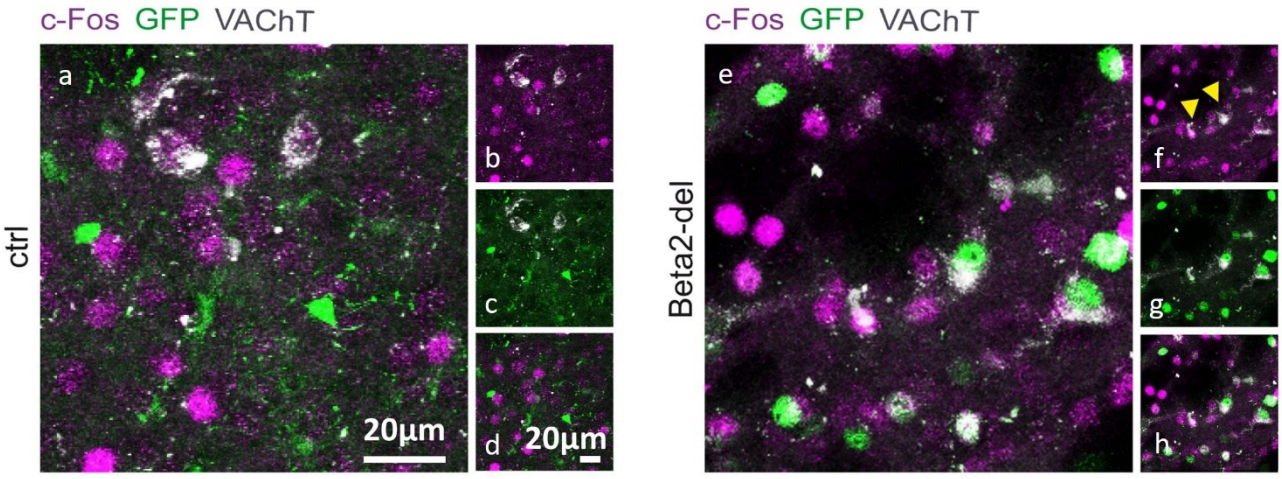

Figure III-29 Triple staining for GFP, c-Fos and VAChT to identify CINs activity - Amphetamine-induced c-Fos expression in control (left) and Beta2-del (right) animals in combination with VAChT and GFP staining is visually estimated. In the two main panels there are merged images for the three markers c-Fos (magenta), GFP (green), and VAChT (grey). On the right

rim of each main square, 3 little squares are showing the different possible combinations of markers 2 by 2. From the top: c-Fos/VAChT, GFP/VAChT, and c-Fos/GFP. Yellow arrowheads indicate two VAChT$^+$/c-Fos- CINs in Beta2-del animals.

B. β2-nAChRs in the prefrontal cortex

a) Model characterization

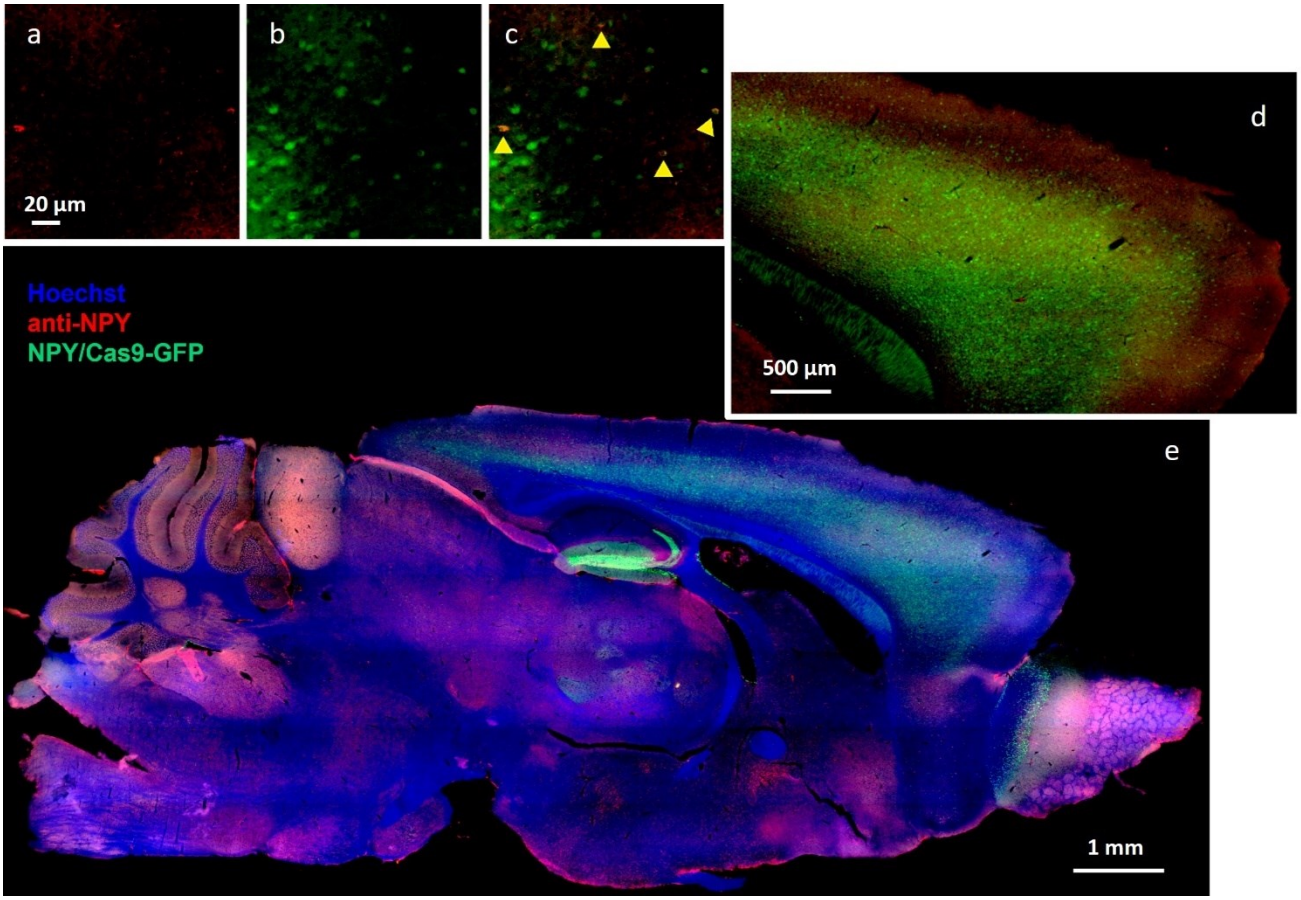

Figure III-30 Overview of the problem of the NPY-driven non-specific expression of GFP. (e) sagittal section co-stained with anti-NPY and anti-GFP antibodies to evaluate the extent of the overlap of the two signals on the Hoechst counterstain for the nuclei. (d) detail of the PFC, where the predominance of GFP$^+$ is striking. (a, b, c) crop of (d) split in the individual channels and merge. The yellow arrow heads show double positive cells, NPY cortical neurons expressing Cas9.

Thanks to the concomitant expression of a GFP tag with the Cas9, we could check for the fidelity of the Cas9-NPY driven expression in the NPY/Cas9 mice. Surprisingly, we saw a massive GFP expression, spreading in areas not reported in other NPY reporter lines (Van Den Pol et al., 2009). We performed immunohistochemistry combining anti-GFP staining, in green, with anti-NPY antibody, in red.

Surprisingly, the overall expression of the green and red signals did not match for the vast majority (Figure III-31). Some neurons were double positive, confirming their NPY$^+$ identity (Figure III-31 c), but most of them were, instead GFP$^+$ only (Figure III-31 d). Not many works have been published using the same NPY-Cre line (Milstein et al., 2015a) and, until recently, no one reported this problem with the specific expression of NPY promoter (Xie et al., 2022).

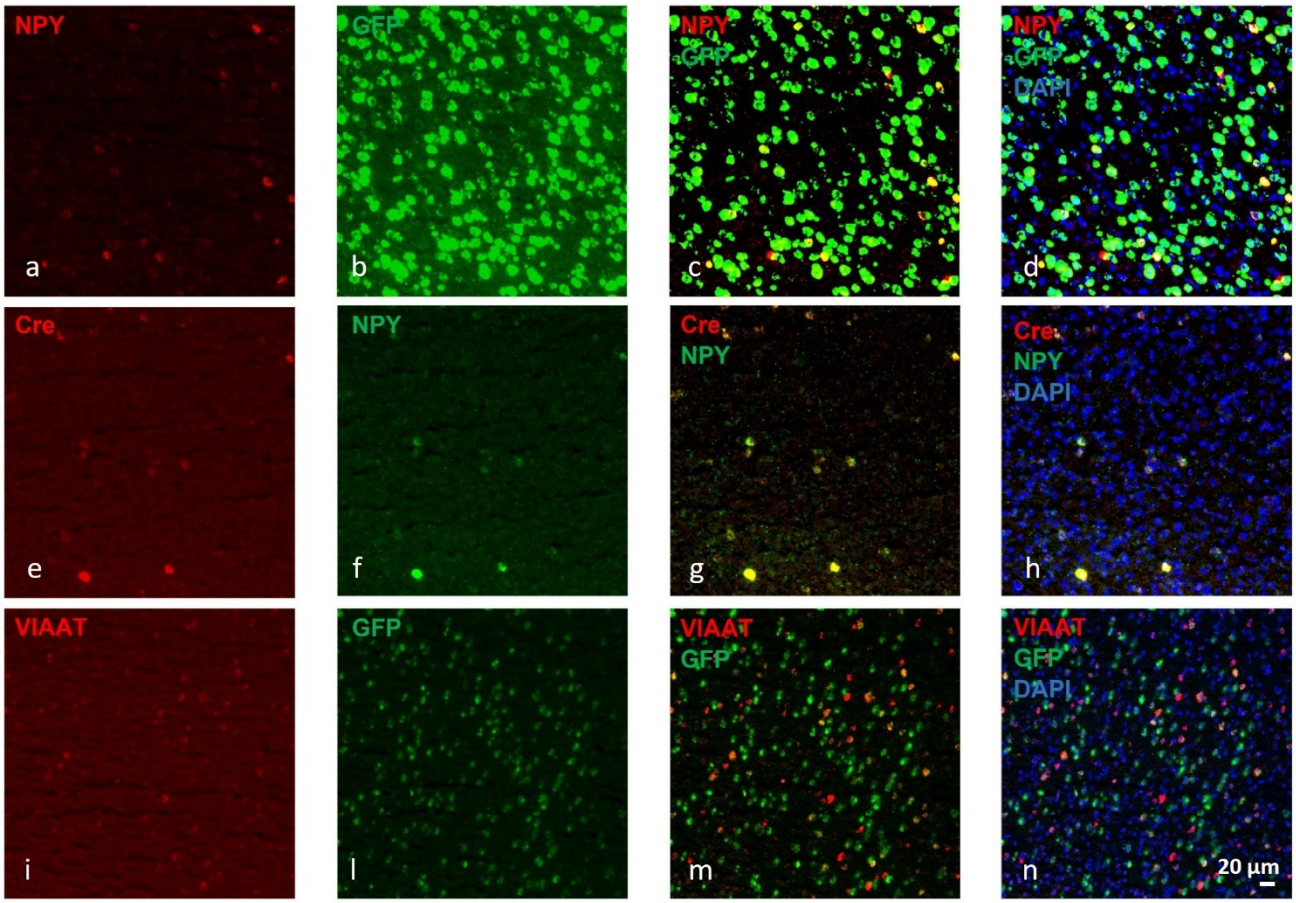

Figure III-31 Combination of different probes in double *in situ* hybridization for detection of Cre and GFP expression in NPY$^+$ cells in the PFC. (d) show NPY and GFP expression, independently and overlapped; (h) Cre expression together with NPY; (i-n) ViAAT and GFP probes are coupled to identify how many GABAergic interneurons express the Cas9-GFP tagged.

To better understand what happened in the NPY/Cas9 line, we designed a FISH experiment for the co-detection of GFP and NPY, and for NPY and Cre, for GFP and VIAAT, targeting the GABA vesicular transporter (Figure III-31 i-n). The expression of NPY mRNA perfectly matches with Cre, but again, most of the GFP-expressing cells did not express NPY anymore, and also, some of these neurons were VIAAT$^+$ (Figure III-31 m). In NPY/Cas9 mice, Cas9 is expressed in Cre dependent manner and Cre expression mediates the removal of a stop codon for Cas9-GFP expression. It follows that if in a cell at any point in time, for example during development, the NPY promoter has been active, then that cell will keep expressing the Cas9-GFP and so it will result as GFP$^+$ even if it is not expressing NPY

anymore. This unexpected inconvenience undermined the plan to use the CRISPR/Cas9 approach to obtain a more specific deletion of β2-nAChRs in the selected targeted population of GABAergic cortical interneurons. Nonetheless the use of NPY/Cas9 mice could be useful for proving the efficacy of the use of a CRISPR/Cas9 approach for obtaining a specific deletion in vivo.

i. The efficiency of CRISPR/Cas9-mediated gene editing in vitro

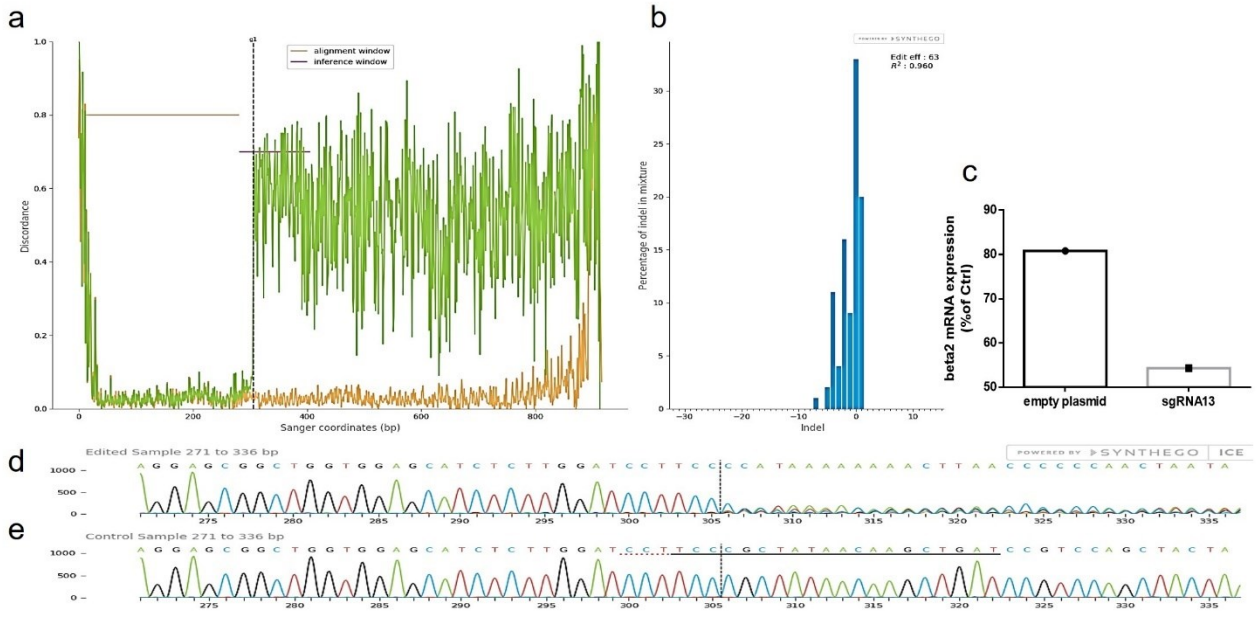

Figure III-32 In vitro assay for assessing the efficiency of the CRISPR/Cas9 editing. a) graphical representation of the degree of discordance obtained in the Sanger sequence calculated by Synthego. The green line represents the mutated sample, while the orange stands for the control. b) distribution of indels in the mixture. c) qPCR showing a decrease in beta2 mRNA in the plasmid transfected with the saRNA13. d) frequency of appearance for bases in their given position for the sample edited with sg13RNA edited or the control sample e).

To assess the efficiency of the CRISPR editing in vitro, we co-transfected F11 cells with a plasmid carrying Cas9 and one carrying CHRNB2gRNA, or with the empty vector as control, we collected the pool of cells and sent them for sequencing. The obtained sequencing data, were further analyzed with ICE v2 Synthego Tool, and the traces obtained are presented in Figure III-32, together with the outcome of a qPCR executed on the same samples (graph with columns on the right). In the output, the curves represents the degree of discordance. It is set-up around 0.5 for the control sample (Figure III-32 a, green), while in orange the analysis of the sample with the guide-RNA, where the discordance drops at 0.0-0.1. In another way to visualize the comparison in the Sanger data, the mutated sample

corresponds to the upper line (Figure III-32 d), while the control is on the bottom (Figure III-32 e). The colored peaks are histograms reporting the frequency of appearance of a single nucleotide in a given position. By focusing on the region starting after 305 bp, it is possible to appreciate how the peaks are flattened in the so-called 'Edited Sample 271 to 336 bp', while in the 'Control Sample 271 to 336 bp' the peaks relative to the different nucleotide change in a range between 200 and 900 (Figure III-32 d, e). The editing efficiency calculated by Synthego software and reported in the graph with the blue histograms, in the middle, equals 63% with an R^2 of 0.960 (Figure III-32 b). The qPCR data (Figure III-32 c) show a 25% less in chrnb2 mRNA expression for the sgRNA13 samples compared to controls.

ii. Stereotaxic surgeries and viral transduction efficiency

Eight weeks old NPY/Cas9 male mice underwent stereotaxic surgeries and got inject in the PFC with either sgRNA13 or scr-RNA. After allowing for the maximal expression of the virus (3 weeks), the cohorts are ready to be tested in behavioural paradigms.

To enhance the chances of obtaining bilateral injections, we injected each animal in both hemispheres, in two different coordinates (Figure III-33 a). Mice were injected bilaterally at 0.4 ML, 2.5 AP, 1.9 DV from bregma, and 0.3 ML, 2.2 AP, 2.1 DV with 500 nl/site at 0.05 µl/min of delivery rate.

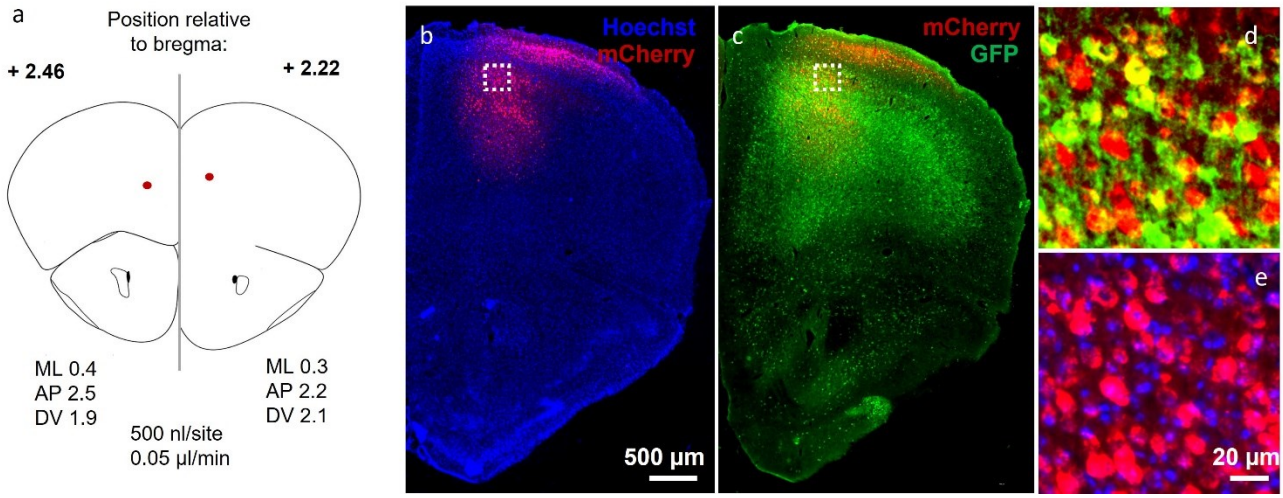

Figure III-33 Stereotaxic coordinates and viral transduction efficiency – (a) scheme adapted from Franklin & Paxinos (2007) Mouse Brain Atlas shows the 2 different bregma levels used for the stereotaxic injections and the full coordinates. (b, c) representative images of a section of a mouse dorsal striatum after AAV-Cre-GFP injection, 10x overview. (e) close-up showing the spreading of the mCherry virus (red) and the transduction efficiency in vivo, in the green cells expressing Cas9-GFP. ML: medio-lateral; AP: antero-posterior; DV: dorso-ventral.

After the behavioural testing, we sacrificed the animals and we performed the histological analysis for the confirmation of the viral expression patterns (Figure III-33). In the control group (NPY/scr), 3

mice out of 12 did not show any presence if the virus in the brain tissue, even after enhancement of the mCherry signal via immunohistochemistry using an anti-RFP antibody. Similarly, in the NPY/sg13 group, 4 mice out of 17 did not show signs of the viral injection. We observed a spreading of the virus in the PFC, recognizable by the mCherry signal, in particular in the prelimbic area (PrL) and we estimated the transduction efficiency of the virus in targeting cortical cells (Figure III-33 b-e).

To get an idea of the viral transduction efficiency, we quantified the area defining the PrL in multiple serial sections for each animal (Figure III-34).

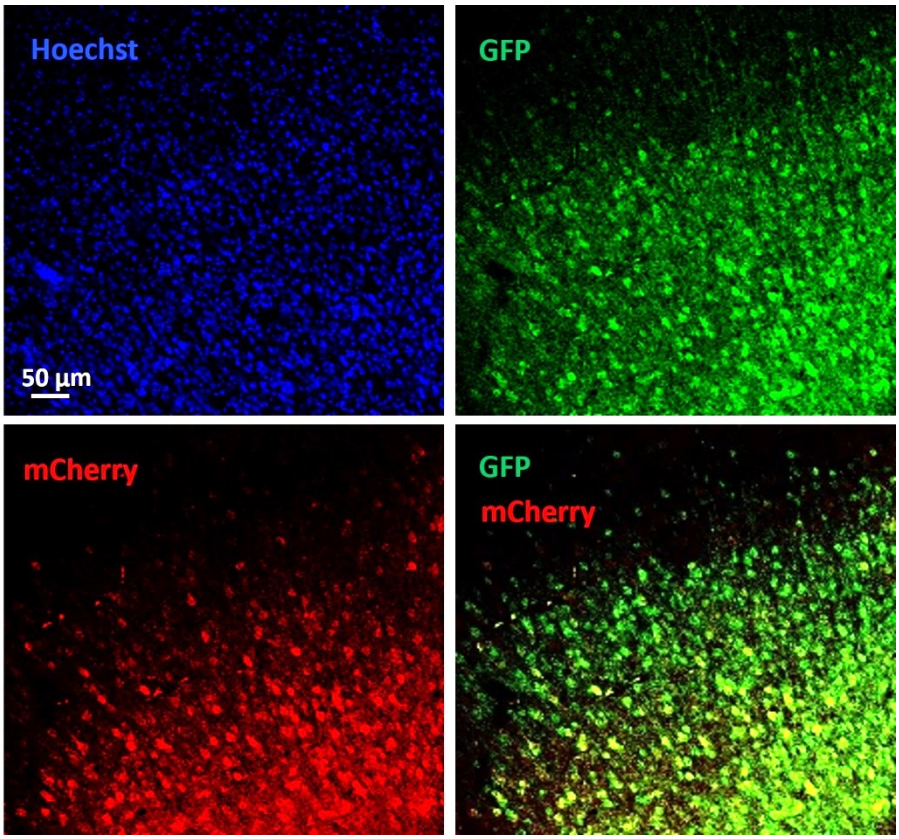

Figure III-34 Representative area of the PFC successfully targeted by viral injection. Confocal images showing three different channels acquired in a representative area of injection in the PFC show the degree of overlap between GFP^+ and mCherry-tagged cells over the total number of nuclei.

We quantified the number of double-positive cells over the total number of nuclei present in the area imaged (Figure III-35 a), and the percentage of double-positive cells was calculated by total number of GFP^+ detected in the field of view (Figure III-35 b). Not surprisingly, there was no difference in the percentage of labelled cells, even when we compared the control group versus mutants. It was not really necessary to keep the two groups separate in this case since we expected the variability could have been only due to the execution of the surgeries. The viral transduction efficiency resulted

around 20% of the total nuclei (t (19) = 0.2310 , p = 0.8198) and it increased to 65% when considered as percentage of the green cells (t (19) = 0.1645, p = 0.8710).

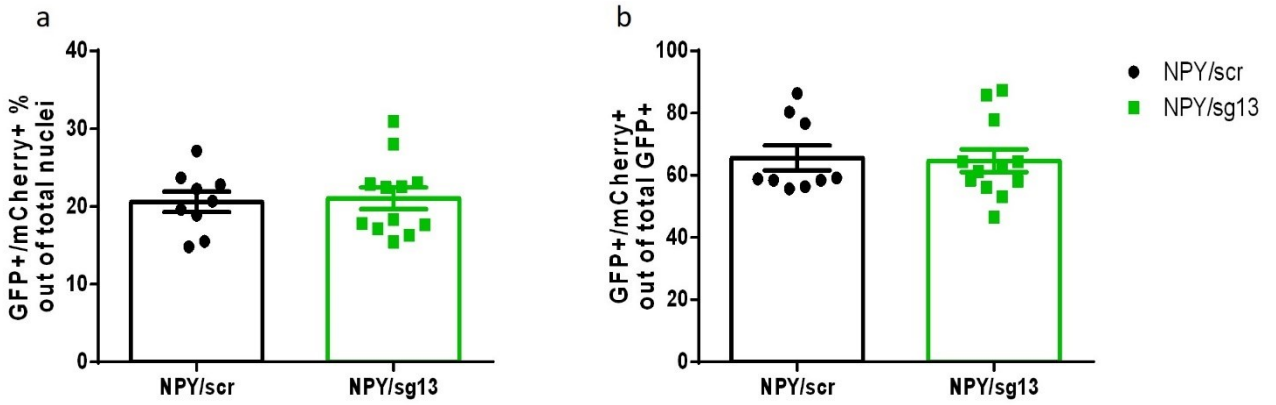

Figure III-35 Quantification of double positive cells GFP⁺/mCherry⁺ in the mouse PFC after stereotaxic surgery. *In black: ctrl mice injected with AAV5-scrRNA-mACherry, in green: Beta2-del mice injected with AAV5-sg13RNA-mCherry.* NPY/scr=9 , NPY/sg13=12.

b) Behaviour

To test the effect of the CRISPR/Cas9 approach in inducing selective deletion of Beta2-nAChRs, we focused, for the behavioural characterization, on the investigation of the social interaction and the anxiety-like behaviour, since it was proved how the lack of Beta2-nAChRs in the PFC affects social interaction (Avale et al., 2011).

i. Social preference and social novelty task

Mice were tested in the three chambers apparatus. This time, the social preference task was followed by the social novelty part, in which the first choice, object (obj) vs mouse (ms 1) during session 1, became known as a mouse (ms 1) vs new mouse (ms 2), in session 2.

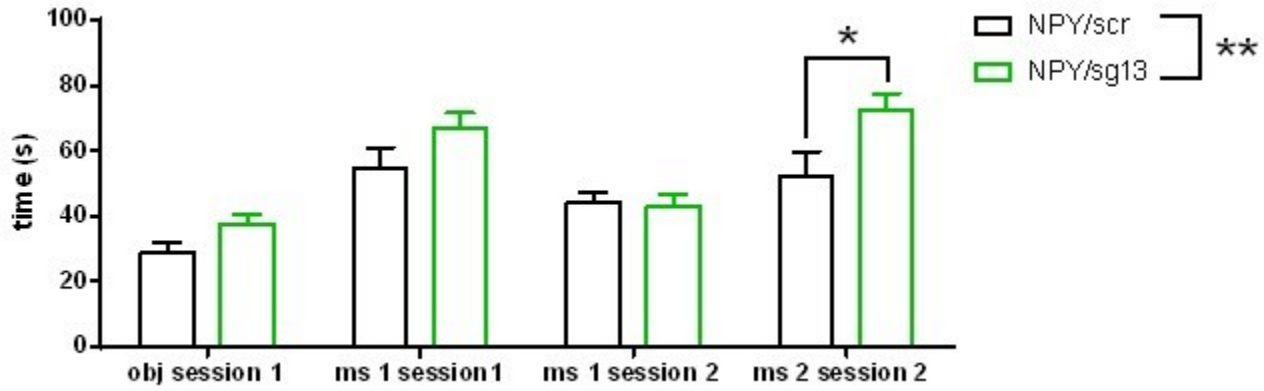

Figure III-36 Interaction time during the social preference and social novelty task. The ** symbolize an overall effect of the groups NPY/scr vs NPY/sg13 $p < 0.001$. Data are shown as mean ± SEM. *In black: ctrl mice injected with AAV5-scrRNA-mACherry, in green: Beta2-del mice injected with AAV5-sg13RNA-mCherry.* NPY/scr=9 , NPY/sg13=12.

When we scored the time mice spent interacting with the obj or ms 1 in session 1, rather than ms 1 or ms2, NPY/sg13 spent longer time than NPY/scr in the exploration of the social stimuli. Beside a general effect of the groups on the behavioural outcome ($F(1, 72) = 9.025$, $p = 0.0037$, two-way ANOVA), NPY/sg13 animals spent more time in the interaction with the novel mouse in the second session of the task (Figure III-36, adjusted $p = 0.0118$, with Sidak's post hoc test). The increase in social interaction was in line with literature data proving that the deletion of Beta2-nAChRs was in place.

ii. Anxiety-like behaviour

Mice were tested in the EPM task. We evaluated the number of entries in the open or closed arms evaluated (Figure III-37 a), together with the time spent in each of the two compartments of the maze (Figure III-37 b). NPY/sg13 had a higher number of transitions between open and closed arms, with a general effect of the group in the number of entries ($F(1, 38) = 10.89$, $p = 0.0021$, two-way ANOVA) and a difference in the entries the mutant did towards the closed arms (adjusted $p = 0.0058$ with Sidak's multiple comparison post hoc test). This difference was shaped by less time spend in the closed arms during the exploration, indicating a less anxious attitude. Interaction group x arms, $F(1, 38) = 7.953$, $p = 0.0076$, two-way ANOVA and NPY/sg13 spent less time in the closed arms compared to NPY/scr, as indicated by Sidak's multiple comparison post hoc test, with adjusted $p = 0.0206$.

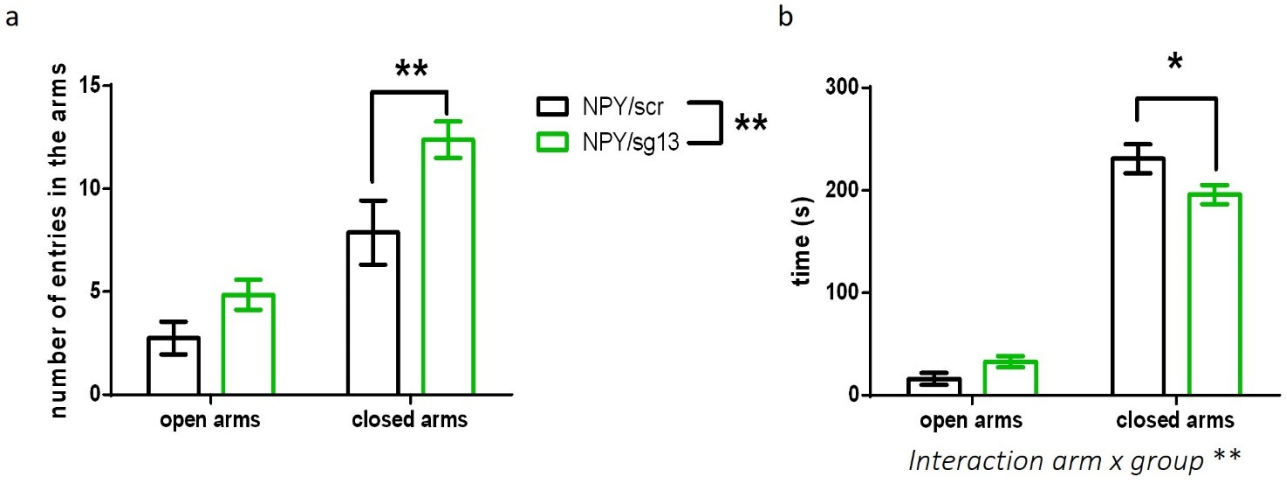

Figure III-37 Elevated Plus Maze for anxiety-like behaviour. a) number of entries in the arms. b) time spent in the arms. In black: ctrl mice injected with AAV5-scrRNA-mACherry, in green: Beta2-del mice injected with AAV5-sg13RNA-mCherry. NPY/scr=9 , NPY/sg13=12. Data are shown as mean ± SEM.

Annex

Table III-1 Statistics relative to Beta2-fx/fx behavioural data

Figure	N (mice)	Statistical analysis		Value	p-value
Figure III-8 **a**	Ctrl=29, Beta2-del=32	Two-way ANOVA	Day	F(1,59) = 17.81	p = 0.0001
			Group	F(1,59) = 1.255	p = 0.2672
			Group x Day	F(1,59) = 3.409	p = 0.0699
Figure III-9 a		Two-way ANOVA	Day	F(1,59) = 38.56	p < 0.0001
			Group	F(1,59) = 8.925	p = 0.0041
			Group x Day	F(1,59) = 6.494	p = 0.0134
Figure III-10		Mann-Whitney U test			p = 0.3994
Figure III-11 **a**	Ctrl=16, Beta2-del=15	Two-way ANOVA	Group	F(1,58) = 0.5290	p = 0.4699
Figure III-11 **b**		Two-way ANOVA	Group	F(1,58) = 0.0078	p = 0.9297
Figure III-12 **a**		Mann-Whitney U test	Group		p = 0.2354
Figure III-12 **b**		Unpaired t-test	Group	t = 1.096	p = 0.2823
Figure III-12 **c**		Mann-Whitney U test	Group		p = 0.1427
Figure III-13		Unpaired t-test	Group	t = 0.2103	p = 0.8349
Figure III-14	Ctrl=29, Beta2-del=32	Two-way ANOVA	Arm	F(1, 110) = 252.6	p < 0.0001
			Group	F(1, 110) = 0.0375	p = 0.8467
Figure III-15	Ctrl=13, Beta2-del=16	Unpaired two-tailed t-test	Group	t(27) = 2.184	p = 0.0378
Figure III-16 **a**	Ctrl=6, Beta2-del=11	Unpaired two-tailed t-test	Group	t(17) = 0.2401	p = 0.8131
Figure III-16 **b**	Ctrl=29, Beta2-del=32	Unpaired two-tailed t-test	Group	t(59) = 0.4466	p = 0.6568
Figure III-17	Ctrl=29, Beta2-del=32	Sidak´s post hoc test	'mouse' vs 'object'		adjusted p = 0.0016
			object' vs 'mouse'		adjusted p = 0.1008

Figure	N (mice)	Statistical analysis		Value	p-value
Figure III-18 **a**		Two-way ANOVA	Chamber x group	F(2, 174) = 10.13	p < 0.0001
		Unpaired two-tailed t-test	Group	t (58) = 0.4590	p = 0.6480
Figure III-18 **b**		Welch's correction of the two-tailed test	Group	t = 3.064	p = 0.0035
Figure III-18 **c**		Welch's correction of the two-tailed test	Group	t = 2.692	p = 0.015
Figure III-19		Unpaired t-test with Welch's correction	Group	t = 1.708	p = 0.1021
Figure III-20		Two-way ANOVA	Group	F(1,29) = 0.3785	p = 0.5432
			Day	F(1,29) = 48.16	p < 0.0001
			Group x day	F(1,29) = 0.6274	p = 0.4347
Figure III-21	Acquisition: Ctrl=15, Beta2-del=16; Reversal: Ctrl=12, Beta2-del=13.	Welch's t test		t(13.96) = 2.521	p = 0.0245
		Two tailed t-test		t(20) = 1.497	p = 0.1499
Figure III-23 **a**	Beta2-del saline (n=11), Beta2-del amphetamine (n=13), ctrl saline (n=9), ctrl amphetamine (n=11)	t-test	Group	t(42) = 2.887	p = 0.006
Figure III-23 **a**		Two-way ANOVA	Treatment	F(1,40) = 19.75	p < 0.0001
			Group	F(1,40) = 3.519	p = 0.068
			Group x treatment	F(1,40) = 1.886	p = 0.1773
		Tukey's post-test	ctrl, saline vs amphetamine		p = 0.1780
Figure III-26 **a**			beta-2-del, saline vs amphetamine		p = 0.0006
Figure III-26 **b**	Beta2-del saline (n=11), Beta2-del amphetamine	Two-way ANOVA	Group	F(1, 33) = 5.958	p = 0.0202
			Treatment	F(1, 33) = 10.15	p = 0.0031

Figure	N (mice)	Statistical analysis		Value	p-value
	(n=9), ctrl saline (n=8), ctrl amphetamine (n=9)		Group x treatment	F(1, 33) = 0.9106	p = 0.3469
Figure III-28 **b**	Beta2-del (n=13), ctrl (n=13)	Two-tailed t-test	Group	t(13) = 2.231	p = 0.0440

Table III-2 Statistics relative to the data presented for NPY/scr and NPY/sg13 mice injected in the PFC

Figure	N (mice)	Statistical analysis		Value	p-value
Figure III-35 a	NPY/scr (n=9), NPY/sg13 (n=12)	Unpaired t-test	Group	t(19) = 0.2310	p = 0.8198
Figure III-35 b		Unpaired t-test	Group	t(19) = 0.1645	p = 0.8710
Figure III-36		Two way ANOVA	Group	F(1, 72) = 9.025	p = 0.0037
		Sidak's post hoc test			p = 0.0118
Figure III-37 a		Two-way ANOVA	Group	F (1, 38) = 10.89	p = 0.0021
		Sidak's multiple comparison post hoc test			adjusted p = 0.0058
Figure III-37 b		Two-way ANOVA	Group x arms	F (1, 38) = 7.953	p = 0.0076
		Sidak's multiple comparison post hoc test			adjusted p = 0.0206.

IV. Discussion

Technological advancement in every field is faster than ever. Nowadays, a growing number of different tools is available to approach scientific questions from many different angles. Recently, the technological advances such as single cell transcriptomics and sophisticated genetic tools have enabled us to recognize the rich diversity of neuronal types in different brain regions and genetically access the individual neuronal types for specific manipulations. However, even though our knowledge of the brain is quickly expanding, it is still relatively difficult to selectively target a specific receptor subtype in a defined neuronal population. Current research pointed out how the evolutionary drive pushed brain development towards tuning the system in the most specialized way, defining each area of the brain within a hierarchical organisation (Kolk & Rakic, 2022; X.-J. Zhang et al., 2017; Crittenden & Graybiel, 2011; Voorn et al., 2004). Different brain regions work as independent functional units but since they are physically interconnected, they act, at the same time, as a whole. They utilize the same set of neurotransmitters and their receptors to integrate and vehiculate the information. In this context, we showed how important is to define and address in a selective fashion specific neuronal population in restricted areas of the brain (Bakken et al., 2016; Close et al., 2017; Tasic et al., 2018).

In the present work, we first used the Cre/loxP system to perform a cell-type non-specific deletion of β2-containing nAChRs expressed by all striatal neurons to investigate their effect on behaviour.

Identification of striatal neurons expressing β2-containing nAChRs.

Our current knowledge of the expression of nAChRs by individual types of striatal neurons primarily arises from functional studies which detected changes in neuronal firing after the application of nicotine or nAChRs antagonists coupled with optogenetic activation of CINs (Assous et al., 2018b; English et al., 2012; Ibanez-Sandoval et al., 2010, 2011; Koós et al., 1999; Koós & Tepper, 2002; Sullivan et al., 2008; Tepper et al., 2008). As main findings, they revealed the expression of nAChRs generally by striatal GABAINs (Assous et al., 2018; Faust et al., 2016; Sullivan et al., 2008; Tepper et al., 2018) mostly identifying fast-spiking INs (putative Pvalb^{+} INs), NPY- and TH-expressing INs as the main populations expressing nAChRs (Dorst et al., 2020; English et al., 2012; Ibanez-Sandoval et al.,

2011; Koós & Tepper, 2002; Muñoz-Manchado et al., 2018; Ünal et al., 2011; Xenias et al., 2015). Due to the lack of specific and reliable antibodies that would allow the visualization of nAChRs containing β2 subunits in the striatum at the protein level, we decided to perform fluorescent *in situ* hybridization to identify striatal neuronal population expressing β2 nicotinic subunit. Through our FISH experiments, we confirmed that β2-containing nAChRs are not expressed by the striatal principal neurons, MSNs, and that, even if they are expressed overall in a low level, their expression is restricted to striatal interneurons. In particular, CINs, besides representing the main source of ACh in the striatum, they also express the vast majority (80%) of β2-containing nAChRs. Among the different GABAINs subpopulations, we found transcripts for the β2 subunit in Pvalb- and NPY-expressing GABAINs. β2 expression in these two neuronal populations displayed a sub-regional specificity as the *Chrnb2*$^{+}$ GABAINs were largely limited to the lateral part of the dorsal striatum. In summary, our FISH approach partially confirmed what has been previously reported, highlighting the relative proportions of expression for the different INs populations. Furthermore, it helped to clarify the roles the distinct types of INs play in the cholinergic control of the striatum through nAChRs activation.

Behavioural role of β2-containing nAChRs expressed by neurons in the dorsal striatum.

In this work, we used numerous behavioural tests to evaluate a broad range of behavioural and cognitive functions that are known to be associated with striatal signalling. Using these tests, we showed that β2-containing nAChRs expressed by striatal INs are involved in the control of specific behaviours. The behavioural phenotype we observed in Beta2-del mice is generally in agreement with previous studies that report centrally expressed nAChRs control social behaviour, anxiety and higher cognitive functions (Avale et al., 2008, 2011; Koukouli & Changeux, 2020; Picciotto, Lewis, Schalkwyk, et al., 2015). Specifically, the global knock out of β2 nicotinic subunit has been reported to lead to an increased interest in social novelty and impaired attentional performance (Avale et al., 2011; Guillem et al., 2011). In addition, the general higher activity of α4β2* nAChRs leads to increased anxiety in mice (Labarca et al., 2000). We did not observe any alterations in spontaneous basic behaviour such as nest building or locomotion and most prominent alterations occurred in exploratory, anxiety-like and social behaviours and in learning. In the social preference task, while the Beta2-del mice spent less time in the social compartment compared to controls, the fraction of time spent directly interacting with the social stimulus was not decreased. Instead, the fraction of

time spent interacting with the non-social object was higher, resulting in a lower sociability ratio. Therefore, the social impairment we observed in our experiments might be more related to altered exploratory behaviour and altered response to novelty in mice with striatal deletion of β2-contaning nAChRs, rather than a social impairment *per se*. In addition to changes in social and exploratory behaviour, we also found evidence of increased anxiety-like behaviour in both the open field and light/dark transition tasks. While the increased anxiety-like behaviour has not been commonly reported in mouse models with striatal alterations, nicotine and nicotinic agonists and antagonists have been implicated in the control of anxiety and they were suggested for the treatment of anxiety disorders and depression (Crouse et al., 2020; Marina Picciotto et al., 2018; Mineur et al., 2007, 2013, 2016; Picciotto, Lewis, Van Schalkwyk, et al., 2015). Finally, we found impairment of discrimination learning in the response-based T-maze. It may reflect an impaired function of striatal GABAINs expressing nAChRs, as recent studies showed the involvement of striatal SST^+ and FS (putative $Pvalb^+$) GABAINs in goal-directed instrumental learning and egocentric navigation in the T-maze (Holley et al., 2019a). A more specific deletion of nAChRs, exclusively in one GABAINs population, would allow to address and distinguish more clearly which of the behavioural changes that we observed are related to individual INs populations.

Evaluation of changes in neuronal activity measured by c-Fos expression.

To obtain a deeper insight into potential changes of striatal signalling and activity following the local deletion of β2 nicotinic subunit, we decided to induced an activation of striatal neurons by administration of a stimulant, amphetamine. In agreement with a body of literature that suggests that activation of nAChRs expressed by striatal neurons results in the inhibition of MSNs (Abudukeyoumu et al., 2018; Aitta-Aho et al., 2017; English et al., 2012; Faust et al., 2016; Guo et al., 2015; Muñoz-Manchado et al., 2016; Sullivan et al., 2008; Ünal et al., 2011), we observed increased locomotor activity and increased general c-Fos expression in the striatum of Beta2-del mice after the amphetamine injection. Importantly, the neuronal activity was decreased specifically in CINs, showed as a reduced c-Fos expression in $VAChT^+$ interneurons. These data suggest that the deletion of β2-containing nAChRs in CINs leads to the decreased activity of CINs and a suppression of their inhibitory effect on striatal circuits. More in general, deleting β2-containing nAChRs can lead to an

excitatory/inhibitory imbalance and related behavioural alterations including social impairments (Han et al., 2020; Holley et al., 2019b; Hori et al., 2020; Lam et al., 2022; Trakoshis et al., 2020).

Use of CRISPR/Cas9 technology for β2 knock down in specific cellular types.

In the present work, we also used the CRISPR/Cas9 technology to perform a cell-type specific deletion of β2-containing nAChRs expressed by NPY interneurons in the PFC to investigate their effect on behaviour.

Inspired by the work of Peng et al. (2019), we wanted to use the CRISPR/Cas9 technology to induce a selective deletion of the β2 subunits of nAChRs in a specific population of GABAINs to clearly characterize the associated behavioural phenotype. We successfully developed the viral vector carrying sgRNA against CHRNB2 gene and we confirmed its efficiency in vitro. Then, our in vivo experiments resulted in a presumed knock down of beta2 nicotinic subunit in NPY^{+} neurons in the site of injection, the PFC. This led to behavioural changes, namely hyper-sociability and decreased anxiety-like behaviour, which was in agreement with data reported in the literature (Avale et al., 2011). Nonetheless, our characterization of the NPY-Cre-Cas9-GFP mice demonstrated that the Cre-driven Cas9-GFP expression is not limited to neurons showing native NPY expression in the adult mice. This is probably due to the transient activation of NPY expression during the embryonic development (leading to the removal of STOP sequence and permanently releasing the Cas9-GFP expression). We plan to investigate this possibility and there is a recent report pointing out a similar issue in the same NPY-IRES-Cre mouse line (Xie et al., 2022). Possibly due to the decreased specificity of our β2 knock down, the behavioural changes that we observed replicated the effect of β2 global knock out in the PFC (Avale et al. 2011). However, even though our NPY-Cre-Cas9-GFP-expressing neuronal population cannot account for total β2-expressing population in the PFC, it likely represents a heterogeneous group of neurons, containing both excitatory and inhibitory neurons. In future experiments, we will establish their identity and quantify the relative proportion of different neuronal types in the Cre-expressing population with beta2 knock down.

Behavioural role of β2-containing nAChRs expressed by NPY neurons in the PFC.

After the functional characterization of striatal β2-expressing nAChRs, we wanted to use a more specific approach to address the effect of their deletion in a different brain region, the PFC, with a more diverse expression of nAChRs and a more complex layer-specific regulation (Bloem et al., 2014; Poorthuis, Bloem, Verhoog, et al., 2013). By using CRISPR/Cas9 technology for inducing a presumably more specific beta2 knock down, we succeeded to replicate the increased interest in social interaction previously reported for the global $\beta2^{-/-}$ mice (Avale et al., 2011; Granon et al., 2003; Serreau et al., 2011). This increased sociability was shown to depend on the PFC, and the re-expression of the β2 subunit in this area was able to rescue it (Avale et al. 2011). When we induced the deletion of β2-containing nAChRs in the PFC we also observed a decreased of the anxiety-like behaviour in the EPM task. This effect on anxiety-like behaviour was the opposite compared to the one we reported in case of striatal deletion of β2-containing nAChRs. Nevertheless, as described above, due to the widespread cortical Cre expression in the NPY-IRES-Cre mouse line, we were not able to limit the β2 knock down to neurons expressing NPY in adult mice. Therefore, we cannot conclude whether the behavioural effect is driven by β2 knock down in projection neurons or a specific type of IN. Only a careful examination of the proportions of individual neuronal types in the NPY-Cre-Cas9-GFP expressing population may partially elucidate this question.

V. Conclusions

We confirmed our hypothesis according to which functional β2-containing nAChRs in a rare neuronal population are necessary for intact cognitive functions and modulation of the behaviour. In particular, the deletion of β2-containing nAChRs in specific types of striatal interneurons resulted in changes in social and anxiety-related behaviours. We also demonstrated that β2-containing nAChRs expressed by striatal CINs play an important role in the control of neuronal activity in the striatum. Finally, we have shown that CRISPR/Cas9 technology is a valid approach for targeting subpopulations of neurons *in vivo*.

References

Abudukeyoumu, N., Hernandez-Flores, T., Garcia-Munoz, M., & Arbuthnott, G. W. (2018). Cholinergic modulation of striatal microcircuits. *European Journal of Neuroscience*, *March*, 1–19. https://doi.org/10.1111/ejn.13949

Adli, M. (2018). The CRISPR tool kit for genome editing and beyond. In *Nature Communications* (Vol. 9, Issue 1). Nature Publishing Group. https://doi.org/10.1038/s41467-018-04252-2

Ahmed, N. Y., Knowles, R., & Dehorter, N. (2019). New Insights Into Cholinergic Neuron Diversity. In *Frontiers in Molecular Neuroscience* (Vol. 12). Frontiers Media S.A. https://doi.org/10.3389/fnmol.2019.00204

Aitta-Aho, T., Phillips, B. U., Pappa, E., Audrey Hay, Y., Harnischfeger, F., Heath, C. J., Saksida, L. M., Bussey, T. J., & Apergis-Schoute, J. (2017). Accumbal cholinergic interneurons differentially influence motivation related to satiety signaling. *ENeuro*, *4*(2). https://doi.org/10.1523/ENEURO.0328-16.2017

Alkondon, M., Pereira, E. F. R., Eisenberg, H. M., & Albuquerque, E. X. (1999). *Nicotinic Receptor Activation in Human Cerebral Cortical Interneurons: a Mechanism for Inhibition and Disinhibition of Neuronal Networks*.

Allaway, K. C., & Machold, R. (2017). Developmental specification of forebrain cholinergic neurons. In *Developmental Biology* (Vol. 421, Issue 1, pp. 1–7). Academic Press Inc. https://doi.org/10.1016/j.ydbio.2016.11.007

Angoa-Pérez, M., Kane, M. J., Briggs, D. I., Francescutti, D. M., & Kuhn, D. M. (2013). Marble burying and nestlet shredding as tests of repetitive, compulsive-like behaviors in mice. *Journal of Visualized Experiments : JoVE*, *82*, 50978. https://doi.org/10.3791/50978

Arrant, A. E., Schramm-Sapyta, N. L., & Kuhn, C. M. (2013). Use of the light/dark test for anxiety in adult and adolescent male rats. *Behavioural Brain Research*, *256*, 119–127. https://doi.org/10.1016/j.bbr.2013.05.035

Arroyo, S., Bennett, C., Aziz, D., Brown, S. P., & Hestrin, S. (2012). *Prolonged Disynaptic Inhibition in the Cortex Mediated by Slow , Non-alfa 7 Nicotinic Excitation of a Specific Subset of Cortical Interneurons*. *32*(11), 3859–3864. https://doi.org/10.1523/JNEUROSCI.0115-12.2012

Assous, M., Faust, T. W., Assini, R., Shah, F., Sidibe, Y., & Tepper, J. M. (2018). Identification and characterization of a novel spontaneously active bursty gabaergic interneuron in the mouse striatum. *Journal of Neuroscience*, *38*(25), 5688–5699. https://doi.org/10.1523/JNEUROSCI.3354-17.2018

Avale, M. E., Chabout, J., Pons, S., Serreau, P., De Chaumont, F., Olivo-Marin, J., Bourgeois, J., Maskos, U., Changeux, J., & Granon, S. (2011). Prefrontal nicotinic receptors control novel social interaction between mice. *The FASEB Journal*, *25*(7), 2145–2155. https://doi.org/10.1096/fj.10-178558

Avale, M. E., Faure, P., Pons, S., Robledo, P., Deltheil, T., David, D. J., Gardier, A. M., Maldonado, R., Granon, S., Changeux, J. P., & Maskos, U. (2008). Interplay of β2* nicotinic receptors and dopamine pathways in the control of spontaneous locomotion. *Proceedings of the National Academy of Sciences of the United States of America*, *105*(41), 15991–15996. https://doi.org/10.1073/pnas.0807635105

Bakken, T. E., Miller, J. A., Ding, S.-L., Sunkin, S. M., Smith, K. A., Ng, L., Szafer, A., Dalley, R. A., Royall, J. J., Lemon, T., Shapouri, S., Aiona, K., Arnold, J., Bennett, J. L., Bertagnolli, D., Bickley, K., Boe, A., Brouner, K., Butler, S., … Lein, E. S. (2016). A comprehensive transcriptional map of primate brain development. *Nature*, *535*(7612), 367–375. https://doi.org/10.1038/nature18637

Barbera, G., Liang, B., Zhang, L., Gerfen, C. R., Culurciello, E., Chen, R., Li, Y., & Lin, D. T. (2016). Spatially Compact Neural Clusters in the Dorsal Striatum Encode Locomotion Relevant Information. *Neuron*, *92*(1), 202–213. https://doi.org/10.1016/j.neuron.2016.08.037

Beckmann, J., & Lips, K. S. (2014). The non-neuronal cholinergic system in health and disease. In *Pharmacology* (Vol. 92, Issues 5–6, pp. 286–302). https://doi.org/10.1159/000355835

Bedwell, S. A., Billett, E. E., Crofts, J. J., & Tinsley, C. J. (2014). The topology of connections between rat prefrontal, motor and sensory cortices. *Frontiers in Systems Neuroscience*, *8*. https://doi.org/10.3389/fnsys.2014.00177

Bernard, V., Laribi, O., Levey, A. I., & Bloch, B. (1998). *Subcellular Redistribution of m2 Muscarinic Acetylcholine Receptors in Striatal Interneurons In Vivo after Acute Cholinergic Stimulation*.

Bernard, V., Levey, A. I., & Bloch, B. (1999). *Regulation of the Subcellular Distribution of m4 Muscarinic Acetylcholine Receptors in Striatal Neurons In Vivo by the Cholinergic Environment: Evidence for Regulation of Cell Surface Receptors by Endogenous and Exogenous Stimulation*.

Bernard, V., Normand, E., & Bloch, B. (1992). Phenotypical Characterization of the Rat Striatal Neurons Expressing Muscarinic Receptor Genes. In *The Journal of Neuroscience* (Vol. 7).

Besson, M., David, V., Suarez, S., Cormier, A., Cazala, P., Changeux, J. P., & Granon, S. (2006). Genetic dissociation of two behaviors associated with nicotine addiction: Beta-2 containing nicotinic receptors are involved in nicotine reinforcement but not in withdrawal syndrome. *Psychopharmacology*, *187*(2), 189–199. https://doi.org/10.1007/s00213-006-0418-z

Besson, M., Suarez, S., Cormier, A., Changeux, J. P., & Granon, S. (2008). Chronic nicotine exposure has dissociable behavioural effects on control and beta2-/- mice. *Behavior Genetics*, *38*(5), 503–514. https://doi.org/10.1007/s10519-008-9216-1

Bloem, B., Poorthuis, R. B., & Mansvelder, H. D. (2014). Cholinergic modulation of the medial prefrontal cortex: The role of nicotinic receptors in attention and regulation of neuronal activity. In *Frontiers in Neural Circuits* (Vol. 8, Issue MAR). Frontiers Research Foundation. https://doi.org/10.3389/fncir.2014.00017

Bourgeois, J., Meas-yeadid, V., Lesourd, A., Faure, P., Maskos, U., Changeux, J., & Granon, S. (2012). *Modulation of the Mouse Prefrontal Cortex Activation by Neuronal Nicotinic Receptors during Novelty Exploration but not by Exploration of a Familiar Environment*. *86*, 1007–1015. https://doi.org/10.1093/cercor/bhr159

Calabresi, P., Picconi, B., Tozzi, A., Ghiglieri, V., & Di Filippo, M. (2014). Direct and indirect pathways of basal ganglia: a critical reappraisal. *Nature Neuroscience*, *17*(8), 1022–1030. https://doi.org/10.1038/nn.3743

Can, A., Dao, D. T., Terrillion, C. E., Piantadosi, S. C., Bhat, S., & Gould, T. D. (2011). The tail suspension test. *Journal of Visualized Experiments*, *58*. https://doi.org/10.3791/3769

Caton, M., Ochoa, E. L. M., & Barrantes, F. J. (2020). The role of nicotinic cholinergic neurotransmission in delusional thinking. In *npj Schizophrenia* (Vol. 6, Issue 1). Nature Research. https://doi.org/10.1038/s41537-020-0105-9

Changeux, J., Corringer, P., & Maskos, U. (2015). Neuropharmacology The nicotinic acetylcholine receptor : From molecular biology to cognition. *Neuropharmacology*, *96*, 135–136. https://doi.org/10.1016/j.neuropharm.2015.03.024

Changeux, J.-P., Kasait, M., & Leet, C.-Y. (1970). *Use of a Snake Venom Toxin to Characterize the Cholinergic Receptor Protein** (Vol. 67, Issue 3).

Close, J. L., Yao, Z., Levi, B. P., Miller, J. A., Bakken, T. E., Menon, V., Ting, J. T., Wall, A., Krostag, A. R., Thomsen, E. R., Nelson, A. M., Mich, J. K., Hodge, R. D., Shehata, S. I., Glass, I. A., Bort, S., Shapovalova, N. V., Ngo, N. K., Grimley, J. S., … Lein, E. (2017). Single-Cell Profiling of an In Vitro Model of Human Interneuron Development Reveals Temporal Dynamics of Cell Type Production and Maturation. *Neuron*, *93*(5), 1035-1048.e5. https://doi.org/10.1016/j.neuron.2017.02.014

Commons, K. G., Cholanians, A. B., Babb, J. A., & Ehlinger, D. G. (2017). The Rodent Forced Swim Test Measures Stress-Coping Strategy, Not Depression-like Behavior. In *ACS Chemical Neuroscience* (Vol. 8, Issue 5, pp. 955–960). American Chemical Society. https://doi.org/10.1021/acschemneuro.7b00042

Crittenden, J. R., & Graybiel, A. M. (2011). Basal ganglia disorders associated with imbalances in the striatal striosome and matrix compartments. In *Frontiers in Neuroanatomy* (Issue SEP). https://doi.org/10.3389/fnana.2011.00059

Crouse, R. B., Kim, K., Batchelor, H. M., Girardi, E. M., Kamaletdinova, R., Chan, J., Rajebhosale, P., Pittenger, S. T., Role, L. W., Talmage, D. A., Jing, M., Li, Y., Gao, X. B., Mineur, Y. S., & Picciotto, M. R. (2020). Acetylcholine is released in the basolateral amygdala in response to predictors of reward and enhances the learning of cue-reward contingency. *ELife*, *9*, 1–31. https://doi.org/10.7554/ELIFE.57335

Dajas-Bailador, F., & Wonnacott, S. (2004). Nicotinic acetylcholine receptors and the regulation of neuronal signalling. *Trends in Pharmacological Sciences*, *25*(6), 317–324. https://doi.org/10.1016/j.tips.2004.04.006

Dani, J. A., & Bertrand, D. (2007). Nicotinic acetylcholine receptors and nicotinic cholinergic mechanisms of the central nervous system. In *Annual Review of Pharmacology and Toxicology* (Vol. 47, pp. 699–729). https://doi.org/10.1146/annurev.pharmtox.47.120505.105214

Dautan, D., Huerta-Ocampo, I., Witten, I. B., Deisseroth, K., Bolam, J. P., Gerdjikov, T., & Mena-Segovia, J. (2014). A Major External Source of Cholinergic Innervation of the Striatum and Nucleus Accumbens Originates in the Brainstem. *Journal of Neuroscience*, *34*(13), 4509–4518. https://doi.org/10.1523/JNEUROSCI.5071-13.2014

Deacon, R. M. J. (2006). Assessing nest building in mice. *Nature Protocols*, *1*(3), 1117–1119. https://doi.org/10.1038/nprot.2006.170

Dorst, M. C., Tokarska, A., Zhou, M., Lee, K., Stagkourakis, S., Broberger, C., Masmanidis, S., & Silberberg, G. (2020). Polysynaptic inhibition between striatal cholinergic interneurons shapes their network activity patterns in a dopamine-dependent manner. *Nature Communications*, *11*(1). https://doi.org/10.1038/s41467-020-18882-y

Dumas, S., & Wallén-Mackenzie, Å. (2019). Developmental Co-expression of Vglut2 and Nurr1 in a Mes-Di-Encephalic Continuum Preceeds Dopamine and Glutamate Neuron Specification. *Frontiers in Cell and Developmental Biology*, *7*. https://doi.org/10.3389/fcell.2019.00307

Economo, M. N., Viswanathan, S., Tasic, B., Bas, E., Winnubst, J., Menon, V., Graybuck, L. T., Nguyen, T. N., Smith, K. A., Yao, Z., Wang, L., Gerfen, C. R., Chandrashekar, J., Zeng, H., Looger, L. L., & Svoboda, K. (2018). Distinct descending motor cortex pathways and their roles in movement. *Nature*, *563*(7729), 79–84. https://doi.org/10.1038/s41586-018-0642-9

English, D. F., Ibanez-sandoval, O., Stark, E., Tecuapetla, F., Buzsáki, G., Deisseroth, K., Tepper, J. M., & Koos, T. (2012). GABAergic circuits mediate the reinforcement-related signals of striatal cholinergic interneurons. *Nature Neuroscience*, *15*(1), 123–130. https://doi.org/10.1038/nn.2984

Faust, T. W., Assous, M., Tepper, J. M., & Koós, T. (2016). Neostriatal GABAergic Interneurons Mediate Cholinergic Inhibition of Spiny Projection Neurons. *The Journal of Neuroscience*, *36*(36), 9505–9511. https://doi.org/10.1523/JNEUROSCI.0466-16.2016

Frahm, S., Ślimak, M. A., Ferrarese, L., Santos-Torres, J., Antolin-Fontes, B., Auer, S., Filkin, S., Pons, S., Fontaine, J. F., Tsetlin, V., Maskos, U., & Ibañez-Tallon, I. (2011). Aversion to Nicotine Is

Regulated by the Balanced Activity of β4 and α5 Nicotinic Receptor Subunits in the Medial Habenula. *Neuron*, *70*(3), 522–535. https://doi.org/10.1016/j.neuron.2011.04.013

Francine M. Benes, M.D., Ph.D. and Sabina Berretta, M. D., & A. (2003). GABAergic Interneurons: Implications for Understanding Schizophrenia and Bipolar Disorder. *Information Sciences*, *149*(1–3), 75–81. https://doi.org/10.1016/S0020-0255(02)00247-5

Franklin, K. B. J., & Paxinos, G. (2007). *The mouse brain* (third edition).

Funahashi, S. (2015). Functions of delay-period activity in the prefrontal cortex and mnemonic scotomas revisited. *Frontiers in Systems Neuroscience*, *9*(FEB). https://doi.org/10.3389/fnsys.2015.00002

Gerfen, C. R., & Bolam, J. P. (2010). The Neuroanatomical Organization of the Basal Ganglia. In *Handbook of Behavioral Neuroscience* (Vol. 20, Issue C, pp. 3–28). https://doi.org/10.1016/B978-0-12-374767-9.00001-9

Gerfen, C. R., & Surmeier, D. J. (2011). Modulation of striatal projection systems by dopamine. *Annual Review of Neuroscience*, *34*, 441–466. https://doi.org/10.1146/annurev-neuro-061010-113641

Gonzales, K. K., & Smith, Y. (2015). Cholinergic interneurons in the dorsal and ventral striatum: Anatomical and functional considerations in normal and diseased conditions. *Annals of the New York Academy of Sciences*, *1349*(1), 1–45. https://doi.org/10.1111/nyas.12762

Goral, R. O., Harper, K. M., Bernstein, B. J., Fry, S. A., Lamb, P. W., Moy, S. S., Cushman, J. D., & Yakel, J. L. (2022). Loss of GABA co-transmission from cholinergic neurons impairs behaviors related to hippocampal, striatal, and medial prefrontal cortex functions. *Frontiers in Behavioral Neuroscience*, *16*. https://doi.org/10.3389/fnbeh.2022.1067409

Gotti, C., & Clementi, F. (2004). Neuronal nicotinic receptors: From structure to pathology. *Progress in Neurobiology*, *74*(6), 363–396. https://doi.org/10.1016/j.pneurobio.2004.09.006

Gotti, C., Zoli, M., & Clementi, F. (2006). Brain nicotinic acetylcholine receptors: native subtypes and their relevance. In *Trends in Pharmacological Sciences* (Vol. 27, Issue 9, pp. 482–491). https://doi.org/10.1016/j.tips.2006.07.004

Govind, A. P., Walsh, H., & Green, W. N. (2012). Nicotine-Induced Upregulation of Native Neuronal Nicotinic Receptors Is Caused by Multiple Mechanisms. *Journal of Neuroscience*, *32*(6), 2227–2238. https://doi.org/10.1523/JNEUROSCI.5438-11.2012

Granon, S., Faure, P., & Changeux, J. P. (2003). Executive and social behaviors under nicotinic receptor regulation. *Proceedings of the National Academy of Sciences of the United States of America*, *100*(16), 9596–9601. https://doi.org/10.1073/pnas.1533498100

Griguoli, M., & Cherubini, E. (2012). Regulation of hippocampal inhibitory circuits by nicotinic acetylcholine receptors. In *Journal of Physiology* (Vol. 590, Issue 4, pp. 655–666). https://doi.org/10.1113/jphysiol.2011.220095

Groleau, M., Kang, J. il, Huppé-Gourgues, F., & Vaucher, E. (2015). Distribution and effects of the muscarinic receptor subtypes in the primary visual cortex. In *Frontiers in Synaptic Neuroscience* (Vol. 7, Issue JUN). Frontiers Research Foundation. https://doi.org/10.3389/fnsyn.2015.00010

Guillem, K., Bloem, B. , Poorthuis, R. B., Loos, M., Smit, A. B., Maskos, U., Spijker, S., & Mansvelder, H. D. (2011). Nicotinic Acetylcholine Receptor b2 Subunits in the Medial Prefrontal Cortex Control Attention. *Science*, *333*(6044), 885–888. https://doi.org/10.1126/science.1208146

Guo, Q., Wang, D., He, X., Feng, Q., Lin, R., Xu, F., Fu, L., & Luo, M. (2015). Whole-brain mapping of inputs to projection neurons and cholinergic interneurons in the dorsal striatum. *PLoS ONE*, *10*(4). https://doi.org/10.1371/journal.pone.0123381

Haber, S. N., & Robbins, T. (2022). The prefrontal cortex. In *Neuropsychopharmacology* (Vol. 47, Issue 1). Springer Nature. https://doi.org/10.1038/s41386-021-01184-2

Han, K., Lee, M., Lim, H. K., Jang, M. W., Kwon, J., Justin Lee, C., Kim, S. G., & Suh, M. (2020). Excitation-inhibition imbalance leads to alteration of neuronal coherence and neurovascular coupling under acute stress. *Journal of Neuroscience*, *40*(47), 9148–9162. https://doi.org/10.1523/JNEUROSCI.1553-20.2020

Hay, Y. A., Lambolez, B., & Tricoire, L. (2016). Nicotinic Transmission onto Layer 6 Cortical Neurons Relies on Synaptic Activation of Non-α7 Receptors. *Cerebral Cortex*, *26*(6), 2549–2562. https://doi.org/10.1093/cercor/bhv085

Hogg, R. C., Raggenbass, M., & Bertrand, D. (2003). Nicotinic acetylcholine receptors: from structure to brain function. *Reviews of Physiology, Biochemistry and Pharmacology*, *147*(March), 1–46. https://doi.org/10.1007/s10254-003-0005-1

Holley, S. M., Galvan, L., Kamdjou, T., Dong, A., Levine, M. S., & Cepeda, C. (2019). Major contribution of somatostatin-expressing interneurons and cannabinoid receptors to increased GABA synaptic

activity in the striatum of Huntington's disease mice. *Frontiers in Synaptic Neuroscience*, *11*(MAY). https://doi.org/10.3389/fnsyn.2019.00014

Hori, K., Yamashiro, K., Nagai, T., Shan, W., Egusa, S. F., Shimaoka, K., Kuniishi, H., Sekiguchi, M., Go, Y., Tatsumoto, S., Yamada, M., Shiraishi, R., Kanno, K., Miyashita, S., Sakamoto, A., Abe, M., Sakimura, K., Sone, M., Sohya, K., … Hoshino, M. (2020). AUTS2 Regulation of Synapses for Proper Synaptic Inputs and Social Communication. *IScience*, *23*(6). https://doi.org/10.1016/j.isci.2020.101183

Howe, M., Ridouh, I., Letizia, A., Mascaro, A., Larios, A., Azcorra, M., & Dombeck, D. A. (2019). *Coordination of rapid cholinergic and dopaminergic signaling in striatum during spontaneous movement*. https://doi.org/10.7554/eLife.44903.001

Hung, S. S. C., Chrysostomou, V., Li, F., Lim, J. K. H., Wang, J. H., Powell, J. E., Tu, L., Daniszewski, M., Lo, C., Wong, R. C., Crowston, J. G., Pébay, A., King, A. E., Bui, B. V., Liu, G. S., & Hewitt, A. W. (2016). AAV-Mediated CRISPR/Cas Gene Editing of Retinal Cells in Vivo. *Investigative Ophthalmology and Visual Science*, *57*(7), 3470–3476. https://doi.org/10.1167/iovs.16-19316

Ibanez-Sandoval, O., Tecuapetla, F., Unal, B., Shah, F., Koos, T., & Tepper, J. M. (2010). Electrophysiological and Morphological Characteristics and Synaptic Connectivity of Tyrosine Hydroxylase-Expressing Neurons in Adult Mouse Striatum. *Journal of Neuroscience*, *30*(20), 6999–7016. https://doi.org/10.1523/JNEUROSCI.5996-09.2010

Ibanez-Sandoval, O., Tecuapetla, F., Unal, B., Shah, F., Koos, T., & Tepper, J. M. (2011). A Novel Functionally Distinct Subtype of Striatal Neuropeptide Y Interneuron. *Journal of Neuroscience*, *31*(46), 16757–16769. https://doi.org/10.1523/JNEUROSCI.2628-11.2011

Joshua, O., Matthijs, B. V., Antonio, L., & Huibert D., M. (2017). *Cholinergic Modulation of Cortical Microcircuits Is Layer-Specific : Evidence from Rodent , Monkey and*. *11*(December), 1–12. https://doi.org/10.3389/fncir.2017.00100

Kaminer, J., Espinoza, D., Bhimani, S., Tepper, J. M., Koos, T., & Shiflett, M. W. (2019). Loss of striatal tyrosine-hydroxylase interneurons impairs instrumental goal-directed behavior. *European Journal of Neuroscience*, *November 2018*, 1–10. https://doi.org/10.1111/ejn.14412

Kennis, M., Rademaker, A. R., & Geuze, E. (2013). Neural correlates of personality: An integrative review. In *Neuroscience and Biobehavioral Reviews* (Vol. 37, Issue 1, pp. 73–95). https://doi.org/10.1016/j.neubiorev.2012.10.012

Kim, H., Kim, M., Im, S.-K., & Fang, S. (2018). Mouse Cre-LoxP system: general principles to determine tissue-specific roles of target genes. *Laboratory Animal Research*, *34*(4), 147. https://doi.org/10.5625/lar.2018.34.4.147

King, S. L., Marks, M. J., Grady, S. R., Caldarone, B. J., Koren, A. O., Mukhin, A. G., Collins, A. C., & Picciotto, M. R. (2003). Conditional expression in corticothalamic efferents reveals a developmental role for nicotinic acetylcholine receptors in modulation of passive avoidance behavior. *Journal of Neuroscience*, *23*(9), 3837–3843. https://doi.org/10.1523/jneurosci.23-09-03837.2003

Kolk, S. M., & Rakic, P. (2022). Development of prefrontal cortex. In *Neuropsychopharmacology* (Vol. 47, Issue 1, pp. 41–57). Springer Nature. https://doi.org/10.1038/s41386-021-01137-9

Konsolaki, E., Tsakanikas, P., Polissidis, A. v., Stamatakis, A., & Skaliora, I. (2016). Early signs of pathological cognitive aging in mice lacking high-affinity nicotinic receptors. *Frontiers in Aging Neuroscience*, *8*(APR). https://doi.org/10.3389/fnagi.2016.00091

Koós, T., & Tepper, J. M. (2002). Dual cholinergic control of fast-spiking interneurons in the neostriatum. *Journal of Neuroscience*, *22*(1529-2401 (Electronic)), 529–535. https://doi.org/22/2/529 [pii]

Koós, T., Tepper, J. M., & Koós, T. (1999). Inhibitory control of neostriatal projection neurons by GABAergic interneurons. *Nature Neuroscience*, *2*(5), 467–472. https://doi.org/10.1038/8138

Koukouli, F., & Changeux, J. (2020). Do Nicotinic Receptors Modulate High-Order Cognitive Processing ? B. *Trends in Neurosciences*, *43*(8), 550–564. https://doi.org/10.1016/j.tins.2020.06.001

Koukouli, F., Rooy, M., Tziotis, D., Sailor, K. A., O'Neill, H. C., Levenga, J., Witte, M., Nilges, M., Changeux, J., Hoeffer, C. A., Stitzel, J. A., Gutkin, B. S., DiGregorio, D. A., & Maskos, U. (2017). Nicotine reverses hypofrontality in animal models of addiction and schizophrenia. *Nature Medicine*, *23*(3), 347–354. https://doi.org/10.1038/nm.4274

Krabbe, S., Paradiso, E., D'Aquin, S., Bitterman, Y., Courtin, J., Xu, C., Yonehara, K., Markovic, M., Müller, C., Eichlisberger, T., Gründemann, J., Ferraguti, F., & Lüthi, A. (2019). Adaptive disinhibitory gating by VIP interneurons permits associative learning. *Nature Neuroscience*, *22*(11), 1834–1843. https://doi.org/10.1038/s41593-019-0508-y

Kruse, A. C., Kobilka, B. K., Gautam, D., Sexton, P. M., Christopoulos, A., & Wess, J. (2014). Muscarinic acetylcholine receptors: Novel opportunities for drug development. In *Nature Reviews Drug Discovery* (Vol. 13, Issue 7, pp. 549–560). Nature Publishing Group. https://doi.org/10.1038/nrd4295

Labarca, C., Schwarz, J., Deshpande, P., Schwarz, S., Nowak, M. W., Fonck, C., Nashmi, R., Kofuji, P., Dang, H., Shi, W., Fidan, M., Khakh, B. S., Chen, Z., Bowers, B. J., Boulter, J., Wehner, J. M., & Lester, H. A. (2000). *Point mutant mice with hypersensitive 4 nicotinic receptors show dopaminergic deficits and increased anxiety*. www.pnas.orgcgidoi10.1073pnas.041582598

Laforet, G. a, Sapp, E., Chase, K., McIntyre, C., Boyce, F. M., Campbell, M., Cadigan, B. a, Warzecki, L., Tagle, D. a, Reddy, P. H., Cepeda, C., Calvert, C. R., Jokel, E. S., Klapstein, G. J., Ariano, M. a, Levine, M. S., DiFiglia, M., & Aronin, N. (2001). Changes in cortical and striatal neurons predict behavioral and electrophysiological abnormalities in a transgenic murine model of Huntington's disease. *The Journal of Neuroscience*, *21*(23), 9112–9123. https://doi.org/21/23/9112 [pii]

Lam, N. H., Borduqui, T., Hallak, J., Roque, A., Anticevic, A., Krystal, J. H., Wang, X. J., & Murray, J. D. (2022). Effects of Altered Excitation-Inhibition Balance on Decision Making in a Cortical Circuit Model. *Journal of Neuroscience*, *42*(6), 1035–1053. https://doi.org/10.1523/JNEUROSCI.1371-20.2021

Lanciego, J. L., Luquin, N., & Obeso, J. A. (2012). Functional neuroanatomy of the basal ganglia. *Cold Spring Harbor Perspectives in Medicine*, *2*(12). https://doi.org/10.1101/cshperspect.a009621

Laroche, S., Davis, S., & Jay, T. M. (2000). Plasticity at hippocampal to prefrontal cortex synapses: Dual roles in working memory and consolidation. *Hippocampus*, *10*(4), 438–446. https://doi.org/10.1002/1098-1063(2000)10:4<438::AID-HIPO10>3.0.CO;2-3

Laubach, M., Amarante, L. M., Swanson, K., & White, S. R. (2018). What, if anything, is rodent prefrontal cortex? In *eNeuro* (Vol. 5, Issue 5). Society for Neuroscience. https://doi.org/10.1523/ENEURO.0315-18.2018

Le Moine, C., Normand, E., Guitteny, A. F., Fouquet, B., Teoulet, R., & Bloch, B. (1990). Dopamine receptor gene expression by enkephalin neurons in rat forebrain (nigrostriatal pathway/D2 receptor/preproenkephalin A/in situ hybridization). In *Proc. NatI. Acad. Sci. USA* (Vol. 87).

Le Moine, C., Svenningsson, P., Fredholm, B. B., & Bloch, B. (1990). Dopamine-Adenosine Interactions in the Striatum and the Globus Pallidus: Inhibition of Striatopallidal Neurons through Either D 2 or A 2A Receptors Enhances D 1 Receptor-Mediated Effects on c-fos Expression. In *The Journal of Neuroscience* (Vol. 17, Issue 20). However.

Le Moine, C., Tison, F., & Bloch, B. (1990). *D2 dopamine receptor gene expression by cholinergic neurons in the rat striatum*.

Ledford, H., & Callaway, E. (2020). *PIONEERS OF CRISPR GENE EDITING WIN CHEMISTRY NOBEL*.

Léna, C., & Changeux, J. P. (1999). The role of β2-subunit-containing nicotinic acetylcholine receptors in the brain explored with a mutant mouse. *Annals of the New York Academy of Sciences*, *868*, 611–616. https://doi.org/10.1111/j.1749-6632.1999.tb11333.x

Léna, C., Popa, D., Grailhe, R., Escourrou, P., Changeux, J. P., & Adrien, J. (2004). β2-Containing nicotinic receptors contribute to the organization of sleep and regulate putative micro-arousals in mice. *Journal of Neuroscience*, *24*(25), 5711–5718. https://doi.org/10.1523/JNEUROSCI.3882-03.2004

Levin, E. D. (2002). Nicotinic receptor subtypes and cognitive function. *Journal of Neurobiology*. https://doi.org/10.1002/neu.10151

Li, X., Yu, B., Sun, Q., Zhang, Y., Ren, M., Zhang, X., Li, A., Yuan, J., Madisen, L., Luo, Q., Zeng, H., Gong, H., & Qiu, Z. (2017). Generation of a whole-brain atlas for the cholinergic system and mesoscopic projectome analysis of basal forebrain cholinergic neurons. *Proceedings of the National Academy of Sciences of the United States of America*, *115*(2), 415–420. https://doi.org/10.1073/pnas.1703601115

Livak, K. J., & Schmittgen, T. D. (2001). Analysis of relative gene expression data using real-time quantitative PCR and the 2-ΔΔCT method. *Methods*, *25*(4), 402–408. https://doi.org/10.1006/meth.2001.1262

Lovinger, D. M. (2010). Neurotransmitter roles in synaptic modulation, plasticity and learning in the dorsal striatum. *Neuropharmacology*, *58*(7), 951–961. https://doi.org/10.1016/j.neuropharm.2010.01.008

Lozovaya, N., Eftekhari, S., Cloarec, R., Gouty-Colomer, L. A., Dufour, A., Riffault, B., Billon-Grand, M., Pons-Bennaceur, A., Oumar, N., Burnashev, N., Ben-Ari, Y., & Hammond, C. (2018). GABAergic inhibition in dual-transmission cholinergic and GABAergic striatal interneurons is abolished in Parkinson disease. *Nature Communications*, *9*(1). https://doi.org/10.1038/s41467-018-03802-y

Luchicchi, A., Bloem, B., Viaña, J. N. M., Mansvelder, H. D., & Role, L. W. (2014). Illuminating the role of cholinergic signaling in circuits of attention and emotionally salient behaviors. *Frontiers in Synaptic Neuroscience*, *6*(OCT), 1–10. https://doi.org/10.3389/fnsyn.2014.00024

Macpherson, T., Morita, M., & Hikida, T. (2014). Striatal direct and indirect pathways control decision-making behavior. *Frontiers in Psychology*, *5*(NOV), 1–7. https://doi.org/10.3389/fpsyg.2014.01301

Mallet, N., Leblois, A., Maurice, N., & Beurrier, C. (2019). Striatal cholinergic interneurons: How to elucidate their function in health and disease. In *Frontiers in Pharmacology* (Vol. 10). Frontiers Media S.A. https://doi.org/10.3389/fphar.2019.01488

Mao, M., Nair, A., & Augustine, G. J. (2019). A novel type of neuron within the Dorsal striatum. *Frontiers in Neural Circuits*, *13*. https://doi.org/10.3389/fncir.2019.00032

Marina Picciotto, C. R., Mineur, Y. S., Mose, T. N., Blakeman, S., & Picciotto, M. R. (2018). Themed Section: Nicotinic Acetylcholine Receptors Hippocampal α7 nicotinic ACh receptors contribute to modulation of depression-like behaviour in C57BL/6J mice LINKED ARTICLES. *British Journal of Pharmacology*, *175*, 1903. https://doi.org/10.1111/bph.v175.11/issuetoc

Martiros, N., Burgess, A. A., & Graybiel, A. M. (2018). Inversely Active Striatal Projection Neurons and Interneurons Selectively Delimit Useful Behavioral Sequences. *Current Biology*, *28*(4), 560-573.e5. https://doi.org/10.1016/j.cub.2018.01.031

Martos, Y. V., Braz, B. Y., Beccaria, J. P., Murer, M. G., & Belforte, J. E. (2017). Compulsive Social Behavior Emerges after Selective Ablation of Striatal Cholinergic Interneurons. *The Journal of Neuroscience*, *37*(11), 2849–2858. https://doi.org/10.1523/JNEUROSCI.3460-16.2017

Maskos, U., Molles, B. E., Pons, S., Besson, M., Guiard, B. P., Guilloux, J., Evrard, A., Cazala, P., Cormier, A., Bemelmans, A., Mallet, J., Gardier, A. M., David, V., Faure, P., Granon, S., & Changeux, J. (2005). *Nicotine reinforcement and cognition restored by targeted expression of nicotinic receptors*. *436*(July), 103–107. https://doi.org/10.1038/nature03694

McLellan, M. A., Rosenthal, N. A., & Pinto, A. R. (2017). Cre-loxP-Mediated Recombination: General Principles and Experimental Considerations. *Current Protocols in Mouse Biology*, *7*(1), 1–12. https://doi.org/10.1002/cpmo.22

Miller, E. K., & Cohen, J. D. (2001). *AN INTEGRATIVE THEORY OF PREFRONTAL CORTEX FUNCTION*. www.annualreviews.org

Milstein, A. D., Bloss, E. B., Apostolides, P. F., Vaidya, S. P., Dilly, G. A., Zemelman, B. v., & Magee, J. C. (2015). Inhibitory Gating of Input Comparison in the CA1 Microcircuit. *Neuron*, *87*(6), 1274–1289. https://doi.org/10.1016/j.neuron.2015.08.025

Mineur, Y. S., Fote, G. M., Blakeman, S., Cahuzac, E. L. M., Newbold, S. A., & Picciotto, M. R. (2016). Multiple nicotinic acetylcholine receptor subtypes in the mouse amygdala regulate affective behaviors and response to social stress. *Neuropsychopharmacology*, *41*(6), 1579–1587. https://doi.org/10.1038/npp.2015.316

Mineur, Y. S., Obayemi, A., Wigestrand, M. B., Fote, G. M., Calarco, C. A., Li, A. M., & Picciotto, M. R. (2013). Cholinergic signaling in the hippocampus regulates social stress resilience and anxiety- and depression-like behavior. *Proceedings of the National Academy of Sciences of the United States of America*, *110*(9), 3573–3578. https://doi.org/10.1073/pnas.1219731110

Mineur, Y. S., & Picciotto, M. R. (2021). The role of acetylcholine in negative encoding bias: Too much of a good thing? In *European Journal of Neuroscience* (Vol. 53, Issue 1, pp. 114–125). Blackwell Publishing Ltd. https://doi.org/10.1111/ejn.14641

Mineur, Y. S., Somenzi, O., & Picciotto, M. R. (2007). Cytisine, a partial agonist of high-affinity nicotinic acetylcholine receptors, has antidepressant-like properties in male C57BL/6J mice. *Neuropharmacology*, *52*(5), 1256–1262. https://doi.org/10.1016/j.neuropharm.2007.01.006

Montag, C., & Reuter, M. (2014). Disentangling the molecular genetic basis of personality: From monoamines to neuropeptides. In *Neuroscience and Biobehavioral Reviews* (Vol. 43, pp. 228–239). Elsevier Ltd. https://doi.org/10.1016/j.neubiorev.2014.04.006

Moon, S. bin, Kim, D. Y., Ko, J. H., & Kim, Y. S. (2019). Recent advances in the CRISPR genome editing tool set. In *Experimental and Molecular Medicine* (Vol. 51, Issue 11). Springer Nature. https://doi.org/10.1038/s12276-019-0339-7

Morales-Perez, C. L., Noviello, C. M., & Hibbs, R. E. (2016). X-ray structure of the human α4β2 nicotinic receptor. *Nature*, *538*(7625), 411–415. https://doi.org/10.1038/nature19785

Morita, K. (2014). Differential cortical activation of the striatal direct and indirect pathway cells: reconciling the anatomical and optogenetic results by using a computational method. *Journal of Neurophysiology*, *112*(1), 120–146. https://doi.org/10.1152/jn.00625.2013

Moser, N., Mechawar, N., Jones, I., Gochberg-Sarver, A., Orr-Urtreger, A., Plomann, M., Salas, R., Molles, B., Marubio, L., Roth, U., Maskos, U., Winzer-Serhan, U., Bourgeois, J. P., le Sourd, A. M., de Biasi, M., Schröder, H., Lindstrom, J., Maelicke, A., Changeux, J. P., & Wevers, A. (2007). Evaluating the suitability of nicotinic acetylcholine receptor antibodies for standard immunodetection procedures. *Journal of Neurochemistry*, *102*(2), 479–492. https://doi.org/10.1111/j.1471-4159.2007.04498.x

Moy, S. S., Nadler, J. J., Young, N. B., Nonneman, R. J., Grossman, A. W., Murphy, D. L., D'Ercole, A. J., Crawley, J. N., Magnuson, T. R., & Lauder, J. M. (2009). Social approach in genetically engineered mouse lines relevant to autism. *Genes, Brain and Behavior*, *8*(2), 129–142. https://doi.org/10.1111/j.1601-183X.2008.00452.x

Mu, R., Tang, S., Han, X., Wang, H., Yuan, D., Zhao, J., Long, Y., & Hong, H. (2022). A cholinergic medial septum input to medial habenula mediates generalization formation and extinction of visual aversion. *Cell Reports*, *39*(9). https://doi.org/10.1016/j.celrep.2022.110882

Muñoz-Manchado, A. B., Bengtsson Gonzales, C., Zeisel, A., Munguba, H., Bekkouche, B., Skene, N. G., Lönnerberg, P., Ryge, J., Harris, K. D., Linnarsson, S., & Hjerling-Leffler, J. (2018). Diversity of Interneurons in the Dorsal Striatum Revealed by Single-Cell RNA Sequencing and PatchSeq. *Cell Reports*, *24*(8), 2179-2190.e7. https://doi.org/10.1016/j.celrep.2018.07.053

Muñoz-Manchado, A. B., Foldi, C., Szydlowski, S., Sjulson, L., Farries, M., Wilson, C., Silberberg, G., & Hjerling-Leffler, J. (2016). Novel Striatal GABAergic Interneuron Populations Labeled in the 5HT3aEGFP Mouse. *Cerebral Cortex*, *26*(1), 96–105. https://doi.org/10.1093/cercor/bhu179

Nadler, J. J., Moy, S. S., Dold, G., Trang, D., Simmons, N., Perez, A., Young, N. B., Barbaro, R. P., Piven, J., Magnuson, T. R., & Crawley, J. N. (2004). Automated apparatus for quantitation of social approach behaviors in mice. *Genes, Brain and Behavior*, *3*(5), 303–314. https://doi.org/10.1111/j.1601-183X.2004.00071.x

Nees, F. (2015). Neuropharmacology The nicotinic cholinergic system function in the human brain. *Neuropharmacology*, *96*, 289–301. https://doi.org/10.1016/j.neuropharm.2014.10.021

Obermayer, J., Luchicchi, A., Heistek, T. S., de Kloet, S. F., Terra, H., Bruinsma, B., Mnie-Filali, O., Kortleven, C., Galakhova, A. A., Khalil, A. J., Kroon, T., Jonker, A. J., de Haan, R., van den Berg, W. D. J., Goriounova, N. A., de Kock, C. P. J., Pattij, T., & Mansvelder, H. D. (2019). Prefrontal cortical ChAT-VIP interneurons provide local excitation by cholinergic synaptic transmission and control attention. *Nature Communications*, *10*(1). https://doi.org/10.1038/s41467-019-13244-9

Opris, I., & Casanova, M. F. (2014). Prefrontal cortical minicolumn: From executive control to disrupted cognitive processing. In *Brain* (Vol. 137, Issue 7, pp. 1863–1875). Oxford University Press. https://doi.org/10.1093/brain/awt359

Parikh, V., Ji, J., Decker, M. W., & Sarter, M. (2010). *Acetylcholine Receptors Differentially Control Glutamatergic and Cholinergic Signaling*. *30*(9), 3518–3530. https://doi.org/10.1523/JNEUROSCI.5712-09.2010

Parikh, V., Kozak, R., Martinez, V., & Sarter, M. (2007). Prefrontal Acetylcholine Release Controls Cue Detection on Multiple Timescales. *Neuron*, *56*(1), 141–154. https://doi.org/10.1016/j.neuron.2007.08.025

Peng, C., Yan, Y., Kim, V. J., Engle, S. E., Berry, J. N., McIntosh, J. M., Neve, R. L., & Drenan, R. M. (2019). Gene editing vectors for studying nicotinic acetylcholine receptors in cholinergic transmission. *European Journal of Neuroscience*, *50*(3), 2224–2238. https://doi.org/10.1111/ejn.13957

Picciotto, M. R., Caldarone, B. J., King, S. L., & Zachariou, V. (2000). Nicotinic receptors in the brain: Links between molecular biology and behavior. *Neuropsychopharmacology*, *22*(5), 451–465. https://doi.org/10.1016/S0893-133X(99)00146-3

Picciotto, M. R., & Corrigall, W. A. (2002). *Neuronal Systems Underlying Behaviors Related to Nicotine Addiction: Neural Circuits and Molecular Genetics*.

Picciotto, M. R., Higley, M. J., & Mineur, Y. S. (2012). Acetylcholine as a Neuromodulator: Cholinergic Signaling Shapes Nervous System Function and Behavior. In *Neuron* (Vol. 76, Issue 1, pp. 116–129). https://doi.org/10.1016/j.neuron.2012.08.036

Picciotto, M. R., Lewis, A. S., Van Schalkwyk, G. I., & Mineur, Y. S. (2015). Mood and anxiety regulation by nicotinic acetylcholine receptors: A potential pathway to modulate aggression and related behavioral states. In *Neuropharmacology* (Vol. 96, Issue PB, pp. 235–243). Elsevier Ltd. https://doi.org/10.1016/j.neuropharm.2014.12.028

Picciotto, M. R., Zoli, M., Léna, C., Bessis, A., Lallemand, Y., LeNovère, N., Vincent, P., Pich, E. M., Brûlet, P., & Changeux, J.-P. P. (1995). Abnormal avoidance learning in mice lacking functional high-affinity nicotine receptor in the brain. *Nature*, *374*(6517), 65–67. https://doi.org/10.1038/374065a0

Picciotto, M. R., Zoli, M., Rimondini, R., Léna, C., Marubio, L. M., Pich, E. M., Fuxe, K., & Changeux, J. P. (1998). Acetylcholine receptors containing the β2 subunit are involved in the reinforcing properties of nicotine. *Nature*, *391*(6663), 173–177. https://doi.org/10.1038/34413

Pickar-Oliver, A., & Gersbach, C. A. (2019). The next generation of CRISPR–Cas technologies and applications. In *Nature Reviews Molecular Cell Biology* (Vol. 20, Issue 8, pp. 490–507). Nature Publishing Group. https://doi.org/10.1038/s41580-019-0131-5

Platt, R. J., Chen, S., Zhou, Y., Yim, M. J., Swiech, L., Kempton, H. R., Dahlman, J. E., Parnas, O., Eisenhaure, T. M., Jovanovic, M., Graham, D. B., Jhunjhunwala, S., Heidenreich, M., Xavier, R. J., Langer, R., Anderson, D. G., Hacohen, N., Regev, A., Feng, G., … Zhang, F. (2014). CRISPR-Cas9 knockin mice for genome editing and cancer modeling. *Cell*, *159*(2), 440–455. https://doi.org/10.1016/j.cell.2014.09.014

Pohanka, M. (2012). Alpha7 nicotinic acetylcholine receptor is a target in pharmacology and toxicology. In *International Journal of Molecular Sciences* (Vol. 13, Issue 2, pp. 2219–2238). https://doi.org/10.3390/ijms13022219

Poorthuis, R. B., Bloem, B., Schak, B., Wester, J., Kock, C. P. J. De, & Mansvelder, H. D. (2013). *Layer-Specific Modulation of the Prefrontal Cortex by Nicotinic Acetylcholine Receptors*. *January*, 148–161. https://doi.org/10.1093/cercor/bhr390

Poorthuis, R. B., Bloem, B., Verhoog, M. B., & Mansvelder, H. D. (2013). *Layer-Specific Interference with Cholinergic Signaling in the Prefrontal Cortex by Smoking Concentrations of Nicotine*. *33*(11), 4843–4853. https://doi.org/10.1523/JNEUROSCI.5012-12.2013

Poorthuis, R. B., & Mansvelder, H. D. (2013). Nicotinic acetylcholine receptors controlling attention: Behavior, circuits and sensitivity to disruption by nicotine. In *Biochemical Pharmacology* (Vol. 86, Issue 8, pp. 1089–1098). Elsevier Inc. https://doi.org/10.1016/j.bcp.2013.07.003

Prado, V. F., Janickova, H., Al-Onaizi, M. A., & Prado, M. A. M. (2017). Cholinergic circuits in cognitive flexibility. *Neuroscience*, *345*, 130–141. https://doi.org/10.1016/j.neuroscience.2016.09.013

Proulx, E., Piva, M., Tian, M. K., Bailey, C. D. C., & Lambe, E. K. (2014). Nicotinic acetylcholine receptors in attention circuitry: The role of layer VI neurons of prefrontal cortex. In *Cellular and Molecular Life Sciences* (Vol. 71, Issue 7, pp. 1225–1244). Birkhauser Verlag AG. https://doi.org/10.1007/s00018-013-1481-3

Quik, M., & Wonnacott, S. (2011). a6b2* and a4b2* Nicotinic Acetylcholine Receptors As Drug Targets for Parkinson' s Disease. *Pharmacological Reviews*, *63*(4), 938–966. https://doi.org/10.1124/pr.110.003269.Abstract

Rada, P., Colasante, C., Skirzewski, M., Hernandez, L., & Hoebel, B. (2006). Behavioral depression in the swim test causes a biphasic, long-lasting change in accumbens acetylcholine release, with partial compensation by acetylcholinesterase and muscarinic-1 receptors. *Neuroscience*, *141*(1), 67–76. https://doi.org/10.1016/j.neuroscience.2006.03.043

Radnikow, G., & Feldmeyer, D. (2018). Layer- and cell type-specific modulation of excitatory neuronal activity in the neocortex. In *Frontiers in Neuroanatomy* (Vol. 12). Frontiers Media S.A. https://doi.org/10.3389/fnana.2018.00001

Ragozzino, M. E. (2000). The contribution of cholinergic and dopaminergic afferents in the rat prefrontal cortex to learning, memory, and attention. In *Psychobiology* (Vol. 28, Issue 2).

Rapanelli, M., Frick, L., Jindachomthong, K., Xu, J., Ohtsu, H., Nairn, A. C., & Pittenger, C. (2018). Striatal Signaling Regulated by the H3R Histamine Receptor in a Mouse Model of tic Pathophysiology. *Neuroscience*, *392*, 172–179. https://doi.org/10.1016/j.neuroscience.2018.09.035

Rapanelli, M., Frick, L. R., & Pittenger, C. (2017). The Role of Interneurons in Autism and Tourette Syndrome. *Trends in Neurosciences*, *40*(7), 397–407. https://doi.org/10.1016/j.tins.2017.05.004

Rapanelli, M., Wang, W., Hurley, E., Feltri, M. L., Pittenger, C., Frick, L. R., & Yan, Z. (2023). Cholinergic neurons in the basal forebrain are involved in behavioral abnormalities associated with Cul3 deficiency: Role of prefrontal cortex projections in cognitive deficits. *Translational Psychiatry*, *13*(1). https://doi.org/10.1038/s41398-023-02306-8

Redman, M., King, A., Watson, C., & King, D. (2016). What is CRISPR/Cas9? *Archives of Disease in Childhood: Education and Practice Edition*, *101*(4), 213–215. https://doi.org/10.1136/archdischild-2016-310459

Riaz, S., Puveendrakumaran, P., Khan, D., Yoon, S., Hamel, L., & Ito, R. (2019). Prelimbic and infralimbic cortical inactivations attenuate contextually driven discriminative responding for reward. *Scientific Reports*, *9*(1). https://doi.org/10.1038/s41598-019-40532-7

Riga, D., Matos, M. R., Glas, A., Smit, A. B., Spijker, S., & Van den Oever, M. C. (2014). Optogenetic dissection of medial prefrontal cortex circuitry. In *Frontiers in Systems Neuroscience* (Vol. 8, Issue DEC). Frontiers Media S.A. https://doi.org/10.3389/fnsys.2014.00230

Rodriguez, A., Zhang, H., Klaminder, J., Brodin, T., Andersson, P. L., & Andersson, M. (2018). ToxTrac: A fast and robust software for tracking organisms. *Methods in Ecology and Evolution*, *9*(3), 460–464. https://doi.org/10.1111/2041-210X.12874

Rossato, J. I., Bevilaqua, L. R. M., Medina, J. H., Izquierdo, I., & Cammarota, M. (2006). Retrieval induces hippocampal-dependent reconsolidation of spatial memory. *Learning and Memory*, *13*(4), 431–440. https://doi.org/10.1101/lm.315206

Rudebeck, P. H., & Izquierdo, A. (2022). Foraging with the frontal cortex: A cross-species evaluation of reward-guided behavior. In *Neuropsychopharmacology* (Vol. 47, Issue 1, pp. 134–146). Springer Nature. https://doi.org/10.1038/s41386-021-01140-0

Saito, M., O'Brien, D., Kovacs, K. M., Wang, R., Zavadil, J., & Vadasz, C. (2005). Nicotine-induced sensitization in mice: Changes in locomotor activity and mesencephalic gene expression. *Neurochemical Research*, *30*(8), 1027–1035. https://doi.org/10.1007/s11064-005-7047-5

Schaaf, C. P. (2014). Nicotinic acetylcholine receptors in human genetic disease. In *Genetics in Medicine* (Vol. 16, Issue 9, pp. 649–656). Nature Publishing Group. https://doi.org/10.1038/gim.2014.9

Seamans, J. K. , Lapish, C. C., & Durstewitz, D. (2008). Comparing the Prefrontal Cortex of Rats and Primates: Insights from Electrophysiology. *Neurotoxicity Research*, *14(2,3)*, 249–262.

Serreau, P., Chabout, J., Suarez, S. V., Naudé, J., & Granon, S. (2011). Beta2-containing neuronal nicotinic receptors as major actors in the flexible choice between conflicting motivations. *Behavioural Brain Research*, *225*(1), 151–159. https://doi.org/10.1016/j.bbr.2011.07.016

Shadlen, M. N. N., & Shohamy, D. (2016). Decision Making and Sequential Sampling from Memory. *Neuron*, *90*(5), 927–939. https://doi.org/10.1016/j.neuron.2016.04.036

Sine, S. M. (2002). The nicotinic receptor ligand binding domain. *Journal of Neurobiology*. https://doi.org/10.1002/neu.10139

Sinkus, M. L., Graw, S., Freedman, R., Ross, R. G., Lester, H. A., & Leonard, S. (2015). The human CHRNA7 and CHRFAM7A genes: A review of the genetics, regulation, and function. In *Neuropharmacology* (Vol. 96, Issue PB, pp. 274–288). Elsevier Ltd. https://doi.org/10.1016/j.neuropharm.2015.02.006

Smiley, J. F., Levey, ‡ A I, & Mesulam, M. M. (1999). *m2 MUSCARINIC RECEPTOR IMMUNOLOCALIZATION IN CHOLINERGIC CELLS OF THE MONKEY BASAL FOREBRAIN AND STRIATUM*.

Smucny, J., & Tregellas, J. (2013). Nicotinic modulation of intrinsic brain networks in schizophrenia. In *Biochemical Pharmacology* (Vol. 86, Issue 8, pp. 1163–1172). Elsevier Inc. https://doi.org/10.1016/j.bcp.2013.06.011

Soga, T., Kamohara, M., Takasaki, J., Matsumoto, S. I., Saito, T., Ohishi, T., Hiyama, H., Matsuo, A., Matsushime, H., & Furuichi, K. (2003). Molecular identification of nicotinic acid receptor. *Biochemical and Biophysical Research Communications*. https://doi.org/10.1016/S0006-291X(03)00342-5

Sullivan, M. A., Chen, H., & Morikawa, H. (2008). Recurrent inhibitory network among striatal cholinergic interneurons. *Journal of Neuroscience*, *28*(35), 8682–8690. https://doi.org/10.1523/JNEUROSCI.2411-08.2008

Sun, Y., Yang, Y., Galvin, V. C., Yang, S., Arnsten, A. F., & Wang, M. (2017). Nicotinic α4β2 cholinergic receptor influences on dorsolateral prefrontal cortical neuronal firing during a working memory task. *Journal of Neuroscience*, *37*(21), 5366–5377. https://doi.org/10.1523/JNEUROSCI.0364-17.2017

Swiech, L., Heidenreich, M., Banerjee, A., Habib, N., Li, Y., Trombetta, J., Sur, M., & Zhang, F. (2015). In vivo interrogation of gene function in the mammalian brain using CRISPR-Cas9. *Nature Biotechnology*, *33*(1), 102–106. https://doi.org/10.1038/nbt.3055

Takao, K., & Miyakawa, T. (2006). Light/dark transition test for mice. *Journal of Visualized Experiments*, *1*. https://doi.org/10.3791/104

Tanimura, A., Du, Y., Kondapalli, J., Wokosin, D. L., & Surmeier, D. J. (2019). Cholinergic Interneurons Amplify Thalamostriatal Excitation of Striatal Indirect Pathway Neurons in Parkinson's Disease Models. *Neuron*, *101*(3), 444-458.e6. https://doi.org/10.1016/j.neuron.2018.12.004

Tasic, B., Yao, Z., Graybuck, L. T., Smith, K. A., Nguyen, T. N., Bertagnolli, D., Goldy, J., Garren, E., Economo, M. N., Viswanathan, S., Penn, O., Bakken, T., Menon, V., Miller, J., Fong, O., Hirokawa, K. E., Lathia, K., Rimorin, C., Tieu, M., … Zeng, H. (2018). Shared and distinct transcriptomic cell types across neocortical areas. *Nature*, *563*(7729), 72–78. https://doi.org/10.1038/s41586-018-0654-5

Tepper, J. M., Koós, T., Ibanez-Sandoval, O., Tecuapetla, F., Faust, T. W., & Assous, M. (2018). Heterogeneity and diversity of striatal GABAergic interneurons: Update 2018. In *Frontiers in Neuroanatomy* (Vol. 12). Frontiers Media S.A. https://doi.org/10.3389/fnana.2018.00091

Tepper, J. M., Wilson, C. J., & Koós, T. (2008). Feedforward and feedback inhibition in neostriatal GABAergic spiny neurons. *Brain Research Reviews*, *58*(2), 272–281. https://doi.org/10.1016/j.brainresrev.2007.10.008

Thiele, A. (2013). Muscarinic signaling in the brain. In *Annual Review of Neuroscience* (Vol. 36, pp. 271–294). https://doi.org/10.1146/annurev-neuro-062012-170433

Tian, M. K., Bailey, C. D. C., de Biasi, M., Picciotto, M. R., & Lambe, E. K. (2011). Plasticity of prefrontal attention circuitry: Upregulated muscarinic excitability in response to decreased nicotinic signaling following deletion of α5 or β2 subunits. *Journal of Neuroscience*, *31*(45), 16458–16463. https://doi.org/10.1523/JNEUROSCI.3600-11.2011

Trakoshis, S., Martínez-Cañada, P., Rocchi, F., Canella, C., You, W., Chakrabarti, B., Ruigrok, A. N. V., Bullmore, E. T., Suckling, J., Markicevic, M., Zerbi, V., Baron-Cohen, S., Gozzi, A., Lai, M. C., Panzeri, S., & Lombardo, M. V. (2020). Intrinsic excitation-inhibition imbalance affects medial prefrontal cortex differently in autistic men versus women. *ELife*, *9*, 1–31. https://doi.org/10.7554/ELIFE.55684

Tremblay, R., Lee, S., & Rudy, B. (2016). GABAergic Interneurons in the Neocortex: From Cellular Properties to Circuits. *Neuron*, *91*(2), 260–292. https://doi.org/10.1016/j.neuron.2016.06.033

Ünal, B., Ibáñez-Sandoval, O., Shah, F., Abercrombie, E. D., & Tepper, J. M. (2011). Distribution of Tyrosine Hydroxylase-Expressing Interneurons with Respect to Anatomical Organization of the Neostriatum. *Frontiers in Systems Neuroscience*, *5*(June), 1–11. https://doi.org/10.3389/fnsys.2011.00041

Uylings, H. B. M., Groenewegen, H. J., & Kolb, B. (2003). Do rats have a prefrontal cortex? In *Behavioural Brain Research* (Vol. 146, Issues 1–2, pp. 3–17). Elsevier. https://doi.org/10.1016/j.bbr.2003.09.028

Valjent, E., & Gangarossa, G. (2021). The Tail of the Striatum: From Anatomy to Connectivity and Function. In *Trends in Neurosciences* (Vol. 44, Issue 3, pp. 203–214). Elsevier Ltd. https://doi.org/10.1016/j.tins.2020.10.016

Valk, S. L., Hoffstaedter, F., Camilleri, J. A., Kochunov, P., Yeo, B. T. T., & Eickhoff, S. B. (2020). Personality and local brain structure: Their shared genetic basis and reproducibility. *NeuroImage*, *220*. https://doi.org/10.1016/j.neuroimage.2020.117067

Vallés, A. S., & Barrantes, F. J. (2021). Dysregulation of Neuronal Nicotinic Acetylcholine Receptor–Cholesterol Crosstalk in Autism Spectrum Disorder. In *Frontiers in Molecular Neuroscience* (Vol. 14). Frontiers Media S.A. https://doi.org/10.3389/fnmol.2021.744597

Van den Pol, A. N., Yao, Y., Fu, L. Y., Foo, K., Huang, H., Coppari, R., Lowell, B. B., & Broberger, C. (2009). Neuromedin B and Gastrin-releasing peptide excite arcuate nucleus neuropeptide y neurons in a novel transgenic mouse expressing strong renilla green fluorescent protein in NPY neurons. *Journal of Neuroscience*, *29*(14), 4622–4639. https://doi.org/10.1523/JNEUROSCI.3249-08.2009

Voorn, P., Vanderschuren, L. J. M. J., Groenewegen, H. J., Robbins, T. W., & Pennartz, C. M. A. (2004). Putting a spin on the dorsal-ventral divide of the striatum. In *Trends in Neurosciences* (Vol. 27, Issue 8, pp. 468–474). https://doi.org/10.1016/j.tins.2004.06.006

Walf, A. A., & Frye, C. A. (2007). The use of the elevated plus maze as an assay of anxiety-related behavior in rodents. *Nature Protocols*, *2*(2), 322–328. https://doi.org/10.1038/nprot.2007.44

Wang, B., Zheng, Y., Shi, H., Du, X., Zhang, Y., Wei, B., Luo, M., Wang, H., Wu, X., Hua, X., Sun, M., & Xu, X. (2017). Zfp462 deficiency causes anxiety-like behaviors with excessive self-grooming in mice. *Genes, Brain and Behavior*, *16*(2), 296–307. https://doi.org/10.1111/gbb.12339

Whiting, P., & Lindstrom, J. O. N. (1987). *Purification and characterization of a nicotinic acetylcholine receptor from rat brain*. *84*(January), 595–599.

Wonnacott, S. (1990). The paradox of nicotinic acetylcholine receptor upregulation by nicotine. *Trends in Pharmacological Sciences*. https://doi.org/10.1016/0165-6147(90)90242-Z

Wonnacott, S. (1991). The relevance of receptor binding studies to tobacco research. *British Journal of Addiction*. https://doi.org/10.1111/j.1360-0443.1991.tb01804.x

Wonnacott, S., & Barik, J. (2007). Nicotinic ACh Receptors. *Tocris Scientific Review Series*.

Xenias, H. S., Ibanez-Sandoval, O., Koos, T., & Tepper, J. M. (2015). Are Striatal Tyrosine Hydroxylase Interneurons Dopaminergic? *Journal of Neuroscience*, *35*(16), 6584–6599. https://doi.org/10.1523/JNEUROSCI.0195-15.2015

Xie, Z., Li, D., Cheng, X., Pei, Q., Gu, H., Tao, T., Huang, M., Shang, C., Geng, D., Zhao, M., Liu, A., Zhang, C., Zhang, F., Ma, Y., & Cao, P. (2022). A brain-to-spinal sensorimotor loop for repetitive self-grooming. *Neuron*, *110*(5), 874-890.e7. https://doi.org/10.1016/j.neuron.2021.11.028

Yang, M., Silverman, J. L., & Crawley, J. N. (2011). Automated three-chambered social approach task for mice. *Current Protocols in Neuroscience*, *SUPPL. 56*. https://doi.org/10.1002/0471142301.ns0826s56

Yang, S. S., Mack, N. R., Shu, Y., & Gao, W. J. (2021). Prefrontal GABAergic Interneurons Gate Long-Range Afferents to Regulate Prefrontal Cortex-Associated Complex Behaviors. In *Frontiers in Neural Circuits* (Vol. 15). Frontiers Media S.A. https://doi.org/10.3389/fncir.2021.716408

Yates, J. W., Meij, J. T. A., Sullivan, J. R., Richtand, N. M., & Yu, L. (2007). *Bimodal effect of amphetamine on motor behaviors in C57BL/6 mice*.

Zhang, R., Xue, G., Wang, S., Zhang, L., Shi, C., & Xie, X. (2012). Novel object recognition as a facile behavior test for evaluating drug effects in AβPP/PS1 Alzheimer's disease mouse model. *Journal of Alzheimer's Disease*, *31*(4), 801–812. https://doi.org/10.3233/JAD-2012-120151

Zhang, X.-J., Li, Z., Han, Z., Sultan, K. T., Huang, K., & Shi, S.-H. (2017). Precise inhibitory microcircuit assembly of developmentally related neocortical interneurons in clusters. *Nature Communications*, *8*(May), 16091. https://doi.org/10.1038/ncomms16091

Zoli, M., Moretti, M., Zanardi, A., McIntosh, J. M., Clementi, F., & Gotti, C. (2002). Identification of the nicotinic receptor subtypes expressed on dopaminergic terminals in the rat striatum. *Journal of Neuroscience*, *22*(20), 8785–8789. https://doi.org/10.1523/jneurosci.22-20-08785.2002

Zoli, M., Pistillo, F., & Gotti, C. (2015). Neuropharmacology Diversity of native nicotinic receptor subtypes in mammalian brain. *Neuropharmacology*, *96*, 302–311. https://doi.org/10.1016/j.neuropharm.2014.11.003